

Valuation of electricity storage contracts based on the COS method

with underlying polynomial electricity prices

by

B.C. Boonstra

to obtain the degree of Master of Science
at the Delft University of Technology,
to be defended publicly on August 28, 2020 at 10:00 AM.



Student number: 4361423
Project duration: January 1, 2020 – August 28, 2020
Supervisor: Prof. dr. ir. C.W. Oosterlee, TU Delft
Thesis committee: Prof. dr. ir. C.W. Oosterlee, TU Delft
Dr. N.V. Budko, TU Delft
Dr. ir. R.J. Fokkink, TU Delft

An electronic version of this thesis is available at <http://repository.tudelft.nl/>.

Abstract

In this thesis we introduce valuation techniques to price electricity storage contracts, where the electricity prices follow a structural model based on polynomial processes. In particular we focus on a Fourier-based pricing method known as the COS method, which performs impressively to price the contracts accurately. We provide details on how to formalize an electricity storage contract, taking into account the physical limitations of an electricity storage and the operational constraints of the electricity grid. In addition to the electricity storage contract, other well-known options are being considered, such as the European option, Bermudan option and Bermudan option with multiple early-exercise rights, where the same asset price model is used based on polynomial processes. We propose an approximation of the characteristic function, so that the Fast Fourier Transform (FFT) can be applied to significantly reduce the computational complexity of the COS method, which is especially suitable for pricing Bermudan options and Bermudan options with multiple early-exercise rights. With the FFT-based algorithm, the computation time of the valuation of the discussed Bermudan-type options with the COS method is reduced from seconds to milliseconds. Furthermore, the Least Squares Monte Carlo (LSMC) method is presented to value the discussed financial derivatives and used to validate the results obtained with the COS method.

Contents

1	Introduction	1
1.1	Relevance and background of electricity storage	1
1.2	Electricity market	2
1.3	Structure of thesis	2
2	Electricity price dynamics	3
2.1	Polynomial model for electricity pricing	3
2.1.1	Defining polynomial processes and the moments formula	4
2.1.2	The polynomial price model	8
2.1.3	Increasing polynomial maps	9
2.1.4	Parameter estimation for the polynomial model	10
3	Options and electricity storage contracts	13
3.1	European option	13
3.2	Bermudan option	13
3.3	Bermudan option with multiple early-exercise rights	14
3.4	Electricity storage contracts	16
3.4.1	Details electricity storage contract	17
3.4.2	The contracts backward induction pricing algorithm	19
3.5	Option and contract valuation	21
3.5.1	Greeks	21
3.6	Risk-neutral measure	22
3.6.1	Risk-neutral measure for the electricity market	22
4	The COS method	24
4.1	Density approximation via the Fourier cosine expansion	24
4.2	The characteristic function	26
4.3	The COS method for European options	27
4.3.1	The coefficients V_k	28
4.3.2	The coefficients V_k for the polynomial model $S_t = \Phi(X_t)$	31
4.4	The COS method for Bermudan options	33
4.4.1	The coefficients $V_k(t_m)$ for Bermudan options	33
4.5	The COS method for Bermudan options with multiple early-exercise rights	36
4.5.1	The coefficients $V_k^j(t_m)$ for Bermudan options with multiple early-exercise rights	36
4.6	The COS method for electricity storage contracts	38
4.6.1	The coefficients $V_k(t_m, e)$ for electricity storage contracts	38
4.7	The integration range for the COS method	43
4.8	The Greeks with the COS method	43
5	The characteristic function approximation	45
5.1	Characteristic function approximation with moments	45
5.2	Characteristic function approximation with cumulants	46
5.3	Empirical characteristic function approximation	48
5.4	Characteristic function approximation with the adjoint expansion	49

5.4.1	General framework of the adjoint expansion method	50
5.4.2	Adjoint expansion for the OU process	51
5.4.3	Adjoint expansion for the second-order polynomial model	54
5.5	An efficient characteristic function approximation for the COS method . .	58
5.6	Error analysis for COS method with approximated characteristic function	60
6	The Least Squares Monte Carlo method	67
6.1	LSMC for Bermudan options	67
6.2	LSMC for Bermudan options with multiple early-exercise rights	69
6.3	LSMC for electricity storage contracts	71
7	Numerical results of the options	73
7.1	Verification of the COS and LSMC method	73
7.1.1	The European and Bermudan option	73
7.1.2	The Bermudan option with multiple early-exercise rights	74
7.2	The Bermudan option	75
7.3	The Bermudan option with multiple early-exercise rights	85
7.4	Implications of the numerical results	87
8	Numerical results electricity contract	88
8.1	The electricity storage contracts	89
8.2	The numerical contract values	92
8.3	The Greeks of the electricity storage contracts	102
8.4	Implications of the numerical results	103
9	Conclusions and outlook	105
9.1	Outlook	106
	Appendices	107
A	The dynamics of stochastic processes	107
A.1	Geometric Brownian Motion	107
A.2	Ornstein-Uhlenbeck process	108
B	The LSMC algorithms	109

1 Introduction

1.1 Relevance and background of electricity storage

In order to limit climate change, the European Union (2011) has the agreed objective to reduce greenhouse gas emissions by 80-95% by 2050, compared to 1990 levels [1]. This reduction of greenhouse gasses needs to go down to a zero emission by 2060-2070 if the European Union wants to meet the Paris Agreement's long-term temperature goal to keep the increase in global average temperature to well below 2 °C above pre-industrial levels [2].

One of the main options for the reduction of greenhouse gasses is the use of renewable energy [3]. To achieve this reduction, the electricity generation will gradually become less dependent on fossil fuels and make more use of renewable energy sources, like wind and solar energy. However, the current renewable energy sources have high variable output, which creates a great challenge in energy generation and maintaining the balance between demand and supply to ensure a reliable and stable energy system [4].

Many valuable endeavors have been made to find a viable solution for the high variable output of renewable energy sources, e.g. electricity storage, grid expansion, demand-side-management and electricity export/import [5]. Among all solutions, electricity storage is acknowledged as the solution with one of the highest potentials [6]. Indeed, by storing electricity when there is too much supply and discharge it during high demand, the renewable electricity output will be more stable and the reliability of renewable energy systems will improve.

There are many different technologies for large-scale electricity storage systems (i.e. lithium-ion batteries, lead-acid batteries, thermal energy storage, pumped hydroelectric storage systems, compressed air energy storage systems, hydrogen storage, flywheel) and each technology has its own technical characteristics (i.e. capacity, efficiency, power output, lifetime) [4], [7], [8]. In the future it is expected that the technical characteristics of the electricity storage will improve. In addition, new techniques and concepts are being developed that can be used for electricity storage (e.g. Car as Power Plant [9] [10]).

Because of the rapid technological improvements of electricity storages, it is also becoming increasingly interesting from a financial point of view. By storing electricity when there is a lot of supply (and therefore low price) and by selling when the demand is high (and therefore high price) a profit can be made. Multiple profitability and business-economic analyses have been done in the literature [11], [12], [13], [14], usually for one technology in a specific application. Besides the value of selling and buying electricity in the market, a storage can have additional value for electricity companies, because of the importance of a reliable and stable energy system.

Due to the great potential of electricity storage, extensive research has been done in this area. The business-economic consequences, profitability analyses, technological developments and applications of electricity storages have been thoroughly researched, while the quantitative financial mathematical research is lacking. In this thesis a quantitative research is conducted into the valuation of various options and contracts for storing electrical energy by trading on the electricity market. This valuation does not take into account additional values of an electricity storage, such as the value of a stable electricity system.

1.2 Electricity market

In the last few decades many countries have liberalized their electricity markets. Prior to the liberalization price fluctuations were minimal and often regulated. Currently, electricity is considered a commodity, which can be bought and sold at market rates. Electricity and electricity derivatives, such as forwards and options, can be traded over the counter (OTC) or on electricity exchanges (e.g. APX Group, Nord Pool AS, NYMEX).

Although electricity is treated as a commodity, its prices behave differently from other commodities because it cannot be stored in big amounts (technological progress could change this) causing the prices to respond more extreme to the relationship between supply and demand. External events, like a shortage of coal or a defective power plant, will result in having significant impact on the electricity prices [15]. The impact of the external events will increase when switching to renewable energy, which entails even more uncertainty. These features make the prices exhibit unique characteristics, such as seasonality, high volatility, mean reversion and extreme price spikes.

1.3 Structure of thesis

The thesis is organized as follows. In Section 2 we introduce a stochastic pricing model based on polynomial processes, which can capture the unique characteristics of electricity prices. Subsequently, in Section 3 we provide details about the European option, the Bermudan option and the Bermudan option with multiple early-exercise rights and in addition the electricity storage contract is formalized. Moreover, it is discussed how these financial derivatives can be valued. In Section 4 the COS method for pricing the options and the electricity contract is presented. In particular, subsection 4.3.2 defines the Fourier cosine coefficients for valuation of derivatives where the asset/electricity prices follow the model based on polynomial processes. In Section 5 various approximations of the characteristic function are introduced, which can be used to significantly reduce the computational complexity of the option valuation by means of the COS method. In addition, a detailed error analysis is given. In Section 6 the Least Squares Monte Carlo method is presented for pricing the discussed options and the electricity storage contract. The results obtained with this simulation based method are used to compare to the results obtained with the COS method. The numerical results of the options and the electricity storage contracts are discussed in respectively Section 7 and Section 8. Finally, in Section 9 we provide a conclusion and outlook reflecting on the results and the methods used.

2 Electricity price dynamics

The relationship between supply and demand in electricity markets has a major influence on the formation of the electricity price, especially in liberalized markets. In contrast to most financial markets, the energy commodity markets show high volatility, occasional extreme spikes and mean reversion.

The first commonly used pure stochastic model for electricity markets is developed by Schwartz and Smith (2000) [16] and Lucia and Schwartz (2002) [17], where a two-factor model with short-term mean reverting effects is presented. Further, Barlow (2002) [18] introduced a tractable structural model, based on the demand and supply, where the electricity price is a linear transformation of an underlying factor, modelled as an Ornstein-Uhlenbeck (OU) process. Many other different models are suggested for pricing in electricity markets, on which the aforementioned models often had a strong influence (cf. [19], [20], [21], [22] for reviews on different models).

Furthermore, since electricity prices exhibit mean reverting behavior, naturally the models use processes with this property. The simplest and most common mean reverting process is the OU process, see Appendix A.2.

The method used in this thesis for modelling the electricity price is introduced by Filipovic, Larsson and Ware (2018) [23]. They described that with the use of a polynomial map the electricity prices can be generated, where a polynomial process is used for the underlying factors. This structural model provides a framework that shows a general and tractable relationship between the underlying factors and the resulting electricity prices. In the sequel of this thesis this model is referred to as the polynomial model.

In the next subsection we elaborate on this model and its features.

2.1 Polynomial model for electricity pricing

The main idea of the polynomial model is the use of an increasing polynomial map, which maps an underlying polynomial process to the electricity price process. It is possible to exploit the freedom in choosing the increasing polynomial map to generate desired dynamics for the price process, e.g. create extreme spikes, while the underlying polynomial process is relatively calm. With the competence of generating certain dynamics, this method still provides a framework that allows a tractable relationship between the underlying factors of the polynomial process and the resulting electricity prices.

The application of polynomial processes has appeared in the literature since Wong (1964) [24], however the use of it in finance began in the early 2000s, where Delbaen and Shirakawa [25] and Zhou [26] introduced a new method on interest rate modelling. In 2011 Cuchiero [27] described a new technique for option pricing and hedging for a class of polynomial processes. More recently, Filipovic and Larsson [28] provided a mathematical foundation for polynomial processes. These polynomial processes are relevant in many financial applications, including financial market models for interest rates, commodities and electricity.

The price model with polynomial processes is as follows. If X_t follows a polynomial process, e.g. GBM or OU process, then the spot price at time t can be modelled in the following form:

$$S_t = \Phi(X_t),$$

where Φ is an increasing polynomial map.

The polynomial model utilizes the properties of polynomial processes. A polynomial process has the property [27] that any conditional expectation of the form $\mathbb{E} [\Phi(X_t) | X_s]$, where Φ is a polynomial, is again a polynomial function of X_s of the same or lower degree than that of Φ . This implies that the conditional moments of all orders of X_t can be computed without its probability distribution or characteristic function.

In the following sections, first the polynomial processes are defined and a formula is given to analytically determine the conditional moments of all orders of a polynomial process. Subsequent, we describe the polynomial model in detail. Moreover, it is also examined how the parameters for this model should be estimated.

2.1.1 Defining polynomial processes and the moments formula

In this section polynomial processes are defined and a lemma is given with which polynomial processes can be easily recognized. In addition, the moments formula is provided, with which it is possible to compute the moments of all orders of a polynomial process without the probability distribution or characteristic function. This section is based on the contents of paper [28] and the approach is inspired by [29].

Polynomial processes

First, general definitions are given about the class of polynomials, after which the definition of a polynomial process and a lemma to easily recognize a polynomial process are presented.

Definition 2.1. (Polynomial) A polynomial p on \mathbb{R}^d is a map, $p : \mathbb{R}^d \rightarrow \mathbb{R}$, of the form:

$$\sum_{\alpha} c_{\alpha} x_1^{\alpha_1} \cdot \dots \cdot x_d^{\alpha_d},$$

where $\alpha = (\alpha_1, \dots, \alpha_d) \in \mathbb{N}^d$ denote the multi-indices of summation and only finitely many coefficients c_{α} are nonzero. This representation is unique and the degree of the polynomial is $\deg(p) = \max\{\alpha_1 + \dots + \alpha_d : c_{\alpha} \neq 0\}$.

Let $\text{Pol}(\mathbb{R}^d)$ indicate the ring of all polynomials on \mathbb{R}^d and $\text{Pol}_n(\mathbb{R}^d)$ the subspace spanned by polynomials of degree at most n . Let E be a subset of \mathbb{R}^d , then a polynomial on E is the constraint $p = q|_E$ to E of a polynomial $q \in \text{Pol}(\mathbb{R}^d)$. The degree of this polynomial p is $\deg(p) = \min\{\deg(q) : p = q|_E, q \in \text{Pol}(\mathbb{R}^d)\}$. Furthermore, let $\text{Pol}(E)$ denote the ring of polynomials on E , and $\text{Pol}_n(E)$ the subspace spanned by polynomials on E of degree at most n .

Consider the following partial differential operator \mathcal{G} :

$$\mathcal{G}\bar{f}(x) = \frac{1}{2}\text{Tr}(a(x)\nabla^2\bar{f}) + b(x)^{\top}\nabla\bar{f}, \quad (2.1)$$

for \bar{f} any \mathcal{C}^2 -function, $x \in \mathbb{R}^d$ and where

$$\begin{aligned} a &: \mathbb{R}^d \rightarrow \mathbb{S}^d, \\ b &: \mathbb{R}^d \rightarrow \mathbb{R}^d, \end{aligned} \quad (2.2)$$

where \mathbb{S}^d is the set of real symmetric $d \times d$ matrices.

Definition 2.2. (well-defined) \mathcal{G} is well-defined as an operator on $\text{Pol}(E)$ if $\mathcal{G}\bar{f} = 0$ on E for any $\bar{f} \in \text{Pol}(\mathbb{R}^d)$ with $\bar{f} = 0$ on E .

For example, assume $d = 2$, $E = \mathbb{R} \times \{0\}$, and the operator as in (2.1) with $a = 1$ and $b = 1$, then the operator \mathcal{G} is not well-defined on $\text{Pol}(E)$, because $\bar{f}(x, y) = y$ is zero on E , but $\mathcal{G}\bar{f} = 1$.

Now the definition of a polynomial process will be described. Let X_t be an E -valued solution to the stochastic differential equation (SDE):

$$dX_t = b(X_t)dt + \sigma(X_t)dW_t, \quad (2.3)$$

where W_t is a d -dimensional Brownian motion, $\sigma : \mathbb{R}^d \rightarrow \mathbb{R}^{d \times d}$ with $\sigma(x)\sigma^\top(x) = a(x)$ on E and $a(x)$ and $b(x)$ defined in (2.2). Definition 2.3 shows when the solution of (2.3) is a polynomial process.

Definition 2.3. (polynomial process) The operator \mathcal{G} is called polynomial on E if it is well-defined on $\text{Pol}(E)$, and thus maps $\text{Pol}_n(E)$ to itself $\forall n \in \mathbb{N}$. In this case, we call any E -valued solution to (2.3) a polynomial process on E .

The next lemma provides a simple way to verify if the solution of the SDE (2.3) is a polynomial process as described in Definition 2.3.

Lemma 2.4. Let \mathcal{G} as defined in (2.1), a and b as (2.2). Assume \mathcal{G} is well defined on $\text{Pol}(E)$. Then the following statements are equivalent:

- (i) \mathcal{G} maps $\text{Pol}_n(E)$ to itself $\forall n \in \mathbb{N}$.
- (ii) \mathcal{G} maps $\text{Pol}_n(E)$ to itself for $n \in \{1, 2\}$.
- (iii) The components of a and b restricted to E lie respectively in $\text{Pol}_2(E)$ and $\text{Pol}_1(E)$.

Proof. See Lemma 2.2. of [28]. □

With Lemma 2.4 it is easy to find out if an E -valued solution to (2.3) is a polynomial process, by looking at the coefficients of \mathcal{G} . Hence, polynomial processes are characterized by a linear drift and the squared volatility parameter being at most quadratic. Furthermore, it follows that if the components $a(x)$ are polynomials of degree at most two and $b(x)$ of degree at most one, that for any $n \in \mathbb{N}$ and any polynomial $p \in \text{Pol}_n(E)$, $\mathcal{G}p$ is also a polynomial of degree at most n on E .

Moments formula

Let N denote the dimension of $\text{Pol}_n(E)$ for any $n \in \mathbb{N}$. Then $\forall p \in \text{Pol}_n(E)$ there $\exists!$ vector $\vec{p} \in \mathbb{R}^N$ such that:

$$\begin{aligned} p(x) &= H(x)^\top \vec{p}, \\ \mathcal{G}p(x) &= H(x)^\top G \vec{p}, \end{aligned} \tag{2.4}$$

where $H(x) = (h_1(x), \dots, h_N(x))^\top$ denotes the vector of basis functions for the space of polynomials of degree n (e.g. for $N = 1$, the basis functions are $H(x) = (h_1(x))^\top = (1, x, x^2, \dots, x^n)^\top$) and $G \in \mathbb{R}^N$ is the unique matrix representation of the partial differential operator \mathcal{G} (2.1).

The following theorem, which is one of the most important properties of the polynomial processes, presents how the moments of all orders of X_T under a filtration can be computed.

Theorem 2.5. (Moment formula). Let X_t be a polynomial process. If $\mathbb{E} [||X_0||^{2n}] < \infty$, then $\forall p \in \text{Pol}_n(E)$ with coordinate vector \vec{p} as in (2.4), it holds that for $0 \leq t \leq T$:

$$\mathbb{E} [p(X_T) | \mathcal{F}_t] = H(X_t)^\top e^{(T-t)G} \vec{p}.$$

Proof. See theorem 3.1. of [28]. □

Example 2.6. In this example Theorem 2.5 is applied to compute the first moment and the variance of the OU process, see Appendix A.2 for the dynamics of the OU process.

First Lemma 2.4 is used to show that the OU process X_t is a polynomial process. The OU process has the following parameters (2.2) for the operator \mathcal{G} :

$$\begin{aligned} a &= \sigma^2, \\ b(x) &= \kappa(\theta - x). \end{aligned} \tag{2.5}$$

It follows that $a \in \text{Pol}_2$ and $b(x) \in \text{Pol}_1$, so according Lemma 2.4 is the OU process indeed a polynomial process.

Now Theorem 2.5 is applied to compute the first two moments of X_T , for which the basis $H(x) = (1, x, x^2)^\top$ is used. For the first moment we compute:

$$\mathbb{E}[X_T | \mathcal{F}_0] = H(X_0)^\top e^{TG} \vec{p},$$

with $\vec{p} = (0, 1, 0)^\top$ and G the unique matrix representation of \mathcal{G} . For the second moment the coefficient vector should be chosen as $\vec{p} = (0, 0, 1)^\top$.

Now G , the matrix representation of \mathcal{G} , is computed. The partial differential operator \mathcal{G} , with parameters a and b defined in (2.5), is given by:

$$\mathcal{G}\bar{f}(x) = \frac{1}{2}\sigma^2 \frac{\partial^2}{\partial x^2} \bar{f}(x) + \kappa(\theta - x) \frac{\partial}{\partial x} \bar{f}(x).$$

Applying the elements of $H(x)$ to \mathcal{G} results in:

$$\mathcal{G}1 = 0, \quad \mathcal{G}x = \kappa\theta - \kappa x, \quad \mathcal{G}x^2 = \sigma^2 + 2\kappa\theta x - 2\kappa x^2,$$

which produces the following matrix representation of the partial differential operator:

$$G = \begin{bmatrix} 0 & \kappa\theta & \sigma^2 \\ 0 & -\kappa & 2\kappa\theta \\ 0 & 0 & -2\kappa \end{bmatrix}.$$

To compute e^{TG} , the matrix G will be diagonalized as $G = UDU^{-1}$, where U , D and U^{-1} are given by:

$$U = \begin{bmatrix} 1 & \theta^2 - \frac{\sigma^2}{2\kappa} & -\theta \\ 0 & -2\theta & 1 \\ 0 & 1 & 0 \end{bmatrix}, \quad D = \begin{bmatrix} 0 & 0 & 0 \\ 0 & -2\kappa & 0 \\ 0 & 0 & -\kappa \end{bmatrix}, \quad U^{-1} = \begin{bmatrix} 1 & \theta & \theta^2 - \frac{\sigma^2}{2\kappa} \\ 0 & 0 & 1 \\ 0 & 1 & 2\theta \end{bmatrix}.$$

It follows that e^{TG} can be computed as:

$$e^{TG} = Ue^{TD}U^{-1} = \begin{bmatrix} 1 & \theta e^{-\kappa T}(e^{\kappa T} - 1) & \frac{e^{-2\kappa T}(e^{\kappa T} - 1)(\sigma^2 e^{\kappa T} + 2\kappa\theta^2 e^{\kappa T} - 2\kappa\theta^2 + \sigma^2)}{2\theta e^{-2\kappa T}(e^{\kappa T} - 1)} \\ 0 & e^{-\kappa T} & e^{-2\kappa T} \\ 0 & 0 & e^{-2\kappa T} \end{bmatrix}.$$

Now we have all the components to compute the first and second moment. The first moment is calculated as follows:

$$\begin{aligned} \mathbb{E}[X_T|\mathcal{F}_0] &= H(X_0)^\top e^{TG}\vec{p} \\ &= (1 \quad X_0 \quad X_0^2) e^{TG} \begin{pmatrix} 0 \\ 1 \\ 0 \end{pmatrix} \\ &= X_0 e^{-\kappa T} + \theta(1 - e^{-\kappa T}), \end{aligned}$$

and the second moment is found as follows:

$$\begin{aligned} \mathbb{E}[X_T^2|\mathcal{F}_0] &= H(X_0)^\top e^{TG}\vec{p} \\ &= (1 \quad X_0 \quad X_0^2) e^{TG} \begin{pmatrix} 0 \\ 0 \\ 1 \end{pmatrix} \\ &= e^{-2\kappa T} X_0^2 + 2e^{-2\kappa T}(-1 + e^{\kappa T})\theta X_0 \\ &\quad + \frac{e^{-2\kappa T}(-1 + e^{\kappa T})(e^{\kappa T}\sigma^2 + \sigma^2 + 2\kappa\theta^2 e^{\kappa T} - 2\kappa\theta^2)}{2\kappa}. \end{aligned}$$

With the first and second moment the variance can be computed:

$$\begin{aligned} Var[X_T|X_0] &= \mathbb{E}[X_T^2|X_0] - \mathbb{E}[X_T|X_0]^2 \\ &= \frac{\sigma^2}{2\kappa}(1 - e^{-2\kappa T}). \end{aligned}$$

The expected value and variance computed with this method are the same as stated in the literature, see Appendix A.2.

2.1.2 The polynomial price model

Now that the polynomial processes and its properties are defined, the polynomial price model, introduced in [23], will be stated. In order to generate electricity prices, the characteristics of the electricity prices need to be captured in the model. This can be done with an increasing polynomial map Φ , which can exploit the freedom in choosing the degree and the parameters to generate the desired characteristics, such as extreme price spikes, high volatility and seasonality. Furthermore, with Theorem 2.5 all the moments of the polynomial model can be computed without the use of the density function or characteristic function.

The polynomial model is defined as follows. If X_t follows a polynomial process, e.g. GBM or OU process, then the spot price at time t can be modelled in the form:

$$S_t = \Phi(X_t) = H(X_t)^\top \vec{p}, \quad (2.6)$$

where $H(X_t)$ denotes the vector of basis functions for the space of polynomials preserved by the polynomial process (e.g. $H(X_t) = (1, X_t, X_t^2, \dots, X_t^n)^\top$ for an one-dimensional polynomial of degree $n \in \mathbb{N}$) and the elements in vector \vec{p} are the coefficients that characterize the polynomial map Φ . The construction of these increasing polynomial maps is explained in detail in Section 2.1.3. Moreover, seasonality can be included by making the coefficients in vector \vec{p} time-dependent.

Furthermore, with the polynomial model electricity forwards can be priced in a direct way. The pricing formulas for the computation of the forwards are given in [30]. The time t price of an electricity forward, where the electricity is directly delivered at time $T \geq t$ is given by:

$$\tilde{f}(t, T, X_t) := \mathbb{E}_{\mathbb{Q}}[S_T | \mathcal{F}_t],$$

where \mathbb{Q} is the risk-neutral measure.

In reality, electricity is not directly delivered, but gradually over a time interval. This leads to the following definition for an electricity forward at time t with the delivery interval $[T_1, T_2]$, with $t \leq T_1 < T_2$:

$$\tilde{F}(t, T_1, T_2, X_t) := \frac{1}{T_2 - T_1} \mathbb{E}_{\mathbb{Q}} \left[\int_{T_1}^{T_2} S_u \, du \middle| \mathcal{F}_t \right].$$

$\tilde{F}(t, T_1, T_2, X_t)$ is often called a swap price.

Proposition 2.7 presents the closed-form solutions of the forward prices.

Proposition 2.7. Let \vec{p} be the vector of coefficients that define the polynomial map $S_t = \Phi(X_t) = H(X_t)^\top \vec{p}$, as defined in (2.6). The time t price of the electricity forward, $\tilde{f}(t, T, X_t)$, for $t \leq T$ is given by:

$$\tilde{f}(t, T, X_t) = H(X_t)^\top e^{(T-t)G} \vec{p},$$

and the time t price of the forward price with delivery interval, for $t \leq T_1 < T_2$ is given by:

$$\tilde{F}(t, T_1, T_2, X_t) = \frac{1}{T_2 - T_1} H(X_t)^\top e^{(T_1-t)G} \int_0^{T_2-T_1} e^{uG} \, du \, \vec{p}.$$

Proof. This follows from Theorem 2.5 and rearranging terms, see [30]. \square

2.1.3 Increasing polynomial maps

To model the spot prices with the polynomial model a polynomial map is needed that provides a 1-1 map from a polynomial process X_t to the spot price S_t . In order to capture the characteristics of the electricity commodity market, increasing polynomial maps $\Phi(\cdot)$ from $[0, \infty)$ onto $[0, \infty)$ will be used.

Such increasing polynomial maps can be constructed from non-negative polynomials on $[0, \infty)$ [31]. To create these increasing polynomial maps the multiplication of positive quadratics will be used. These quadratics are defined as [32]:

$$\tilde{q}_{\alpha, \gamma}(x) = \frac{\alpha}{2}x^2 + (1 - \alpha - \gamma)x + \gamma, \quad (2.7)$$

where the quadratic polynomials $\tilde{q}_{\alpha, \gamma}$ are normalized such that:

$$\int_0^{\infty} e^{-x} \tilde{q}_{\alpha, \gamma}(x) dx = 1.$$

To produce all the possible quadratic polynomials that are on $[0, \infty)$, the parameter set (α, γ) is chosen as follows:

$$\begin{aligned} \alpha &= \hat{r} \cos(\xi), \\ \gamma &= \hat{r} \sin(\xi), \end{aligned} \quad (2.8)$$

where $\xi \in [0, \pi/2]$ and $\hat{r} \in [0, \cos(\xi) + \sin(\xi) + \sqrt{\sin(2\xi)}]$.

With the quadratic polynomials as described above the increasing polynomial map, $\Phi(\cdot) : [0, \infty) \mapsto [0, \infty)$, can be constructed from pairs of parameters $(\alpha_1, \gamma_1), \dots, (\alpha_K, \gamma_K)$ where $K \in \mathbb{N}^+$:

$$\Phi(x) = \int_0^x \prod_{k=1}^K \tilde{q}_{\alpha_k, \gamma_k}(u) du. \quad (2.9)$$

Note that if $\alpha_k \neq 0 \forall k \in [1, K]$ the degree of Φ is $2K + 1$. Furthermore, under this general construction of the polynomial map (2.9) a polynomial process with even order can be obtained by setting $\alpha_k = 0$ for some $k \in [1, K]$.

Example 2.8. The cubic polynomial is an example of a polynomial map with degree 3:

$$\Phi_3(x) = a_3x^3 + a_2x^2 + a_1x + a_0.$$

The cubic polynomial can be obtained by setting $K = 1$ in equation (2.9)

$$\begin{aligned} \Phi_3(x) &= \int_0^x \tilde{q}_{\alpha, \gamma}(u) du = \frac{\alpha}{6}x^3 + \frac{(1 - \alpha - \gamma)}{2}x^2 + \gamma x + \alpha_0 \\ &= \frac{r \cos(\xi)}{6}x^3 + \frac{(1 - r \cos(\xi) - r \sin(\xi))}{2}x^2 + r \sin(\xi)x + \alpha_0. \end{aligned} \quad (2.10)$$

Now by setting $\xi = \pi/3$, $\hat{r} = 1$ and $\alpha_0 = 0$ the following cubic polynomial is obtained, see Figure 1, which in theory could be used to map a polynomial process X_t to the spot prices S_t .

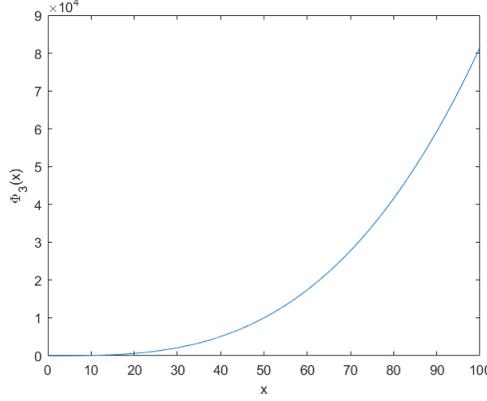


Figure 1: Increasing polynomial map (2.10), where $\xi = \frac{\pi}{3}$, $\hat{r} = 1$ and $\alpha_0 = 0$.

2.1.4 Parameter estimation for the polynomial model

In this subsection it is described how the parameters of the underlying process X_t and the polynomial map Φ can be estimated using maximum likelihood estimation (MLE), as discussed in [33]. First the Geometric Brownian Motion (GBM) is examined as underlying polynomial process, then it is shown how the same method can be applied to an underlying OU process.

Geometric Brownian Motion

Assume that the asset price S_t can be generated by the polynomial model, which takes the form of (2.6):

$$S_t = \Phi(X_t),$$

where the underlying polynomial process X_t follows the GBM, which characteristics are defined in Appendix A.1.

First we let the time interval $[0, T]$ be equally divided by N parts, such that $dt = \frac{T}{N}$ and $(0, t_1, t_2, \dots, t_{N-1}, T)$. Note that the increments of $x_{t_n} = \log(X_{t_n}) = \log(\Phi^{-1}(S_{t_n}))$ are normally distributed:

$$x_{t_n} - x_{t_{n-1}} = \log\left(\frac{X_{t_n}}{X_{t_{n-1}}}\right) \sim N\left(\left(\mu - \frac{\sigma^2}{2}\right)(t_n - t_{n-1}), \sigma^2(t_n - t_{n-1})\right). \quad (2.11)$$

The polynomial model Φ of degree $2n + 1$ is thus determined by the parameter set $\xi = (\mu, \sigma, (\alpha_1, \gamma_1), \dots, (\alpha_n, \gamma_n))$, where an even degree is obtained by setting one of the α_i 's to zero. To calibrate the parameters in the set ξ MLE can be used. From the distribution (2.11) the log-likelihood of (S_0, \dots, S_N) , i.e. (X_0, \dots, X_N) or (x_0, \dots, x_N) , can be computed. The log-likelihood is given by:

$$LL := l(\mu, \sigma; x_{t_0}, \dots, x_{t_N}) = -\frac{N}{2} \log(\hat{\sigma}^2 2\pi) - \frac{1}{2\hat{\sigma}^2} \sum_{n=1}^N (x_{t_n} - x_{t_{n-1}} - \hat{\mu})^2, \quad (2.12)$$

where $\hat{\mu} = \left(\mu - \frac{\sigma^2}{2}\right) dt$ and $\hat{\sigma}^2 = \sigma^2 dt$.

The MLE estimates the parameters $(\hat{\mu}, \hat{\sigma})$ by maximizing the log-likelihood function. This method estimates parameters for which the observed data is most probable:

$$(\hat{\mu}_{MLE}, \hat{\sigma}_{MLE}) = \arg \max_{\hat{\mu}, \hat{\sigma}} l(\hat{\mu}, \hat{\sigma}; x_{t_0}, \dots, x_{t_N}).$$

This results in the following parameters:

$$\begin{aligned} \hat{\mu}_{MLE} &= \frac{x_{t_N} - x_{t_0}}{N}, \\ \hat{\sigma}_{MLE}^2 &= \frac{1}{N} \sum_{n=1}^N (x_{t_n} - x_{t_{n-1}} - \hat{\mu}_{MLE})^2. \end{aligned} \quad (2.13)$$

Now by substitution of the parameters (2.13) in the log-likelihood function (2.12), the following log-likelihood function is obtained:

$$LL = -\frac{N}{2} \log \left(\frac{2\pi}{N} \sum_{n=1}^N \left(x_{t_n} - x_{t_{n-1}} - \frac{x_{t_N} - x_{t_0}}{N} \right)^2 \right) - \frac{N}{2}. \quad (2.14)$$

Finally, the optimal polynomial coefficients of the polynomial map (2.6) need to be estimated. The closed-form solution log-likelihood function for this problem is not available, so numerical methods will be necessary to find the maximum likelihood estimators [33].

Summarizing, we got the following problem that needs to be calibrated:

$$\max\{LL\} = \max \left\{ -\frac{N}{2} \log \left(\frac{2\pi}{N} \sum_{n=1}^N \left(x_{t_n} - x_{t_{n-1}} - \frac{x_{t_N} - x_{t_0}}{N} \right)^2 \right) - \frac{N}{2} \right\}, \quad (2.15)$$

$$x_n = \log(\Phi^{-1}(S_n)), \quad (2.16)$$

$$\Phi(x) = \int_0^x \prod_{k=1}^K \tilde{q}_{\alpha_k, \gamma_k}(t) dt. \quad (2.17)$$

To calibrate the model, the problem (2.15)-(2.17) can be fitted to electricity market prices, S_0, \dots, S_N . Note that maximizing the log-likelihood function (2.15) is done by minimizing the following expression:

$$\sum_{n=1}^N \left(x_{t_n} - x_{t_{n-1}} - \frac{x_{t_N} - x_{t_0}}{N} \right). \quad (2.18)$$

This minimization problem (2.18) is not easy to solve analytically. If a second-order polynomial model is taken, i.e. $K = 1$ and $\alpha_1 = 0$ in (2.17), the expression that needs to be minimized is already a complicated function of the polynomial coefficients. Therefore numerical methods need to be used to find the maximum likelihood estimators. Global optimization is a numerical method to perform this task.

Remark 2.9. For the polynomial model with an underlying OU process a similar derivation can be done to calibrate the model. In Appendix A.2 it is shown that the OU process is normally distributed with mean and variance defined in (A.9).

Using the same discretization of $[0, T]$ by N parts as used in the MLE for the GBM, it follows that the next expression is normally distributed:

$$X_{t_n} - e^{-\kappa dt} X_{t_{n-1}} \sim N \left(\theta(1 - e^{-\kappa dt}), \frac{\sigma^2}{2\kappa}(1 - e^{-2\kappa dt}) \right). \quad (2.19)$$

Therefore the log-likelihood is given by:

$$LL := -\frac{N}{2} \log(\hat{\sigma}^2 2\pi) - \frac{1}{2\hat{\sigma}^2} \sum_{n=1}^N \left(X_{t_n} - \hat{\lambda} X_{t_{n-1}} - \hat{\mu} \right)^2, \quad (2.20)$$

where $\hat{\sigma}^2 = \frac{\sigma^2}{2\kappa}(1 - e^{-2\kappa dt})$, $\hat{\lambda} = e^{-\kappa dt}$ and $\hat{\mu} = \theta(1 - e^{-\kappa dt})$.

Thus for the n^{th} -order polynomial model with an underlying OU process we need to maximize the log-likelihood function (2.20) over the parameter set $\xi = (\hat{\mu}, \hat{\lambda}, \hat{\sigma}, (\alpha_1, \gamma_1), \dots, (\alpha_n, \gamma_n))$. Similar as with the MLE for GBM, numerical methods are needed to find the maximum likelihood estimators.

An example of the MLE for calibration of the third-order polynomial model with an underlying OU process is given in [32].

Example 2.10. Let our price model take the form of (2.6), with X_t following the Geometric Brownian Motion (A.1) and a polynomial map Φ of degree 3 as described in section 2.1.3. By using Ito's formula we can define the solution for X_t as

$$X_t = X_0 \exp \left(\left(\mu - \frac{1}{2} \sigma^2 \right) (t - t_0) + \sigma (W_t - W_0) \right). \quad (2.21)$$

The parameters used for this model are set as follows:

$$\mu = 0.05, \quad \sigma = 0.8, \quad \alpha = 0.75, \quad \gamma = 0.75. \quad (2.22)$$

The results are shown in Figure 2.

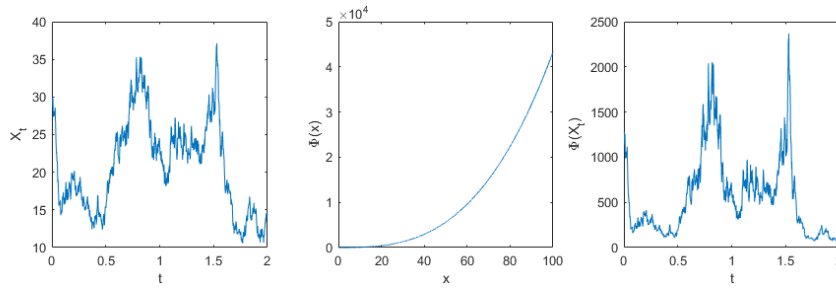


Figure 2: Polynomial model with the parameters as described in (2.22). From left to right: The simulation of process X_t following the GBM; The degree 3 increasing polynomial map Φ ; The resulting spot prices $S_t = \Phi(X_t)$.

As showed in Figure 2, the increasing polynomial map Φ is used to change the dynamics of the polynomial process X_t to the more extreme dynamics of the price process $S_t = \Phi(X_t)$.

3 Options and electricity storage contracts

In this section several different options are described. An option is a financial contract that gives the option holder the right, but not the obligation, to trade an underlying asset for a predetermined strike price K at a fixed time in the future. Within these financial contracts there is a general distinction between a call and a put option. A call option gives the holder the right to buy the asset for the strike price K , whereas a put option gives the right to sell.

In addition to the options, this section defines another financial contract, the electricity storage contract. This is a contract where electricity can be sold/bought at fixed moments by trading on the electricity market in order to make a profit while the energy level in the storage changes. The electricity storage contract does not use a predetermined strike price K but trades with the market prices of electricity.

3.1 European option

A European option is a financial contract which limits the holder to exercise at only one prescribed time T , which is called the maturity time. At the maturity time the holder can decide to exchange the asset for the agreed strike price K . Generally, the holder will only exercise the option when it has a positive value. Therefore, the option value at time T , $v(T, S_T)$, is equal to the payoff function, $g(T, S_T)$:

$$v(T, S_T) \equiv g(T, S_T) = \begin{cases} \max(S_T - K, 0), & \text{for a call,} \\ \max(K - S_T, 0), & \text{for a put.} \end{cases} \quad (3.1)$$

Due to the fact that there are no early-exercise features, the value of a European option at time t can be computed as the expectation of the discounted option value at exercise time T , by means of the risk-neutral valuation formula:

$$v(t, S_t) = e^{-r(T-t)} \mathbb{E}_{\mathbb{Q}}[v(T, S_T) | \mathcal{F}_t], \quad (3.2)$$

where $\mathcal{F}_t = \sigma(S_s; s \leq t)$, r the constant interest rate and $\mathbb{E}_{\mathbb{Q}}[\cdot]$ the expectation under the risk-neutral measure \mathbb{Q} .

3.2 Bermudan option

A Bermudan option gives the holder the right to exercise the option once at a predetermined finite set of exercise moments before expiry. The holder receives the payoff when the option is exercised.

Consider a Bermudan option with M exercise moments, where t_0 is the initial time and $\{t_1, \dots, t_M\}$ the set of exercise moments, where $0 = t_0 < t_1 < \dots < t_M = T$ and the time between exercise moments is equally distributed, $\Delta t := (t_{m+1} - t_m)$. The payoff function of a Bermudan option with strike price K when exercised at time t_m is given by:

$$g(t_m, S_{t_m}) = \begin{cases} \max(S_{t_m} - K, 0), & \text{for a call,} \\ \max(K - S_{t_m}, 0), & \text{for a put.} \end{cases} \quad (3.3)$$

At maturity time t_M the choices for the holder are to exercise the option or to let the option expire, therefore the value of a Bermudan option at time t_M is equal to the payoff function:

$$v(t_M, S_{t_M}) \equiv g(t_M, S_{t_M}).$$

At each exercise moment before maturity, $t_m \in \{t_1, \dots, t_{M-1}\}$, the holder has the choice to exercise or continue. This results in the following values for the two choices:

1. If the holder exercises the option, the value of the option at time t_m will be equal to the payoff at that time, $g(t_m, S_{t_m})$.
2. If the holder does not exercise the option, the Bermudan option at time t_m still has value, because the option can be exercised at a later exercise moment. This value is called the continuation value and is defined by $c(t_m, S_{t_m})$.

The holder will select the choice which results in the highest value. Therefore, the value of the Bermudan option at time t_m , for $m \in \{1, \dots, M-1\}$, is as follows:

$$v(t_m, S_{t_m}) = \max(g(t_m, S_{t_m}), c(t_m, S_{t_m})).$$

At initial time t_0 the option can not be exercised, so the value at time t_0 is equal to the continuation value:

$$v(t_0, S_{t_0}) \equiv c(t_0, S_{t_0}).$$

Between two exercise moments t_m and t_{m+1} , for $m \in \{0, \dots, M-1\}$, the continuation value of a Bermudan option can be considered as that of the value of a European option, and can be computed with the risk-neutral valuation formula (3.2):

$$c(t_m, S_{t_m}) = e^{-r\Delta t} \mathbb{E}_{\mathbb{Q}}[v(t_{m+1}, S_{t_{m+1}}) | \mathcal{F}_{t_m}]. \quad (3.4)$$

Due to the fact that the option value at maturity time t_M is known and the continuation value at time t_m can be computed with the option value at time t_{m+1} , a backward induction method is used to result in the Bermudan option value at initial time t_0 . The backward induction algorithm to value the Bermudan option is summarized as follows:

$$\begin{cases} v(t_M, S_{t_M}) &= g(t_M, S_{t_M}), \\ v(t_m, S_{t_m}) &= \max(g(t_m, S_{t_m}), c(t_m, S_{t_m})), & \text{for } m \in \{M-1, \dots, 1\}, \\ c(t_m, S_{t_m}) &= e^{-r\Delta t} \mathbb{E}_{\mathbb{Q}}[v(t_{m+1}, S_{t_{m+1}}) | \mathcal{F}_{t_m}], & \text{for } m \in \{M-1, \dots, 0\}, \\ v(t_0, S_{t_0}) &= c(t_0, S_{t_0}). \end{cases} \quad (3.5)$$

3.3 Bermudan option with multiple early-exercise rights

In this subsection the Bermudan option, where the holder has the right to exercise the option once, is extended so that the holder has the right to exercise the option multiple times at a predetermined finite set of exercise moments before expiry. The number of rights that a holder is entitled to exercise the option before expiry will be denoted by R , so for a Bermudan option $R = 1$. With this option the holder can only use at most one right at each exercise moment. Thus it is not possible to have more exercise rights than exercise moments, therefore $R \leq M$. We let $\mathcal{R} := \{1, \dots, R\}$ denote the set of all the possible numbers of early-exercise rights left.

Now we create an extra dimension in the notation for the multiple exercise framework: the number of early-exercise rights left. This will be denoted as a superscript j in the notation. So $v^j(t_m, S_{t_m})$ and $c^j(t_m, S_{t_m})$ are respectively the value of the option and the continuation value at time t_m with j rights left. The continuation value $c^j(t_m, S_{t_m})$ is computed with the risk-neutral valuation formula (3.2), just like with the Bermudan option:

$$c^j(t_m, S_{t_m}) = e^{-r\Delta t} \mathbb{E}_{\mathbb{Q}}[v^j(t_{m+1}, S_{t_{m+1}}) | \mathcal{F}_{t_m}]. \quad (3.6)$$

To make a pricing algorithm for the Bermudan option with multiple early-exercise rights we must be able to determine the value $v^j(t_m, S_{t_m})$ in (3.6). Two different settings are taken in consideration:

1. The holder has as many exercise rights left as there are exercise moments.
2. The holder has less exercise rights than there are exercise moments.

These two settings are elaborated below.

1. In the first setting there are as many exercise rights left as there are exercise moments, therefore the holder will use the right to exercise at every exercise moment if the value of the option is positive. Therefore the value at t_{M-j+1} with j exercise moments left is equal to the payoff function at every exercise moment discounted to time t_{M-j+1} . For example, the value at time t_{M-1} with two exercise moments left, $v^2(t_{M-1}, S_{t_{M-1}})$, is equal to the payoff at time t_{M-1} plus the discounted payoff at time t_M .

Now it is shown that the value of the option with j exercise rights left at moments t_{M-j+1} in equation (3.6) can be written as the payoff at time t_{M-j+1} plus the continuation value with one right less at time t_{M-j+1} .

We start with the continuation value where $j = 1$:

$$\begin{aligned} c^1(t_{M-1}, S_{t_{M-1}}) &= e^{-r\Delta t} \mathbb{E}_{\mathbb{Q}}[v^1(t_M, S_{t_M}) | \mathcal{F}_{t_{M-1}}] \\ &= e^{-r\Delta t} \mathbb{E}_{\mathbb{Q}}[g(t_M, S_{t_M}) | \mathcal{F}_{t_{M-1}}]. \end{aligned} \quad (3.7)$$

Note that the continuation value with zero rights left equals zero, so indeed $v^1(t_M, S_{t_M})$ can be written as the payoff at time t_M plus the continuation value with one right less (which equals zero).

For two exercise rights and two exercise moments left the following derivation is done:

$$\begin{aligned} c^2(t_{M-2}, S_{t_{M-2}}) &= e^{-r\Delta t} \mathbb{E}_{\mathbb{Q}}[v^2(t_{M-1}, S_{t_{M-1}}) | \mathcal{F}_{t_{M-2}}] \\ &= e^{-r\Delta t} \mathbb{E}_{\mathbb{Q}}[g(t_{M-1}, S_{t_{M-1}}) + e^{-r\Delta t} g(t_M, S_{t_M}) | \mathcal{F}_{t_{M-2}}] \\ &= e^{-r\Delta t} \left(\mathbb{E}_{\mathbb{Q}}[g(t_{M-1}, S_{t_{M-1}}) | \mathcal{F}_{t_{M-2}}] + \mathbb{E}_{\mathbb{Q}}[e^{-r\Delta t} g(t_M, S_{t_M}) | \mathcal{F}_{t_{M-2}}] \right) \\ &= e^{-r\Delta t} \left(\mathbb{E}_{\mathbb{Q}}[g(t_{M-1}, S_{t_{M-1}}) | \mathcal{F}_{t_{M-2}}] + \mathbb{E}_{\mathbb{Q}}[e^{-r\Delta t} \mathbb{E}_{\mathbb{Q}}[g(t_M, S_{t_M}) | \mathcal{F}_{t_{M-1}}] | \mathcal{F}_{t_{M-2}}] \right) \\ &\stackrel{(3.7)}{=} e^{-r\Delta t} \left(\mathbb{E}_{\mathbb{Q}}[g(t_{M-1}, S_{t_{M-1}}) | \mathcal{F}_{t_{M-2}}] + \mathbb{E}_{\mathbb{Q}}[c^1(t_{M-1}, S_{t_{M-1}}) | \mathcal{F}_{t_{M-2}}] \right) \\ &= e^{-r\Delta t} \mathbb{E}_{\mathbb{Q}}[g(t_{M-1}, S_{t_{M-1}}) + c^1(t_{M-1}, S_{t_{M-1}}) | \mathcal{F}_{t_{M-2}}], \end{aligned}$$

where the tower rule and the linearity of the conditional expectation is used.

By applying the tower rule repetitive it can be shown that the value of the option with j exercise rights left at moments t_{M-j+1} in equation (3.6) can be written as:

$$v^j(t_{M-j+1}, S_{t_{M-j+1}}) = g(t_{M-j+1}, S_{t_{M-j+1}}) + c^{j-1}(t_{M-j+1}, S_{t_{M-j+1}}), \quad \forall j \in \mathcal{R}. \quad (3.8)$$

We call this value the initialization for the level of exercise rights left.

2. The second setting contains the cases where there are fewer exercise rights left than there are exercise moments left. The holder of the option at time t_m for $m \in \{M-j, \dots, 1\}$ with j rights left has to make the decision between the following two choices:

- Exercise the option and receive the payoff $g(t_m, S_{t_m})$ and continue with $j-1$ rights, resulting in the value $g(t_m, S_{t_m}) + c^{j-1}(t_m, S_{t_m})$.
- Not exercising the option and continue with j rights, resulting in the value $c^j(t_m, S_{t_m})$.

The holder will make the choice that gives the highest value. Therefore, the value of the option at time t_m for $m \in \{M-j, \dots, 1\}$ with j rights left is defined as follows:

$$v^j(t_m, S_{t_m}) = \max(g(t_m, S_{t_m}) + c^{j-1}(t_m, S_{t_m}), c^j(t_m, S_{t_m})), \quad \forall j \in \mathcal{R}. \quad (3.9)$$

By combining the two setting described above we can compute all the continuation values at all exercise moments for any number of exercise rights left backward in time. Note that, just like the Bermudan option, the option with multiple early-exercise rights at initial time t_0 cannot be exercised, so the value is equal to the continuation value at time t_0 . Summarizing, the backward induction algorithm to value the Bermudan option with R early-exercise rights at initial time t_0 is given by:

$$\begin{cases} c^0(t_m, S_{t_m}) & = 0, \quad \forall m, \\ v^j(t_{M-j+1}, S_{t_{M-j+1}}) & = g(t_{M-j+1}, S_{t_{M-j+1}}) + c^{j-1}(t_{M-j+1}, S_{t_{M-j+1}}), \quad \forall j \in \mathcal{R}, \\ v^j(t_m, S_{t_m}) & = \max(g(t_m, S_{t_m}) + c^{j-1}(t_m, S_{t_m}), c^j(t_m, S_{t_m})), \\ & \quad \forall j \text{ and } m \in \{M-j, \dots, 1\}, \\ c^j(t_m, S_{t_m}) & = e^{-r\Delta t} \mathbb{E}_{\mathbb{Q}}[v^j(t_{m+1}, S_{t_{m+1}}) | \mathcal{F}_{t_m}], \quad \forall j \text{ and } m \in \{M-1, \dots, 0\}, \\ v^R(t_0, S_{t_0}) & = c^R(t_0, S_{t_0}). \end{cases} \quad (3.10)$$

3.4 Electricity storage contracts

To acquire an electricity storage contract we alter the Bermudan option with multiple early-exercise rights. Similar to the Bermudan option with multiple early-exercise rights the holder of the electricity storage contract has to decide which action to take at every exercise moment. The actions that can be taken are withdrawing electricity from the storage, injecting electricity in the storage or doing nothing. Because the holder of the contract can make this choice at any exercise moment, it applies that there are as many early-exercise rights as exercise moments (i.e. $R = M$).

Furthermore, compared to the Bermudan option with multiple early-exercise rights there are more features to be taken into account:

1. Physical limitations of the electricity storage, e.g. capacity and endurance.
2. Efficiency of the electricity storage.
3. Restrictions to the amount of electricity that can be withdrawn and injected from the electricity grid.
4. The possibility to have negative payoff by withdrawing electricity.
5. A storage contract often includes a penalty function that is activated if the holder of the contract does not comply with the contract conditions.

These additional features make it a more complex problem than a standard Bermudan option or Bermudan option with multiple early-exercise rights. In the following two subsections an electricity storage contract with such features is defined in more detail and the backward induction algorithm for the contract valuation is given.

3.4.1 Details electricity storage contract

In this section a storage contract is defined in a similar way as in [34], where a gas storage contract is discussed, although it is adapted so that it is applicable to an electricity storage.

Similarly as with the Bermudan option with multiple early-exercise rights there are M exercise moments, where t_0 is the initial time and $\{t_1, \dots, t_M\}$ the set of exercise moments, where the time between the exercise moments is evenly distributed, $\Delta t = (t_{m+1} - t_m)$. However, the storage contract includes an extra moment t_{M+1} on which it is not possible to exercise, called the settlement date of the contract.

On the settlement date, the holder of the contract can receive a penalty if there is not the agreed amount of energy in the storage. For example, if the battery of an electric car is used for storage, there must be a certain level of energy in the battery at the end of the contract so that the car can still drive. The penalty function at the settlement date is denoted by $q_s(t_{M+1}, S_{t_{M+1}}, e(t_{M+1}))$, where the notation $e(t_m)$ represents the amount of energy left in the storage at time t_m , for all $m \in \{0, \dots, M+1\}$.

As described, the holder of the contract can take three actions: do nothing, withdraw energy or inject energy. These actions correspond to a change in energy level in the storage, denoted as $\Delta e(t_m) = e(t_{m+1}) - e(t_m)$. If nothing is done at moment t_m , the energy level does not change, $\Delta e(t_m) = 0$, withdrawing energy is taken as a negative energy change, $\Delta e(t_m) < 0$, and injecting energy as a positive energy change, $\Delta e(t_m) > 0$. By definition, at initial time t_0 the holder can not take any action and the volume change is zero, $\Delta e(t_0) := 0$.

The payoff function depends on the action taken by the holder of the contract, and is defined by:

$$g(t_m, S_{t_m}, \Delta e(t_m)) = \begin{cases} -\bar{c}(S_{t_m})\Delta e(t_m) & , \Delta e(t_m) > 0, \\ 0 & , \Delta e(t_m) = 0, \\ -\bar{p}(S_{t_m})\Delta e(t_m) & , \Delta e(t_m) < 0, \end{cases} \quad (3.11)$$

where $\bar{c}(S_{t_m})$ and $\bar{p}(S_{t_m})$ are respectively the cost of injection and the profit of withdrawing energy as a function of the electricity spot price.

This thesis includes the efficiency of the storage, e.g. an electric motor is typically between 85% and 90% efficient [10]. The efficiency of the storage will be denoted by η , which means it converts $\eta \cdot 100\%$ of the purchased electricity into electricity which can be sold. Therefore the following cost and profit functions are used:

$$\begin{aligned}\bar{c}(S_{t_m}) &= \frac{S_{t_m}}{\eta}, \\ \bar{p}(S_{t_m}) &= S_{t_m}.\end{aligned}\tag{3.12}$$

These functions imply that we have to buy $(1/\eta) > 1$ units of energy in order to sell 1 unit of energy.

There are also physical limitations to the capacity of the storage, therefore we introduce a maximum and minimum energy level for the storage, respectively e^{min} and e^{max} . The energy level of the electricity storage should satisfy for all t_m , $m \in \{0, \dots, M + 1\}$:

$$e^{min} \leq e(t_m) \leq e^{max}.\tag{3.13}$$

Furthermore, there are operational restrictions on the minimum and maximum levels of energy that can be injected and withdrawn, respectively i_{op}^{min} and i_{op}^{max} . In most markets there is also a required minimum energy injection, denoted as i_{market}^{min} . So the allowed energy level changes at an exercise moment are limited by:

$$\Delta e(t_m) \in [i_{op}^{min}, i_{market}^{min}] \cup [0, i_{op}^{max}], \quad \forall m \in \{1, \dots, M\},\tag{3.14}$$

where $i_{op}^{min} \leq i_{market}^{min} \leq 0 \leq i_{op}^{max}$.

In addition, the endurance of the storage facility should be taken into account, e.g. charging/discharging a battery too quickly has been known to reduce the battery lifetime [35]. That is why we have set an interval $[i_b^{min}, i_b^{max}]$ for energy changes in which the storage can last as long as possible. A constant penalty function is introduced in case the holder of the contract wants to make a change in the energy level that lies outside this interval. This penalty function for exercise moment t_m depends only on the action $\Delta e(t_m)$ that is taken and is denoted as $q_b(\Delta e(t_m))$.

Summarizing the storage limitations, the set of allowed actions $\Delta e(t_m)$ is limited by the capacity and the operational constraints. We define this set of all allowed actions at time t_m , for all $m \in \{1, \dots, M\}$, as follows:

$$\mathcal{A}(t_m, e(t_m)) = \{\Delta e \mid e^{min} \leq e(t_m) + \Delta e \leq e^{max} \text{ and } \Delta e \in [i_{op}^{min}, i_{market}^{min}] \cup [0, i_{op}^{max}]\},\tag{3.15}$$

and the set of allowed actions $\Delta e(t_m)$ without getting a penalty $q_b(t_m, \Delta e(t_m))$ is defined as follows:

$$\mathcal{D}(t_m, e(t_m)) = \{\Delta e \mid e^{min} \leq e(t_m) + \Delta e \leq e^{max} \text{ and } \Delta e \in [i_b^{min}, i_{market}^{min}] \cup [0, i_b^{max}]\}.\tag{3.16}$$

Note that the set of allowed actions where a penalty is handed out is given by $\mathcal{A} \setminus \mathcal{D}$.

The value of the contract at initial time t_0 is given by the discounted future payoff and penalties, where the holder of the contract chooses the optimal allowed action at each exercise moment. Thus the following pricing problem is considered:

$$v(t_0, S_{t_0}) = \max_{\Delta e^*} \mathbb{E}_{\mathbb{Q}} \left[\sum_{m=1}^M e^{-rt_m} \left(g(t_m, S_{t_m}, \Delta e(t_m)) + q_b(\Delta e(t_m)) \right) + e^{-rt_{M+1}} q_s(t_{M+1}, S_{t_{M+1}}, e(t_{M+1})) \right], \quad (3.17)$$

where \mathbb{Q} is the risk-neutral pricing measure, r the risk-neutral interest rate and the optimal actions are given by the set $\Delta e^* = \{\Delta e^*(t_1), \dots, \Delta e^*(t_M)\}$.

In Table 1 the characteristics of the electricity storage contract are described.

Start date	t_0
Number of exercise moments	M
Time to maturity	T
Time between exercise moments	$\Delta t = \frac{T}{M}$
Settlement date	t_{M+1}
Start energy level	$e(t_0)$
Min. capacity	e^{min}
Max. capacity	e^{max}
Min. energy level change	$i_{op}^{min} \leq 0$
Max. energy level change	$i_{op}^{max} \geq 0$
Required min. injection in market	i_{market}^{min}
Min. energy level change without penalty	$i_b^{min} \leq 0$
Max. energy level change without penalty	$i_b^{max} \geq 0$
Penalty of charging/discharging too rapidly	$q_b(\Delta e)$
Penalty at settlement date	$q_s(e)$
The efficiency of the storage	η

Table 1: The electricity storage contract characteristics

3.4.2 The contracts backward induction pricing algorithm

This section shows how the electricity storage contract, with the details described in Section 3.4.1, can be priced with a backward induction algorithm.

First, the total electricity storage capacity is discretized into N_e equally distributed energy levels, with $\delta := (e^{max} - e^{min})/N_e$ the energy between two consecutive energy levels. This results in the set $E := \{e^{min}, e^{min} + \delta, e^{min} + 2\delta, \dots, e^{max}\}$ of all the possible energy levels that the storage can have. It is assumed that the action $\Delta e(t_m)$ at any exercise moment t_m is a multiple of δ .

Furthermore, the pricing algorithm is computed backward in time and it is not known which energy levels will be visited beforehand. Therefore, the contract values need to be computed for all the possible energy levels $e \in E$. So the notation of the contract value at each exercise moment needs to be extended by the level of energy in storage at that

time. The contract value at time t_m with $e(t_m)$ energy in storage and the electricity price S_{t_m} is denoted by $v(t_m, S_{t_m}, e(t_m))$. Note that the number of early-exercise rights does not need to be kept track of, as with the Bermudan option with multiple early-exercise rights, because the holder can exercise at any exercise moment.

On the settlement date t_{M+1} it is not possible for the holder to change the energy level in the storage. However, if there is not the agreed amount of energy left in the storage the holder of the contract will receive a penalty. Therefore, the value of the contract at time t_{M+1} is equal to the penalty function:

$$v(t_{M+1}, S_{t_{M+1}}, e) = q_s(t_{M+1}, S_{t_{M+1}}, e), \quad \forall e \in E \quad (3.18)$$

At all the exercise moments t_m , $m \in \{M, \dots, 1\}$, before the settlement date the holder of the contract can choose an action $\Delta e(t_m) \in \mathcal{A}$. The holder will choose the action that ultimately gives him/her the highest value. To make this decision, continuation values are needed to show what the expected value is after choosing a specific action. So the continuation value depends on the energy level in storage after the action is taken, $e(t_m) + \Delta e(t_m) = e(t_{m+1})$. Therefore the continuation value is denoted by:

$$c(t_m, S_{t_m}, e(t_m) + \Delta e(t_m)) = c(t_m, S_{t_m}, e(t_{m+1})) \quad (3.19)$$

Note that this makes it possible that at time t_m the continuation value can be the same for different levels of energy in storage, by choosing certain actions. As an example, the situation with energy level $e(t_m) = 2$ and action $\Delta e(t_m) = 1$ results in the same continuation value as the situation with energy level $e(t_m) = 4$ and action $\Delta e(t_m) = -1$, assuming that $\Delta e(t_m) \in \mathcal{A}$. These situations result in the same continuation value due to the fact that they have the same energy level at time t_{m+1} .

Therefore, the continuation value does not have to be determined for every energy level $e(t_m)$ and all its corresponding allowed actions $\Delta e(t_m) \in \mathcal{A}$, but only for the possible energy levels in the set E . The continuation value, for all the possible energy levels $e \in E$, can be computed with the risk-neutral valuation formula, similar as with the Bermudan option with multiple early-exercise rights:

$$c(t_m, S_{t_m}, e) = e^{-r\Delta t} \mathbb{E}_{\mathbb{Q}}[v(t_{m+1}, S_{t_{m+1}}, e) | \mathcal{F}_{t_m}], \quad \forall e \in E. \quad (3.20)$$

Now that the continuation function has been defined, the value of the contract can be given. The holder of the contract at time t_m with $e \in E$ electricity in storage and electricity price S_{t_m} chooses the action $\Delta e \in \mathcal{A}(t_m, e)$ that gives him/her the highest value, taking into account the penalty function. This results in the following contract value at time t_m :

$$v(t_m, S_{t_m}, e) = \max_{\Delta e \in \mathcal{A}(t_m, e(t_m))} \left\{ g(t_m, S_{t_m}, \Delta e) + c(t_m, S_{t_m}, e + \Delta e) + q_b(\Delta e) \right\}, \quad \forall e \in E. \quad (3.21)$$

The value of the contract at initial time t_0 is equal to the continuation value, similar as with the Bermudan option with multiple early-exercise rights, because no actions can be taken at this time:

$$v(t_0, S_{t_0}, e(t_0)) = c(t_0, S_{t_0}, e(t_0)) = e^{-r\Delta t} \mathbb{E}_{\mathbb{Q}}[v(t_1, S_{t_1}, e(t_0)) | \mathcal{F}_{t_0}]. \quad (3.22)$$

Now we have all the building blocks to determine the contract value backward in time. This is summarized in the following backward induction algorithm:

$$\left\{ \begin{array}{ll} v(t_{M+1}, S_{t_{M+1}}, e) & = q_s(t_{M+1}, S_{t_{M+1}}, e), \quad \forall e \in E, \\ c(t_m, S_{t_m}, e) & = e^{-r\Delta t} \mathbb{E}_{\mathbb{Q}}[v(t_{m+1}, S_{t_{m+1}}, e) | \mathcal{F}_{t_m}], \quad \forall e \in E \text{ and } m \in \{M, \dots, 0\}, \\ v(t_m, S_{t_m}, e) & = \max_{\Delta e \in \mathcal{A}} \left\{ g(t_m, S_{t_m}, \Delta e) \right. \\ & \quad \left. + c(t_m, S_{t_m}, e + \Delta e) \right. \\ & \quad \left. + q_b(\Delta e) \right\}, \quad \forall e \in E \text{ and } m \in \{M, \dots, 1\}, \\ v(t_0, S_{t_0}, e) & = c(t_0, S_{t_0}, e), \quad \forall e \in E. \end{array} \right. \quad (3.23)$$

3.5 Option and contract valuation

As shown in the descriptions of the options and the electricity contract, option/contract pricing usually comes down to computing the conditional expectation of the discounted value of the financial derivative under the risk-neutral measure, the so-called risk-neutral valuation formula.

There are several ways to compute this conditional expectation. Ideally there is an analytical solution, however this is generally only the case with the simplest option types (European options) with the most basic asset price dynamics (e.g. the dynamics assumed with the Black-Scholes equation). Alternatively, we can apply numerical techniques to approximate the conditional expectation for the derivation of the option value. Commonly used numerical techniques for this are numerical integration and Monte Carlo methods. A comparison for various numerical techniques is made in [36], where Fourier-based integration techniques have performed as one of the best for pricing many options.

Furthermore, in financial mathematics it is an important branch of research to price options as quickly and/or accurately as possible. For calibration of a model the speed of the computation is most essential, while for pricing a specific derivative contract the accuracy and robustness is crucial [37].

In this thesis we introduce valuation techniques to price various options and the electricity storage contract, which are defined in this section, where the electricity price process follows the polynomial model. In particular we focus on a Fourier-based method known as the COS method. Additionally, the Least Squares Monte Carlo (LSMC) method is used to validate the results obtained with the COS method.

3.5.1 Greeks

In addition to the option value, there is also relevant information in the so-called Greeks (also called hedge parameters or risk sensitivities). These Greeks are quantities that measure the sensitivity of the option value with respect to a change in the underlying parameters, e.g. the asset price S or the volatility σ .

The Greeks are defined as follows, respectively Delta, Gamma and Vega:

$$\Delta := \frac{\partial v}{\partial S}, \quad \Gamma := \frac{\partial^2 v}{\partial S^2} = \frac{\partial \Delta}{\partial S}, \quad \nu := \frac{\partial v}{\partial \sigma}. \quad (3.24)$$

3.6 Risk-neutral measure

In risk and portfolio management, where asset movements are uncertain, the probability space $(\Omega, \mathcal{F}, \mathbb{P})$ is considered, where Ω denotes the sample space of all scenarios, \mathcal{F} the σ -algebra on Ω and \mathbb{P} the probability measure that assigns a probability to every event $\omega \in \Omega$. The probability measure \mathbb{P} is called the real world measure.

However, when pricing derivatives another measure is used, namely the risk-neutral measure \mathbb{Q} (also called martingale measure). Under the risk-neutral measure \mathbb{Q} the discounted prices of assets are martingales, which is not assured under the real world measure \mathbb{P} , i.e.

$$\mathbb{E}_{\mathbb{Q}}[e^{-r(T-t)}S_T|\mathcal{F}_t] = S_t,$$

where $\mathcal{F}_t \subset \mathcal{F}$ is the natural filtration on (Ω, \mathcal{F}) and S_t the price of an asset at time t .

The fundamental theorems of asset pricing (FTAPs) give conditions for a market to be free of arbitrage and to be complete. The first FTAP states that a market is arbitrage free if and only if there exists a risk-neutral probability measure, equivalent¹ to the real world measure. The second FTAP states that an arbitrage-free market is complete, that is that every risky derivative can be hedged, if and only if there exists a unique risk-neutral measure that is equivalent to the real world measure.

3.6.1 Risk-neutral measure for the electricity market

As described in the second FTAP, in complete markets the risk-neutral pricing measure is unique, ensuring only one arbitrage-free price of the option/storage contract. Furthermore, in a complete market the risk can be removed to a large extent by a trading strategy, called delta hedging. By means of delta hedging, the drift has no influence on the pricing of options. In contrast to a complete market, an incomplete market has many different risk-neutral measures and there does not exist such a property to hedge the risk.

The electricity market is a typical example of an incomplete market, due to its characteristics, therefore the risk-neutral measure is not unique. In the literature there are different ways to deal with this incompleteness. It is possible to obtain a risk-neutral probability measure \mathbb{Q} with the Esscher transform, which is often used in derivative pricing for incomplete markets. Another commonly used approach is to assume that the measure is already risk-neutral, and directly perform the pricing. This latter approach calibrates the model through implied parameters from a liquid market, however the electricity market is illiquid.

In this thesis we follow another common approach (see e.g. [17] [34] [38]), it is assumed there exists a risk premium to compensate for the risk. The risk premium, defined by $\lambda\sigma(t, X_t)$, is subtracted from the real drift of the process, where λ is the market price per unit risk linked to the state variable X_t and $\sigma(t, X_t)$ the volatility parameter of the process. This risk premium, calibrated from observed market data, determines the choice of one specific risk-neutral measure.

Next, we show how to use the risk premium for the OU process and the second-order polynomial model.

¹Given a space (Ω, \mathcal{F}) , two measure are equivalent on (Ω, \mathcal{F}) if they agree on which sets in \mathcal{F} have probability zero.

Ornstein-Uhlenbeck process

Consider the OU process, described in Appendix A.2:

$$dX_t = \kappa(\theta - X_t)dt + \sigma dW_t. \quad (3.25)$$

Let the risk premium, $\lambda\sigma(t, X_t)$, be subtracted from the drift term of the process, the drift of the OU process is $\mu(t, X_t) = \kappa(\theta - X_t)$. This results in the following adjusted drift term:

$$\hat{\mu}(t, X_t) = \kappa \left(\theta - \frac{\lambda\sigma}{\kappa} - X_t \right).$$

Moreover, through the Radon-Nikodym derivative and the Girsanov theorem, the following measure change is considered:

$$dW_t = dW_t^* - \lambda dt,$$

and equivalently:

$$W_t = W_t^* - \lambda t,$$

where W_t^* is the Brownian motion under the risk-neutral measure \mathbb{Q} .

Under the measure change the stochastic process (3.25) can be rewritten as:

$$dX_t = \kappa \left(\theta - \frac{\lambda\sigma}{\kappa} - X_t \right) dt + \sigma dW_t^*. \quad (3.26)$$

Second-order polynomial model

The second-order polynomial model is defined by choosing the parameters $K = 1$ and $\alpha_1 = 0$ in the increasing polynomial map (2.9). These parameters result in the following second-order polynomial model:

$$S_t = \Phi(X_t) = \int_0^{X_t} (1-c)u + c \, du = CX_t^2 + cX_t, \quad (3.27)$$

where $C := \frac{1-c}{2}$ and the underlying process X_t has the following general dynamics:

$$dX_t = \mu(t, X_t)dt + \sigma(t, X_t)dW_t.$$

With Ito's lemma the following SDE is obtained, using (3.27):

$$dS_t = (2CX_t + c)dX_t + 2C(dX_t)^2.$$

Note that $(dX_t)^2 = \sigma(t, X_t)^2 dt$. Therefore, by substitution of dX_t and simplification, the SDE is given by:

$$\begin{aligned} dS_t &= (\mu(t, X_t)(2CX_t + c) + 2C\sigma(t, X_t)^2) dt + \sigma(t, X_t)(2CX_t + c)dW_t \\ &= \tilde{\mu}(t, X_t)dt + \tilde{\sigma}(t, X_t)dW_t. \end{aligned} \quad (3.28)$$

By subtracting the risk premium, $\lambda\tilde{\sigma}(t, X_t)$, from the drift term of the process and changing the measure with the Girsanov theorem, the SDE (3.28) can be rewritten as:

$$dS_t = (\tilde{\mu}(t, X_t) - \lambda\tilde{\sigma}(t, X_t)) dt + \tilde{\sigma}(t, X_t)dW_t^*, \quad (3.29)$$

where dW_t^* is the risk-neutral Brownian motion increment and the drift and volatility parameters are defined as follows:

$$\begin{aligned} \tilde{\mu}(t, X_t) &= \mu(t, X_t)(2CX_t + c) + 2C\sigma(t, X_t)^2, \\ \tilde{\sigma}(t, X_t) &= \sigma(t, X_t)(2CX_t + c). \end{aligned} \quad (3.30)$$

4 The COS method

The COS method is a pricing method, introduced by Fang and Oosterlee [39], which approximates the risk-neutral valuation formula. The risk-neutral valuation formula can be written as an integral representation, where v denotes the option value, x the state variable at time t and y at time T :

$$v(t, x) = e^{-r\Delta t} \mathbb{E}_{\mathbb{Q}}[v(T, y) | \mathcal{F}_t] = e^{-r\Delta t} \int_{-\infty}^{\infty} v(T, y) f(y|T, t, x) dy. \quad (4.1)$$

Furthermore, besides the accurate approximation of the option value, the COS method can compute the Greeks at almost no extra computational costs.

The main idea of the COS method is to approximate the conditional probability density function, $f(y|T, t, x)$, via the Fourier cosine expansion (also called cosine expansion). Moreover, the COS method makes use of the relation between the coefficients of the Fourier cosine expansion and the characteristic function. The use of the characteristic function is convenient, because the density function is often unknown for relevant asset processes, in contrast to the characteristic function. For processes with affine dynamics, the characteristic function can be derived by solving the Riccati differential equations [40]. However, affinity is not invariant under polynomial transformations [41] and therefore the characteristic function of the polynomial model, $S_t = \Phi(X_t)$, generally does not exist.

So the characteristic function does not exist in closed-form for every pricing model, e.g. the characteristic function of the polynomial model $S_t = \Phi(X_t)$ is not available. However, by choosing the state variables in equation (4.1) conveniently, the characteristic function of the underlying process X_t can be used. Furthermore, if the characteristic function has a certain form, an efficient fast Fourier transform (FFT) based algorithm can be applied to significantly reduce the computational complexity of calculating the values of the Bermudan option, the Bermudan option with multiple early-exercise rights and the electricity storage contract. If the closed-form characteristic function does not have this form, the characteristic function can be approximated to establish this form, this is described in Section 5.

4.1 Density approximation via the Fourier cosine expansion

In this section the probability density function is approximated via the Fourier cosine expansion. This approximation makes use of the closed-form relation between the density and the characteristic function. The characteristic function is given by the Fourier transform of the probability density function, whereas the density function is obtained by the inverse Fourier transform of the characteristic function. This combination is called a Fourier transform pair and is defined as follows:

Fourier transform pair

The density function $f(y|T, t, x)$ and the characteristic function $\phi(u|T, t, x)$ is an example of a Fourier pair, where x denotes the state variable at time t and y at time T :

$$\phi(u|T, t, x) = \int_{-\infty}^{\infty} e^{iuy} f(y|T, t, x) dy, \quad (4.2)$$

and

$$f(y|T, t, x) = \frac{1}{2\pi} \int_{-\infty}^{\infty} e^{-iuy} \phi(u|T, t, x) du. \quad (4.3)$$

Consider a function $f(\theta)$, supported on the interval $[0, \pi]$. The Fourier cosine expansion for this function is defined by:

$$f(\theta) = \sum'_{k=0}^{\infty} A_k \cos(k\theta), \quad (4.4)$$

where \sum' implies that the first term of the summation is multiplied by $\frac{1}{2}$ and the coefficients A_k are given by:

$$A_k = \frac{2}{\pi} \int_0^{\pi} f(\theta) \cos(k\theta) d\theta. \quad (4.5)$$

For functions supported on a finite interval $[a, b] \in \mathbb{R}$, the Fourier cosine expansion can be obtained by a change of variables:

$$\theta = \frac{y-a}{b-a} \pi, \quad y = \frac{b-a}{\pi} \theta + a.$$

By changing the variables the Fourier cosine expansion is as follows:

$$f(y) = \sum'_{k=0}^{\infty} A_k \cos\left(k\pi \frac{y-a}{b-a}\right), \quad (4.6)$$

where the coefficients are given by:

$$A_k = \frac{2}{b-a} \int_a^b f(y) \cos\left(k\pi \frac{y-a}{b-a}\right) dy. \quad (4.7)$$

The Fourier cosine expansion of the conditional density function $f(y|T, t, x)$ (4.3) is similar. Next the Fourier cosine expansion of $f(y|T, t, x)$ will be rewritten such that the characteristic function is used instead of the density function.

Firstly we notice that the characteristic function (4.2) can be approximated by truncating the integral range, this is possible due to the conditions for the existence of a Fourier transform and the fact that the density function $f(y|T, t, x)$ has no mass in the tails. Assume that the integration range $[a, b]$ is chosen such that the characteristic function (4.2) can be approximated adequately. This results in the following approximation:

$$\phi(u|T, t, x) \approx \hat{\phi}(u|T, t, x) = \int_a^b e^{iuy} f(y|T, t, x) dy. \quad (4.8)$$

Secondly it is noticed that A_k (4.7) can be rewritten to use the truncated characteristic function instead of the density function. For this derivation the Euler formula is used:

$$e^{iu} = \cos(u) + i \sin(u),$$

which shows that $\operatorname{Re}\{e^{iu}\} = \cos(u)$. Therefore the coefficients A_k of the Fourier cosine expansion of $f(y|T, t, x)$ can be rewritten as:

$$\begin{aligned} A_k &= \frac{2}{b-a} \int_a^b f(y|T, t, x) \cdot \cos\left(k\pi \frac{y-a}{b-a}\right) dy \\ &= \frac{2}{b-a} \int_a^b f(y|T, t, x) \cdot \operatorname{Re}\left\{e^{ik\pi \frac{y-a}{b-a}}\right\} dy \\ &= \frac{2}{b-a} \operatorname{Re}\left\{\int_a^b f(y|T, t, x) \cdot e^{ik\pi \frac{y-a}{b-a}} dy \cdot e^{-ik\pi \frac{a}{b-a}}\right\} \\ &= \frac{2}{b-a} \operatorname{Re}\left\{\hat{\phi}\left(\frac{k\pi}{b-a} \middle| T, t, x\right) \cdot e^{ik\pi \frac{-a}{b-a}}\right\}. \end{aligned} \quad (4.9)$$

By using (4.8) the coefficients A_k can be approximated by \hat{A}_k :

$$A_k \approx \hat{A}_k = \frac{2}{b-a} \operatorname{Re}\left\{\phi\left(\frac{k\pi}{b-a} \middle| T, t, x\right) \cdot e^{ik\pi \frac{-a}{b-a}}\right\}. \quad (4.10)$$

Summarizing, the Fourier cosine series expansion of $f(y|T, t, x)$ supported on the interval $[a, b] \in \mathbb{R}$ can be written as (4.6):

$$f(y|T, t, x) = \sum_{k=0}^{\infty}{}' A_k \cos\left(k\pi \frac{y-a}{b-a}\right), \quad (4.11)$$

where the coefficients A_k are described as in (4.7):

$$A_k = \frac{2}{b-a} \int_a^b f(y|T, t, x) \cos\left(k\pi \frac{y-a}{b-a}\right) dy. \quad (4.12)$$

By truncating the series summation and replacing the coefficients A_k by its approximation (4.10), the following approximation of the conditional density function is obtained:

$$f(y|T, t, x) \approx \frac{2}{b-a} \sum_{k=0}^{N-1}{}' \operatorname{Re}\left\{\phi\left(\frac{k\pi}{b-a} \middle| T, t, x\right) \cdot e^{-ik\pi \frac{a}{b-a}}\right\} \cos\left(k\pi \frac{y-a}{b-a}\right). \quad (4.13)$$

4.2 The characteristic function

In section 4.1 the characteristic function is defined, i.e. the Fourier transform of the density:

$$\phi(u|x, \Delta t) = \mathbb{E}[e^{iuy}|x] = \int_{-\infty}^{\infty} e^{iuy} f(y|T, t, x) dy, \quad (4.14)$$

where $\Delta t = T - t$.

For a large group of pricing models, including the models with available characteristic functions used in this thesis, the characteristic function can be written in the following form:

$$\phi(u|x, \Delta t) = e^{iu\beta x} \phi(u|\Delta t), \quad (4.15)$$

where $\phi(u|\Delta t)$ does not depend on x . For processes with independent and stationary increments, e.g. exponential Lévy processes, it holds that $\beta = 1$. For the OU process it holds that $\beta = e^{-\kappa\Delta t}$. In the sequel this form (4.15) will be used to describe the general characteristic function.

For processes where $\beta = 1$, an efficient FFT-based algorithm can be used to reduce the computational complexity of the calculation of the continuation values used in the pricing of options with the COS method [42], this is further explained in Remark 4.3.

It is not the case that the closed-form characteristic function can be determined for any process. However, for processes with affine dynamics (e.g. GBM, exponential Lévy processes, the OU process) the characteristic function exists [40], it can be obtained by solving the Ricatti differential equations. Affinity is not invariant under polynomial transformations [41], therefore generally the characteristic function of the polynomial model is not available.

In Section 5, we introduce approximations of the characteristic function, which can be used for the efficient FFT-based algorithm. Furthermore, the characteristic function of the process does not have to exist for these approximations.

4.3 The COS method for European options

As described in Section 3.1, the value of a European option is given by the risk-neutral valuation formula. This risk-neutral valuation formula can be written in the integral form defined in (4.1).

By truncation of the infinite integration range to $[a, b] \in \mathbb{R}$ in the integral form of (3.2), similar as for the integral in (4.8), the European option value v can be approximated by:

$$v(t_0, x) = e^{-r\Delta t} \mathbb{E}_{\mathbb{Q}}[v(T, y)|\mathcal{F}_{t_0}] \approx e^{-r\Delta t} \int_a^b v(T, y) f(y|T, t_0, x) dy, \quad (4.16)$$

where the state variables x and y can be any function of respectively the asset prices S_{t_0} and S_T , e.g. $x = \Phi^{-1}(S_{t_0}) = X_{t_0}$ or $x = S_{t_0}$.

The COS method for pricing European options is obtained by replacing the conditional density function $f(y|T, t_0, x)$ by its Fourier cosine expansion approximation (4.13). This results in the following approximation for the option value:

$$v(t_0, x) \approx e^{-r\Delta t} \int_a^b v(T, y) \sum_{k=0}^{N-1} \frac{2}{b-a} \operatorname{Re} \left\{ \phi \left(\frac{k\pi}{b-a} \middle| T, t_0, x \right) e^{ik\pi \frac{-a}{b-a}} \right\} \cos \left(k\pi \frac{y-a}{b-a} \right) dy. \quad (4.17)$$

By interchanging the integral and the summation the following formula is obtained, the so-called COS formula:

$$v(t_0, x) \approx e^{-r\Delta t} \sum_{k=0}^{N-1} \operatorname{Re} \left\{ \phi \left(\frac{k\pi}{b-a} \middle| T, t_0, x \right) e^{ik\pi \frac{-a}{b-a}} \right\} V_k, \quad (4.18)$$

where coefficients V_k are defined by:

$$V_k = \frac{2}{b-a} \int_a^b v(T, y) \cos\left(k\pi \frac{y-a}{b-a}\right) dy. \quad (4.19)$$

The closed-form solution of the coefficients V_k is available for several choices of the state variables x and y , see Section 4.3.1.

4.3.1 The coefficients V_k

In this subsection the closed-form solutions of the coefficients V_k (4.19) for the European option are computed. The variable to be integrated in equation (4.19) depends on the state variables x and y chosen in equation (4.16) and thus subsequently on which characteristic function is taken in the COS formula (4.18). For example, when the characteristic function of the price process S_t generated with the polynomial model $S_t = \Phi(X_t)$ is used, the variable $y = S_T$ is integrated. However, if the characteristic function of the underlying process X_t is used, the variable $y = \Phi^{-1}(S_T) = X_T$ is integrated in equation (4.19). Note that when integrating over the underlying process, the payoff function must be written in terms of the underlying process.

In general, the characteristic function of the price process generated with the polynomial model is not available, however it is possible that the characteristic function of the underlying process does exist. Furthermore, many frequently used asset processes, such as the GBM and the one-factor model by Schwartz, have a log-normal distribution. The characteristic function of such processes is unknown, which is why the available characteristic function of the log-adjusted process is typically used.

The payoff function, defined for a European option in (3.1), must represent the variable of the process used for the characteristic function. In this subsection two different state variables are examined for the computation of the coefficients V_k , for the asset price $y = S_T$ and for the log-adjusted asset price $y = \log(S_T/K)$. In the next subsection the coefficients V_k are computed for the payoff function which represents the underlying process of the polynomial model, $y = \Phi^{-1}(S_T) = X_T$.

For the calculations of the coefficients V_k we look at a generalized form on the interval $[x_1, x_2] \subseteq [a, b]$, so that the computations can also be used for the COS method of the other options and the electricity storage contract. This generalized coefficient will be denoted as $G_k(x_1, x_2)$:

$$G_k(x_1, x_2) = \frac{2}{b-a} \int_{x_1}^{x_2} v(T, y) \cos\left(k\pi \frac{y-a}{b-a}\right) dy. \quad (4.20)$$

Note that $V_k = G_k(a, b)$.

1. The coefficients V_k for the state variable $y = S_T$.

The variable S_T in the payoff function can be directly integrated, if the characteristic function of the price process itself is used. This results in the following option value at maturity time T , where $y = S_T$ is the asset process at time T :

$$v(T, y) = g(T, y) = \begin{cases} \max(y - K, 0), & \text{for a call,} \\ \max(K - y, 0), & \text{for a put.} \end{cases} \quad (4.21)$$

This results in the following coefficients $G_k(x_1, x_2)$:

$$G_k(x_1, x_2) = \begin{cases} \frac{2}{b-a} \int_{x_1}^{x_2} \mathbb{I}_{(y>K)}(y-K) \cos\left(k\pi \frac{y-a}{b-a}\right) dy, & \text{for a call,} \\ \frac{2}{b-a} \int_{x_1}^{x_2} \mathbb{I}_{(y<K)}(K-y) \cos\left(k\pi \frac{y-a}{b-a}\right) dy, & \text{for a put.} \end{cases} \quad (4.22)$$

where $V_k = G_k(a, b)$ and \mathbb{I} is the indicator function.

After integration and simplifying the notation, the following coefficients for the call and put options are obtained:

- For $k = 0$

$$G_0^{call}(x_1, x_2) = \begin{cases} \frac{2}{b-a} \left[Ky - \frac{y^2}{2} \right]_{x_1}^{x_2}, & \text{for } K < x_1, \\ \frac{2}{b-a} \left[Ky - \frac{y^2}{2} \right]_K^{x_2}, & \text{for } x_1 \leq K \leq x_2, \\ 0 & \text{for } K > x_2. \end{cases} \quad (4.23)$$

$$G_0^{put}(x_1, x_2) = \begin{cases} 0 & \text{for } K < x_1, \\ \frac{2}{b-a} \left[\frac{y^2}{2} - Ky \right]_{x_1}^K, & \text{for } x_1 \leq K \leq x_2, \\ \frac{2}{b-a} \left[\frac{y^2}{2} - Ky \right]_{x_1}^{x_2}, & \text{for } K > x_2. \end{cases} \quad (4.24)$$

- For $k > 0$

$$G_k^{call}(x_1, x_2) = \begin{cases} \left[\frac{-2\left((a-b) \cos\left(k\pi \frac{a-y}{a-b}\right) + k\pi(y-K) \sin\left(k\pi \frac{y-a}{a-b}\right)\right)}{k^2\pi^2} \right]_{x_1}^{x_2}, & \text{for } K < x_1, \\ \left[\frac{-2\left((a-b) \cos\left(k\pi \frac{a-y}{a-b}\right) + k\pi(y-K) \sin\left(k\pi \frac{y-a}{a-b}\right)\right)}{k^2\pi^2} \right]_K^{x_2}, & \text{for } x_1 \leq K \leq x_2, \\ 0 & \text{for } K > x_2. \end{cases} \quad (4.25)$$

$$G_k^{put}(x_1, x_2) = \begin{cases} 0 & \text{for } K < x_1, \\ \left[\frac{2\left((a-b) \cos\left(k\pi \frac{a-y}{a-b}\right) + k\pi(y-K) \sin\left(k\pi \frac{y-a}{a-b}\right)\right)}{k^2\pi^2} \right]_{x_1}^K, & \text{for } x_1 \leq K \leq x_2, \\ \left[\frac{2\left((a-b) \cos\left(k\pi \frac{a-y}{a-b}\right) + k\pi(y-K) \sin\left(k\pi \frac{y-a}{a-b}\right)\right)}{k^2\pi^2} \right]_{x_1}^{x_2}, & \text{for } K > x_2. \end{cases} \quad (4.26)$$

2. The coefficients V_k for the state variable $y = \log(S_T/K)$.

The log-adjusted process is typically used for the GBM and the one-factor model by Schwartz, because for these models the characteristic function of the log-adjusted process is known in closed-form. The log-adjusted process results in the following payoff at maturity time T , where $y = \log(S_T/K)$:

$$v(T, y) = g(T, y) = \begin{cases} \max(Ke^y - K, 0), & \text{for a call,} \\ \max(K - Ke^y, 0), & \text{for a put.} \end{cases} \quad (4.27)$$

By substitution of (4.27) in (4.20) the coefficients $G_k(x_1, x_2)$ can be computed as follows:

$$G_k(x_1, x_2) = \begin{cases} \frac{2}{b-a} \int_{x_1}^{x_2} \mathbb{I}_{(y>0)} (Ke^y - K) \cos\left(k\pi \frac{y-a}{b-a}\right) dy, & \text{for a call,} \\ \frac{2}{b-a} \int_{x_1}^{x_2} \mathbb{I}_{(y<0)} (Ke^y - K) \cos\left(k\pi \frac{y-a}{b-a}\right) dy, & \text{for a put.} \end{cases} \quad (4.28)$$

This results in the following coefficients for a call, with $x_1 \geq 0$, and a put, with $x_2 \leq 0$, where the notation of Section 3.1 of [39] is used:

$$G_k(x_1, x_2) = \begin{cases} \frac{2}{b-a} K (\chi_k(x_1, x_2) - \psi_k(x_1, x_2)), & \text{for a call,} \\ \frac{2}{b-a} K (-\chi_k(x_1, x_2) + \psi_k(x_1, x_2)), & \text{for a put,} \end{cases} \quad (4.29)$$

where $\chi_k(x_1, x_2)$ and $\psi(x_1, x_2)$ are defined by:

$$\begin{aligned} \chi_k(x_1, x_2) &:= \int_{x_1}^{x_2} e^y \cos\left(k\pi \frac{y-a}{b-a}\right) dy \\ &= \frac{1}{1 + \left(\frac{k\pi}{b-a}\right)^2} \left[\cos\left(k\pi \frac{x_2-a}{b-a}\right) e^{x_2} - \cos\left(k\pi \frac{x_1-a}{b-a}\right) e^{x_1} \right. \\ &\quad \left. + \frac{k\pi}{b-a} \sin\left(k\pi \frac{x_2-a}{b-a}\right) e^{x_2} - \frac{k\pi}{b-a} \sin\left(k\pi \frac{x_1-a}{b-a}\right) e^{x_1} \right], \end{aligned} \quad (4.30)$$

$$\psi_k(x_1, x_2) := \begin{cases} \left[\sin\left(k\pi \frac{x_2-a}{b-a}\right) - \sin\left(k\pi \frac{x_1-a}{b-a}\right) \right], & k \neq 0, \\ x_2 - x_1, & k = 0. \end{cases}$$

The Fourier coefficients V_k for the European option are given by [39]:

$$V_k = \begin{cases} G_k(0, b), & \text{for a call,} \\ G_k(a, 0), & \text{for a put.} \end{cases} \quad (4.31)$$

4.3.2 The coefficients V_k for the polynomial model $S_t = \Phi(X_t)$

As mentioned before, the characteristic function of the polynomial model is not available. However, the COS method can use the characteristic function of the underlying process X_t to compute the option value. This results in the following payoff function used in the coefficients V_k (4.19), where $y = \Phi^{-1}(S_T) = X_T$ is the underlying asset value at time T :

$$v(T, y) = g(T, y) = \begin{cases} \max(\Phi(y) - K, 0), & \text{for a call,} \\ \max(K - \Phi(y), 0), & \text{for a put.} \end{cases} \quad (4.32)$$

By substitution of the payoff function (4.32) in (4.20) the coefficients $G(x_1, x_2)$ can be computed as follows:

$$G_k(x_1, x_2) = \begin{cases} \frac{2}{b-a} \int_{x_1}^{x_2} \mathbb{I}_{(\Phi(y) > K)} (\Phi(y) - K) \cos\left(k\pi \frac{y-a}{b-a}\right) dy, & \text{for a call,} \\ \frac{2}{b-a} \int_{x_1}^{x_2} \mathbb{I}_{(\Phi(y) < K)} (K - \Phi(y)) \cos\left(k\pi \frac{y-a}{b-a}\right) dy, & \text{for a put,} \end{cases} \quad (4.33)$$

where $V_k = G_k(a, b)$.

The coefficients $G_k(x_1, x_2)$ in (4.33) can be computed analytically for any finite-order polynomial map $\Phi(\cdot)$ if the inverse $\Phi^{-1}(K)$ exists. However, if this inverse is not available in closed-form, the coefficients can still be determined by using a numerical approximation of $\Phi^{-1}(K)$.

Example 4.1. In this example the coefficients $G_k(x_1, x_2)$ are computed for a European put option where the asset prices follow a second-order polynomial process:

$$S_t = \Phi(X_t) = \frac{1-c}{2} X_t^2 + cX_t = CX_t^2 + cX_t. \quad (4.34)$$

The coefficients $G_k(x_1, x_2)$ for the put option are calculated as follows:

$$G_k^{put}(x_1, x_2) = \frac{2}{b-a} \int_{x_1}^{x_2} \mathbb{I}_{(\Phi(y) < K)} (K - \Phi(y)) \cos\left(k\pi \frac{y-a}{b-a}\right) dy. \quad (4.35)$$

This leads to the following coefficients $G_k(x_1, x_2)$ for the put option:

$$G_k^{put}(x_1, x_2) = \begin{cases} 0 & , K < Cx_1^2 + cx_1, \\ \frac{2}{b-a} \int_{x_1}^K (K - y) \cos\left(k\pi \frac{y-a}{b-a}\right) dy & , C = 0 \text{ and } x_1 \leq K \leq x_2, \\ \frac{2}{b-a} \int_{x_1}^{\frac{\sqrt{c^2+4CK-c}}{2C}} (K - Cy^2 - cy) \cos\left(k\pi \frac{y-a}{b-a}\right) dy & , C \neq 0 \text{ and} \\ & Cx_1^2 + cx_1 \leq K \leq Cx_2^2 + cx_2, \\ \frac{2}{b-a} \int_{x_1}^{x_2} (K - Cy^2 - cy) \cos\left(k\pi \frac{y-a}{b-a}\right) dy & , K > Cx_2^2 + cx_2. \end{cases} \quad (4.36)$$

After integration the following coefficients are obtained:

- for $k = 0$:

$$G_0^{put}(x_1, x_2) = \begin{cases} 0 & , K < Cx_1^2 + cx_1, \\ \frac{2}{b-a} [Ky - \frac{1}{2}y^2]_{x_1}^K & , C = 0 \text{ and } x_1 \leq K \leq x_2, \\ \frac{2}{b-a} [Ky - \frac{c}{2}y^2 - \frac{C}{3}y^3]_{x_1}^{\frac{\sqrt{c^2+4CK-c}}{2C}} & , C \neq 0 \text{ and} \\ & Cx_1^2 + cx_1 \leq K \leq Cx_2^2 + cx_2, \\ \frac{2}{b-a} [Ky - \frac{c}{2}y^2 - \frac{C}{3}y^3]_{x_1}^{x_2} & , K > Cx_2^2 + cx_2. \end{cases} \quad (4.37)$$

- for $k > 0$:

$$G_k^{put}(x_1, x_2) = \begin{cases} 0 & , K < Cx_1^2 + cx_1, \\ \frac{2}{b-a} \left[\frac{(a-b)(\pi k(y-K) \sin(\frac{\pi k(a-y)}{a-b}) + (b-a) \cos(\frac{\pi k(y-a)}{a-b}))}{\pi^2 k^2} \right]_{x_1}^K & , C = 0 \text{ and } x_1 \leq K \leq x_2, \\ \frac{2}{b-a} \left[\begin{array}{l} -\frac{1}{\pi^3 k^3} (a-b) \left(\sin\left(\frac{\pi k(y-a)}{a-b}\right) (-2a^2C + \right. \\ \left. 4abC - 2b^2C + \pi^2 k^2 (y(c+Cy) - K)) + \right. \\ \left. \left. \pi k(a-b)(c+2Cy) \cos\left(\frac{\pi k(y-a)}{a-b}\right) \right) \right]_{x_1}^{\frac{\sqrt{c^2+4CK-c}}{2C}} & , C \neq 0 \text{ and} \\ & Cx_1^2 + cx_1 \leq K \leq Cx_2^2 + cx_2, \\ \frac{2}{b-a} \left[\begin{array}{l} -\frac{1}{\pi^3 k^3} (a-b) \left(\sin\left(\frac{\pi k(y-a)}{a-b}\right) (-2a^2C + \right. \\ \left. 4abC - 2b^2C + \pi^2 k^2 (y(c+Cy) - K)) + \right. \\ \left. \left. \pi k(a-b)(c+2Cy) \cos\left(\frac{\pi k(y-a)}{a-b}\right) \right) \right]_{x_1}^{x_2} & , K > Cx_2^2 + cx_2. \end{array} \end{cases} \quad (4.38)$$

The coefficients V_k^{put} for the European put option where the prices follow the second-order polynomial model are $V_k^{put} = G_k^{put}(a, b)$, $\forall k$.

A similar computation can be performed for the coefficients of a European call option and/or for a higher-order polynomial model.

4.4 The COS method for Bermudan options

The Bermudan option is valued backwards in time, as described in the backward induction algorithm (3.5). Moreover, the continuation values in this algorithm are defined by the risk-neutral valuation formula, and therefore can be approximated by the COS method [42].

The approximation of the continuation value can be obtained with the COS method in a similar way as for the European option value (4.18). This results in the following COS formula for the continuation value, where x denotes the state variable at time t_{m-1} and y at time t_m :

$$c(t_{m-1}, x) \approx \hat{c}(t_{m-1}, x) := e^{-r\Delta t} \sum_{k=0}^{N-1} \operatorname{Re} \left\{ \phi \left(\frac{k\pi}{b-a} \middle| \Delta t, x \right) e^{ik\pi \frac{-a}{b-a}} \right\} V_k(t_m), \quad (4.39)$$

where the coefficients $V_k(t_m)$ are defined by:

$$V_k(t_m) = \frac{2}{b-a} \int_a^b v(t_m, y) \cos \left(k\pi \frac{y-a}{b-a} \right) dy. \quad (4.40)$$

Using (4.39) and the fact that at initial time t_0 the Bermudan option value equals the continuation value, the value of the Bermudan option at time t_0 can be approximated by the following COS formula:

$$v(t_0, x) \approx \hat{c}(t_0, x) = e^{-r\Delta t} \sum_{k=0}^{N-1} \operatorname{Re} \left\{ \phi \left(\frac{k\pi}{b-a} \middle| \Delta t, x \right) e^{ik\pi \frac{-a}{b-a}} \right\} V_k(t_1). \quad (4.41)$$

Therefore, the idea of valuating the Bermudan option with the COS method is to compute the coefficient $V_k(t_1)$ and substitute this into (4.41). Next it is shown that the coefficients $V_k(t_m)$ can be recovered from $V_k(t_{m+1})$, by means of a backward induction method.

4.4.1 The coefficients $V_k(t_m)$ for Bermudan options

In this section it is shown how the coefficients $V_k(t_m)$, (4.40), for $m = \{M, \dots, 1\}$, can be computed in a backward manner. The coefficients $V_k(t_m)$ for a Bermudan option are defined as follows:

$$V_k(t_m) = \frac{2}{b-a} \int_a^b v(t_m, y) \cos \left(k\pi \frac{y-a}{b-a} \right) dy, \quad (4.42)$$

where $v(t_m, y)$, for $m = \{M, \dots, 1\}$, is given by:

$$v(t_m, y) = \begin{cases} g(t_m, y), & \text{for } m = M, \\ \max(g(t_m, y), c(t_m, y)), & \text{for } m = \{M-1, \dots, 1\}, \end{cases} \quad (4.43)$$

with the functions written in terms of state variable y .

First $V_k(t_M)$ is obtained by substituting $v(t_M, y) = g(t_M, y)$ in (4.42), resulting in the same calculation of the integral as for the European option.

For $V_k(t_m)$, $m = \{M - 1, \dots, 1\}$, the integral is split in two parts, due to the fact that the integral is taken as the maximum of the payoff function $g(t_m, y)$ and the continuation value $c(t_m, y)$. The split of the integral is based on the so-called early-exercise point x_m^* , which is the point where the continuation value equals the payoff function, i.e. $c(t_m, x_m^*) = g(t_m, x_m^*)$. The early-exercise point x_m^* can be determined by for example Newton's method, see [43] for more information about the use of Newton's method for this problem.

For a Bermudan put option it holds on the interval $y \in [a, x_m^*]$ that $g(t_m, y) \geq c(t_m, y)$ and on the interval $y \in (x_m^*, b]$ that $g(t_m, y) < c(t_m, y)$. The opposite applies for a Bermudan call option, namely that on the interval $y \in [a, x_m^*]$ that $g(t_m, y) \leq c(t_m, y)$ and on the interval $y \in (x_m^*, b]$ that $g(t_m, y) > c(t_m, y)$.

Therefore, once x_m^* is found, the integral to compute the coefficients $V_k(t_m)$, for $m \in \{M - 1, \dots, 1\}$ and $\forall k$, can be split into two parts:

$$V_k(t_m) = \begin{cases} C_k(a, x_m^*, t_m) + G_k(x_m^*, b), & \text{for a call,} \\ G_k(a, x_m^*, t_m) + C_k(x_m^*, b, t_m), & \text{for a put,} \end{cases} \quad (4.44)$$

and at maturity time t_M the coefficients are given by:

$$V_k(t_M) = \begin{cases} G_k(a, b), & \text{for a call,} \\ G_k(a, b), & \text{for a put,} \end{cases} \quad (4.45)$$

where the Fourier cosine series coefficients of the payoff function, $G_k(x_1, x_2)$, and of the continuation value, $C_k(x_1, x_2, t_m)$, are defined by:

$$G_k(x_1, x_2) = \frac{2}{b-a} \int_{x_1}^{x_2} g(t_m, y) \cos\left(k\pi \frac{y-a}{b-a}\right) dy, \quad (4.46)$$

$$C_k(x_1, x_2, t_m) = \frac{2}{b-a} \int_{x_1}^{x_2} c(t_m, y) \cos\left(k\pi \frac{y-a}{b-a}\right) dy, \quad (4.47)$$

It remains to compute $G_k(x_1, x_2)$ and $C_k(x_1, x_2, t_m)$.

The coefficients $G_k(x_1, x_2)$

The Fourier coefficients of the payoff function, $G_k(x_1, x_2)$, can be found in closed-form for several choices of state variables x and y . The integral to be calculated in (4.46) is similar to the integral used for the computation of the Fourier coefficients V_k for European options, (4.20). Therefore the same coefficients $G(x_1, x_2)$ can be used as computed in Section 4.3.1 and for the polynomial model in Section 4.3.2.

Remark 4.2. Note that in the computation of $G_k(x_1, x_2)$ for the log-adjusted process $y = \log(\frac{S_T}{K})$, described in (4.29), it must hold that $x_1 \geq 0$ for a call option and $x_2 \leq 0$ for a put option. This feature is a fact for the early-exercise points x_m^* , $m \in \{1, \dots, M - 1\}$, allowing formula (4.29) to be used to compute the closed-form solution of $G_k(a, x_m^*)$ and $G_k(x_m^*, b)$ for the log-adjusted process. However at time t_M the option value equals the payoff function and therefore the coefficient $V_k(t_M)$ equals (4.45), where the integral is taken between $[a, b]$. Therefore, similar as for the coefficient V_k for the European option,

it holds for the log-adjusted process that the coefficient $V_k(t_M)$ for the Bermudan option equals:

$$V_k(t_M) = \begin{cases} G_k(0, b), & \text{for a call,} \\ G_k(a, 0), & \text{for a put.} \end{cases} \quad (4.48)$$

The coefficients $C_k(x_1, x_2, t_m)$

To obtain the coefficients $C_k(x_1, x_2, t_m)$, the approximation of the continuation value with the COS formula $\hat{c}(t_m, y)$, defined in (4.39), is used. By inserting $\hat{c}(t_m, y)$ in equation (4.47) and interchanging summation and integration gives the following approximation of coefficients $C_k(x_1, x_2, t_m)$, where it is assumed that the characteristic function can be written in the general form $\phi(u|y, \Delta t) = e^{iuy\beta} \phi(u|\Delta t)$, as described in (4.15):

$$\hat{C}_k(x_1, x_2, t_m) = e^{-r\Delta t} \sum_{l=0}^{N-1} \text{Re} \left\{ \phi \left(\frac{k\pi}{b-a} \middle| \Delta t \right) \hat{V}_l(t_{m+1}) \mathcal{M}_{k,l}(x_1, x_2) \right\}, \quad (4.49)$$

with the coefficients $\hat{V}_l(t_m)$ for $m = \{1, \dots, M-1\}$ given by:

$$\hat{V}_l(t_m) = \begin{cases} \hat{C}_l(a, x_m^*, t_m) + G_l(x_m^*, b), & \text{for a call,} \\ G_l(a, x_m^*) + \hat{C}_l(x_m^*, b, t_m), & \text{for a put,} \end{cases} \quad (4.50)$$

where for $m = M$ the coefficient is $\hat{V}_l(t_M) = V_l(t_M)$, as described in (4.45), and the coefficients $\mathcal{M}_{k,l}(x_1, x_2)$ are defined as:

$$\mathcal{M}_{k,l}(x_1, x_2) = \frac{2}{b-a} \int_{x_1}^{x_2} e^{il\pi \frac{\beta y - a}{b-a}} \cos \left(k\pi \frac{y-a}{b-a} \right) dy. \quad (4.51)$$

From basic calculus the coefficients $\mathcal{M}_{k,l}(x_1, x_2)$ can be rewritten into two parts [44]:

$$\mathcal{M}_{k,l}(x_1, x_2) = -\frac{i}{\pi} (\mathcal{M}_{k,l}^s(x_1, x_2) + \mathcal{M}_{k,l}^c(x_1, x_2)),$$

where it holds that

$$\mathcal{M}_{k,l}^c(x_1, x_2) = \begin{cases} \frac{(x_2-x_1)\pi i}{b-a}, & \text{for } k = j = 0 \\ \frac{1}{l\beta+k} \left[e^{\frac{((j\beta+k)x_2 - (l+k)a)\pi i}{b-a}} - e^{\frac{((l\beta+k)x_1 - (l+k)a)\pi i}{b-a}} \right], & \text{otherwise,} \end{cases} \quad (4.52)$$

$$\mathcal{M}_{k,l}^s(x_1, x_2) = \begin{cases} \frac{(x_2-x_1)\pi i}{b-a}, & \text{for } k = j = 0 \\ \frac{1}{l\beta-k} \left[e^{\frac{((l\beta-k)x_2 - (l-k)a)\pi i}{b-a}} - e^{\frac{((l\beta-k)x_1 - (l-k)a)\pi i}{b-a}} \right], & \text{otherwise.} \end{cases} \quad (4.53)$$

Remark 4.3. For characteristic functions where $\beta = 1$ an efficient FFT-based algorithm for the computation of the Fourier coefficients $\hat{\mathbf{C}}(t_m) = \{\hat{C}_0(t_m), \dots, \hat{C}_{N-1}(t_m)\}$ can be used [42]. The key to this efficient algorithm is that the matrices $\mathcal{M}^s = \{\mathcal{M}_{k,l}^s(x_1, x_2)\}_{k,l=0}^{N-1}$ and $\mathcal{M}^c = \{\mathcal{M}_{k,l}^c(x_1, x_2)\}_{k,l=0}^{N-1}$ have respectively a Toeplitz and Hankel structure, $\forall k, l, x_1, x_2$:

$$\mathcal{M}_{k,l}^s(x_1, x_2) = \mathcal{M}_{k+1, l+1}^s(x_1, x_2) \quad \text{and} \quad \mathcal{M}_{k,l}^c(x_1, x_2) = \mathcal{M}_{k+1, l-1}^c(x_1, x_2).$$

With these matrix structures, the FFT can be applied directly for an efficient matrix-vector multiplication to compute the continuation value coefficients $\hat{C}_k(x_1, x_2, t_m)$ for all k in $O(N \log_2(N))$ computational complexity. The algorithm to compute these coefficients with this method is described in Algorithm 2 in section 2.3 of [42].

4.5 The COS method for Bermudan options with multiple early-exercise rights

In this section the COS method for Bermudan options is extended to options with multiple early-exercise rights, discussed in Section 3.3. The COS method will be used to approximate the continuation value for the number of exercise rights left.

In the paper [44], Zhang and Oosterlee introduced the COS method for swing options. In their model the swing options have the property to be exercised early more than once continuous in time before expiry and adopted the concept of recovery time (if the holder has exercised the option early, he/she has to wait the recovery time before they can exercise again). This method for the swing options is more difficult than for the Bermudan option with multiple early-exercise rights considered in this section, since we are dealing with discrete exercise moments instead of continuous ones.

As described in the backward induction algorithm (3.10) the value of the Bermudan option with R early-exercise rights at initial time t_0 can be computed by the continuation value, i.e. $v^R(t_0, x) = c^R(t_0, x)$.

The continuation value for the Bermudan option with $j \in \mathcal{R}$ early-exercise rights left can be approximated directly with the COS formula in a similar way as for the Bermudan option (4.39). The difference is that the coefficients V_k depend on the number of early-exercise rights left. It follows that the COS formula to compute the continuation value of the Bermudan option with j early-exercise rights left at time t_{m-1} , $\forall m \in \{1, \dots, M\}$, where x and y respectively denote the state variables at time t_{m-1} and t_m , is defined by:

$$c^j(t_{m-1}, x) \approx \hat{c}^j(t_{m-1}, x) := e^{-r\Delta t} \sum_{k=0}^{N-1} \text{Re} \left\{ \phi \left(\frac{k\pi}{b-a} \middle| \Delta t, x \right) e^{ik\pi \frac{-a}{b-a}} \right\} V_k^j(t_m), \quad (4.54)$$

where the coefficients $V_k^j(t_m)$ are given by:

$$V_k^j(t_m) = \frac{2}{b-a} \int_a^b v^j(t_m, y) \cos \left(k\pi \frac{y-a}{b-a} \right) dy. \quad (4.55)$$

So the value of the Bermudan option with R early-exercise rights can be approximated if the coefficients $V_k^R(t_1)$ are found. In the next section it is shown how these coefficients $V_k^j(t_m)$, for all $j \in \mathcal{R}$ and $m \in \{1, \dots, M\}$, can be derived backward in time.

4.5.1 The coefficients $V_k^j(t_m)$ for Bermudan options with multiple early-exercise rights

In this subsection the coefficients $V_k^j(t_m)$, defined in (4.55), used in the COS formula for the Bermudan option with multiple early-exercise rights are recovered. Similarly as the derivation of the backward induction algorithm described in Section 3.3, the recovery of the coefficients $V_k^j(t_m)$ is done in two settings/steps in a backward manner in time $\forall j \in \mathcal{R}$:

1. First the coefficients are recovered where the number of exercise rights left is equal to the number of exercise moments left, the so-called initialization. As described in Section 3.3, in this initialization setting the value of the option, $v^j(t_{M-j+1}, S_{t_{M-j+1}})$, used for computing the continuation value can be written as the payoff function at

time t_{M-j+1} plus the continuation value with one right less, see formula (3.8). So the coefficients $V_k^j(t_{M-j+1})$ for this initialization step can be written as:

$$\begin{aligned}
V_k^j(t_{M-j+1}) &= \frac{2}{b-a} \int_a^b v^j(t_{M-j+1}, y) \cos\left(k\pi \frac{y-a}{b-a}\right) dy \\
&= \frac{2}{b-a} \int_a^b (g(t_{M-j+1}, y) + c^{j-1}(t_{M-j+1}, y)) \cos\left(k\pi \frac{y-a}{b-a}\right) dy \\
&= \frac{2}{b-a} \int_a^b g(t_{M-j+1}, y) \cos\left(k\pi \frac{y-a}{b-a}\right) dy \\
&\quad + \frac{2}{b-a} \int_a^b c^{j-1}(t_{M-j+1}, y) \cos\left(k\pi \frac{y-a}{b-a}\right) dy \\
&:= G_k(a, b) + C_k^{j-1}(a, b, t_{M-j+1}).
\end{aligned} \tag{4.56}$$

2. In the second step the setting is taken where there are less exercise rights than exercise moments left. As shown in the backward induction algorithm (3.10) the value of the option in this setting is given for all $j \in \mathcal{R}$ by:

$$v^j(t_m, y) = \max\{c^j(t_m, y), c^{j-1}(t_m, y) + g(t_m, y)\} \quad , \text{ for } m \in \{M-j, \dots, 1\}. \tag{4.57}$$

The coefficient $V_k^j(t_m)$ can be recovered by substituting this maximum in equation (4.55). Furthermore, similar as the Bermudan option, there exists a point x_m^{*j} , called the early-exercise point for j level of rights left, where $c^j(t_m, x_m^{*j}) = c^{j-1}(t_m, x_m^{*j}) + g(t_m, x_m^{*j})$.

For a put option it holds on the interval $y \in [a, x_m^{*j}]$ that $c^{j-1}(t_m, y) + g(t_m, y) \geq c^j(t_m, y)$ and on the interval $y \in (x_m^{*j}, b]$ that $c^{j-1}(t_m, y) + g(t_m, y) < c^j(t_m, y)$. Vice versa for the call option, i.e. on the interval $y \in [a, x_m^{*j}]$ that $c^{j-1}(t_m, y) + g(t_m, y) \leq c^j(t_m, y)$ and on the interval $y \in (x_m^{*j}, b]$ that $c^{j-1}(t_m, y) + g(t_m, y) > c^j(t_m, y)$.

Therefore, based on the early-exercise point x_m^{*j} the integral of (4.55) can be split in two parts, such that the maximum of (4.57) is always taken. Hence for the put option the coefficients $V_k^j(t_m)$ for $m \in \{M-j, \dots, 1\}$ and $\forall j \in \mathcal{R}$ are given by:

$$\begin{aligned}
V_k^j(t_m) &= \frac{2}{b-a} \int_a^b v^j(t_m, y) \cos\left(k\pi \frac{y-a}{b-a}\right) dy \\
&= \frac{2}{b-a} \int_a^b \max\{c^j(t_m, y), c^{j-1}(t_m, y) + g(t_m, y)\} \cos\left(k\pi \frac{y-a}{b-a}\right) dy \\
&= \frac{2}{b-a} \int_a^{x_m^{*j}} (c^{j-1}(t_m, y) + g(t_m, y)) \cos\left(k\pi \frac{y-a}{b-a}\right) dy \\
&\quad + \frac{2}{b-a} \int_{x_m^{*j}}^b c^j(t_m, y) \cos\left(k\pi \frac{y-a}{b-a}\right) dy \\
&:= G_k(a, x_m^{*j}) + C_k^{j-1}(a, x_m^{*j}, t_m) + C_k^j(x_m^{*j}, b, t_m).
\end{aligned} \tag{4.58}$$

A similar derivation can be done for the call option.

Summarizing, the coefficients $V_k^j(t_m)$ for the Bermudan put option with $j \in \mathcal{R}$ exercise rights left is given by:

$$V_k^j(t_m) = \begin{cases} G_k(a, b) + C_k^{j-1}(a, b, t_{M-j+1}), & \text{for } m = M - j + 1, \\ G_k(a, x_m^{*j}) + C_k^{j-1}(a, x_m^{*j}, t_m) + C_k^j(x_m^{*j}, b, t_m), & \text{for } m \in \{M - j, \dots, 1\}. \end{cases} \quad (4.59)$$

The closed-form solution of the Fourier cosine series coefficients of the payoff function, $G_k(x_1, x_2)$, are computed in Section 4.3.1 for various state variables y and for the polynomial model in Section 4.3.2. Furthermore, the Fourier cosine series coefficients of the continuation value, $C_k^j(x_1, x_2, t_m)$, can be approximated in the same way as described in (4.49), however $V_k^j(t_{m+1})$ is used instead of $V_k(t_{m+1})$. Note that the continuation value with zero rights left is always zero.

4.6 The COS method for electricity storage contracts

In this section the COS method for electricity storage contracts is discussed. The main idea is to approximate the continuation values, described in the backward induction pricing algorithm (3.23), with the COS method for each allowed energy level $e \in E$ in storage.

The approximation of the continuation values can be obtained by means of the COS method in a similar way as for the Bermudan option with multiple early-exercise rights. The difference is that the coefficients V_k now depend on the energy level $e \in E$ instead of the number of early-exercise rights left. The COS formula for approximating the continuation value with $e \in E$ energy in storage is defined, for $m \in \{M + 1, \dots, 1\}$, by:

$$c(t_{m-1}, x, e) \approx \hat{c}(t_{m-1}, x, e) := e^{-r\Delta t} \sum_{k=0}^{N-1} \text{Re} \left\{ \phi \left(\frac{k\pi}{b-a} \middle| \Delta t, x \right) e^{ik\pi \frac{-a}{b-a}} \right\} V_k(t_m, e). \quad (4.60)$$

The value of the electricity contract with $e(t_0)$ electricity in storage can be approximated if the coefficients $V_k(t_1, e(t_0))$ have been recovered, due to the fact that the initial value of the contract is equal to the continuation value at time t_0 .

The next section will show how to determine the coefficients $V_k(t_m, e)$ backward in time for each energy level $e \in E$.

4.6.1 The coefficients $V_k(t_m, e)$ for electricity storage contracts

In this section it is shown how the coefficients $V_k(t_m, e)$, used in the COS formula (4.60), can be recovered backward in time. The coefficients $V_k(t_m, e)$ are defined, for $m \in \{M + 1, \dots, 1\}$, by:

$$V_k(t_m, e) = \frac{2}{b-a} \int_a^b v(t_m, y, e) \cos \left(k\pi \frac{y-a}{b-a} \right) dy, \quad \forall e \in E. \quad (4.61)$$

First, the coefficients are recovered at the settlement date t_{M+1} , where the value of the contract equals the penalty function, $v(t_{M+1}, y, e) = q_s(t_{M+1}, y, e)$. Therefore, by substitution of this penalty function in formula (4.61) the coefficients $V_k(t_{M+1}, e)$ are

obtained for each energy level:

$$V_k(t_{M+1}, e) = \frac{2}{b-a} \int_a^b q_s(t_{M+1}, y, e) \cos\left(k\pi \frac{y-a}{b-a}\right) dy, \quad \forall e \in E. \quad (4.62)$$

At moments t_m , $m \in \{M, \dots, 1\}$, with energy level $e \in E$ in storage, the holder of the contract chooses an allowed action $\Delta e \in \mathcal{A}(t_m, e)$ which ensures the maximum ultimate value. This decision results in the contract value $v(t_m, y, e)$ defined in (3.21). By substitution of this value in (4.61), it follows that the coefficients at time t_m , $m \in \{M, \dots, 1\}$, with $e \in E$ energy in storage are obtained by:

$$V_k(t_m, e) = \frac{2}{b-a} \int_a^b \max_{\Delta e \in \mathcal{A}(t_m, e)} \left\{ g(t_m, y, \Delta e) + c(t_m, y, e + \Delta e) + q_b(\Delta e) \right\} \cos\left(k\pi \frac{y-a}{b-a}\right) dy, \quad \forall e \in E. \quad (4.63)$$

Note that the coefficients $V_k^j(t_m)$ for the Bermudan option with multiple early-exercise rights are realized by taking the integral of a maximum of two functions. This integral can always be divided into two parts by means of the early-exercise point, so that the maximum of the two functions is always taken. When determining the coefficients for the electricity contract, $V_k(t_m, e)$ (4.63), a maximum of $Dim(\mathcal{A}(t_m, e))$ functions is taken.

To take the integral of the maximum in formula (4.63), the integration range $[a, b]$ is split into intervals, $[a, x_1], [x_1, x_2], [x_3, x_4], \dots, [x_n, b]$, so that the maximum is always taken. This split is based on the so-called optimal actions $\Delta e_i^* \in \mathcal{A}(t_m, e)$, for which the contract value $v(t_m, y, e)$ results in the maximum on interval $[x_i, x_{i+1}]$, for $i \in \{0, \dots, n\}$.

These intervals with corresponding optimal actions can be found by discretizing the interval $[a, b]$, i.e. $[a, a + \delta, a + 2\delta, \dots, b]$, and compare the values $v(t_m, y, e)$ for all the actions $\Delta e \in \mathcal{A}(t_m, e)$ at each element in the discretization and choose the action which gives the maximum value. This results for example in the interval $[x_i, x_{i+1}] = [a + 200\delta, a + 235\delta]$ where the action Δe_i^* gives the maximum value $v(t_m, y, e)$ for each element $y \in [a + 200\delta, a + 201\delta, \dots, a + 235\delta]$. Note, it is possible that the same action can be an optimal action at various different intervals, e.g. $\Delta e_2^* = \Delta e_5^*$.

Once the intervals and the corresponding optimal actions for splitting the integral are found, the coefficients $V_k(t_m, e)$ (4.63) for all $e \in E$ at moment t_m , $m \in \{M, \dots, 1\}$, can be written as:

$$\begin{aligned} V_k(t_m, e) &= \frac{2}{b-a} \left[\int_a^{x_1} \left(g(t_m, y, \Delta e_0^*) + c(t_m, y, e + \Delta e_0^*) + q_b(\Delta e_0^*) \right) \cos\left(k\pi \frac{y-a}{b-a}\right) dy \right. \\ &\quad + \int_{x_1}^{x_2} \left(g(t_m, y, \Delta e_1^*) + c(t_m, y, e + \Delta e_1^*) + q_b(\Delta e_1^*) \right) \cos\left(k\pi \frac{y-a}{b-a}\right) dy \\ &\quad + \dots \\ &\quad \left. + \int_{x_n}^b \left(g(t_m, y, \Delta e_n^*) + c(t_m, y, e + \Delta e_n^*) + q_b(\Delta e_n^*) \right) \cos\left(k\pi \frac{y-a}{b-a}\right) dy \right] \\ &= \sum_{i=0}^n \left[G_k(x_i, x_{i+1}, \Delta e_i^*) + C_k(x_i, x_{i+1}, e + \Delta e_i^*) + Q_k(x_i, x_{i+1}, \Delta e_i^*) \right], \end{aligned} \quad (4.64)$$

where $x_0 = a$, $x_{n+1} = b$, $\Delta e_i^* \in \mathcal{A}(t_m, e)$ the optimal action on interval $[x_i, x_{i+1}]$ and the Fourier cosine series coefficients of the payoff function, the continuation value and the penalty function are respectively defined, $\forall \Delta e \in \mathcal{A}(t_m, e)$, by:

$$G_k(x_i, x_{i+1}, \Delta e) = \frac{2}{b-a} \int_{x_i}^{x_{i+1}} g(t_m, y, \Delta e) \cos\left(k\pi \frac{y-a}{b-a}\right) dy \quad (4.65)$$

$$C_k(x_i, x_{i+1}, e + \Delta e) = \frac{2}{b-a} \int_{x_i}^{x_{i+1}} c(t_m, y, e + \Delta e) \cos\left(k\pi \frac{y-a}{b-a}\right) dy \quad (4.66)$$

$$Q_k(x_i, x_{i+1}, \Delta e) = \frac{2}{b-a} \int_{x_i}^{x_{i+1}} q_b(\Delta e) \cos\left(k\pi \frac{y-a}{b-a}\right) dy. \quad (4.67)$$

The Fourier coefficients $C_k(x_i, x_{i+1}, e + \Delta e)$ are approximated in the same way as described in (4.49), however the coefficients $V_k(t_{m+1}, e + \Delta e)$ are used instead of $V_k(t_{m+1})$. Next it is shown how the coefficient $G_k(x_i, x_{i+1}, \Delta e)$ and $Q_k(x_i, x_{i+1}, \Delta e)$ are computed in closed-form.

The coefficients $G_k(x_i, x_{i+1}, \Delta e)$

The coefficients $G_k(x_i, x_{i+1}, \Delta e)$ can be obtained by substitution of the payoff function of the electricity contract (3.11) in equation (4.65), after which the integral can be calculated. Furthermore, we assume that the electricity price process follows the polynomial model, $S_t = \Phi(X_t)$, described in Section 2.1.

Since the characteristic function of the polynomial model does not exist, the characteristic function of the underlying process X_t is used. Therefore, the state variables are defined as $x = \Phi^{-1}(S_{t_{m-1}})$ and $y = \Phi^{-1}(S_{t_m})$. So the coefficients $G_k(x_1, x_2, \Delta e)$ (3.11) can be calculated as follows:

$$G_k(x_i, x_{i+1}, \Delta e) = \begin{cases} \frac{2}{b-a} \int_{x_i}^{x_{i+1}} \frac{-\Phi(y)}{\eta} \Delta e \cos\left(k\pi \frac{y-a}{b-a}\right) dy & , \Delta e > 0, \\ 0 & , \Delta e = 0, \\ \frac{2}{b-a} \int_{x_i}^{x_{i+1}} -\Phi(y) \Delta e \cos\left(k\pi \frac{y-a}{b-a}\right) dy & , \Delta e < 0. \end{cases} \quad (4.68)$$

The coefficients $G_k(x_i, x_{i+1}, \Delta e)$ can be computed in closed-form for any finite-order polynomial map $\Phi(\cdot)$.

Example 4.4. In this example the coefficients $G_k(x_i, x_{i+1}, \Delta e)$ are computed where the electricity price follows a second-order polynomial model, defined by:

$$S_t = \Phi(X_t) = \frac{1-c}{2} X_t^2 + cX_t = CX_t^2 + cX_t.$$

After substitution of the second-order polynomial model in (4.68), the integral can be computed. This results in the following coefficients $G_k(x_i, x_{i+1}, \Delta e)$:

- For $k = 0$

$$G_k(x_i, x_{i+1}, \Delta e) = \begin{cases} \frac{2}{b-a} \frac{\Delta e}{\eta} \left[-\frac{c}{2} y^2 - \frac{C}{3} y^3 \right]_{x_i}^{x_{i+1}} & , \Delta e > 0, \\ 0 & , \Delta e = 0, \\ \frac{2}{b-a} \Delta e \left[-\frac{c}{2} y^2 - \frac{C}{3} y^3 \right]_{x_i}^{x_{i+1}} & , \Delta e < 0, \end{cases} \quad (4.69)$$

- For $k > 0$

$$G_k(x_i, x_{i+1}, \Delta e) = \begin{cases} \frac{2}{b-a} \frac{\Delta e}{\eta} \left[\begin{array}{l} -\frac{1}{\pi^3 k^3} (a-b) \left(\sin \left(\frac{\pi k (y-a)}{a-b} \right) (-2a^2 C + \right. \\ \left. 4abC - 2b^2 C + \pi^2 k^2 y (c + Cy)) + \right. \\ \left. \left. \pi k (a-b) (c + 2Cy) \cos \left(\frac{\pi k (y-a)}{a-b} \right) \right) \right]_{x_i}^{x_{i+1}}, & \Delta e > 0, \\ 0 & \Delta e = 0, \\ \frac{2}{b-a} \Delta e \left[\begin{array}{l} -\frac{1}{\pi^3 k^3} (a-b) \left(\sin \left(\frac{\pi k (y-a)}{a-b} \right) (-2a^2 C + \right. \\ \left. 4abC - 2b^2 C + \pi^2 k^2 y (c + Cy)) + \right. \\ \left. \left. \pi k (a-b) (c + 2Cy) \cos \left(\frac{\pi k (y-a)}{a-b} \right) \right) \right]_{x_i}^{x_{i+1}}, & \Delta e < 0, \end{array} \right. \end{cases} \quad (4.70)$$

Example 4.5. In this example the coefficients $G_k(x_i, x_{i+1}, \Delta e)$ are calculated where the electricity price follows a third-order polynomial model, defined by:

$$S_t = \Phi(X_t) = AX_t^3 + BX_t^2 + CX_t + D.$$

This third-order polynomial model results in the following coefficients $G_k(x_1, x_{i+1}, e)$:

- For $k = 0$

$$G_k(x_i, x_{i+1}, \Delta e) = \begin{cases} \frac{2}{b-a} \frac{\Delta e}{\eta} \left[-\frac{A}{4} y^4 - \frac{B}{3} y^3 - \frac{C}{2} y^2 - Dy \right]_{x_i}^{x_{i+1}}, & \Delta e > 0, \\ 0 & \Delta e = 0, \\ \frac{2}{b-a} \Delta e \left[-\frac{A}{4} y^4 - \frac{B}{3} y^3 - \frac{C}{2} y^2 - Dy \right]_{x_i}^{x_{i+1}}, & \Delta e < 0, \end{cases} \quad (4.71)$$

- For $k > 0$

$$G_k(x_i, x_{i+1}, \Delta e) = \begin{cases} \frac{2}{b-a} \frac{\Delta e}{\eta} \left[\begin{array}{l} \frac{(a-b)}{\pi^4 k^4} \left(\pi k \sin \left(\frac{\pi k(a-y)}{a-b} \right) (-2a^2(3Ay+B) + \right. \\ 4ab(3Ay+B) - 2b^2(3Ay+B) + \\ \left. \pi^2 k^2 (y(y(Ay+B)+C)+D) \right) + \\ (a-b) \cos \left(\frac{\pi k(y-a)}{a-b} \right) (6a^2A - 12aAb + \\ \left. A(6b^2 - 3\pi^2 k^2 y^2) - \pi^2 k^2 (2By+C)) \right) \end{array} \right]_{x_i}^{x_{i+1}}, & \Delta e > 0, \\ 0 & \Delta e = 0, \\ \frac{2}{b-a} \Delta e \left[\begin{array}{l} \frac{(a-b)}{\pi^4 k^4} \left(\pi k \sin \left(\frac{\pi k(a-y)}{a-b} \right) (-2a^2(3Ay+B) + \right. \\ 4ab(3Ay+B) - 2b^2(3Ay+B) + \\ \left. \pi^2 k^2 (y(y(Ay+B)+C)+D) \right) + \\ (a-b) \cos \left(\frac{\pi k(y-a)}{a-b} \right) (6a^2A - 12aAb + \\ \left. A(6b^2 - 3\pi^2 k^2 y^2) - \pi^2 k^2 (2By+C)) \right) \end{array} \right]_{x_i}^{x_{i+1}}, & \Delta e < 0. \end{cases} \quad (4.72)$$

The coefficients $Q_k(x_1, x_2, \Delta e)$

The penalty function $q_b(\Delta e)$ depends only on the action $\Delta e \in \mathcal{A}$ taken and not on the electricity price. Furthermore, the penalty function will only be nonzero if an action $\Delta e \in \mathcal{A} \setminus \mathcal{D}$ is taken. Substitution of the penalty function in equation (4.67) results in the following Fourier cosine series coefficients of the penalty function:

- For $k = 0$

$$Q_k(x_i, x_{i+1}, \Delta e) = \begin{cases} 0 & , \Delta e \in \mathcal{D}, \\ \frac{2}{b-a} q_b(\Delta e)(x_{i+1} - x_i) & , \Delta e \in \mathcal{A} \setminus \mathcal{D}. \end{cases} \quad (4.73)$$

- For $k > 0$

$$Q_k(x_i, x_{i+1}, \Delta e) = \begin{cases} 0 & , \Delta e \in \mathcal{D}, \\ \frac{2}{\pi k} q_b(\Delta e) \left(\sin \left(\frac{\pi k(a-x_{i+1})}{a-b} \right) - \sin \left(\frac{\pi k(a-x_i)}{a-b} \right) \right) & , \Delta e \in \mathcal{A} \setminus \mathcal{D}. \end{cases} \quad (4.74)$$

4.7 The integration range for the COS method

The interval of integration, $[a, b]$, for the COS method is essential for the accuracy of valuation. If an interval is set too small, a significant integration-range truncation error occurs, whereas if an interval is chosen too large, a large value for N should be selected to remain accurate, which increases the computation time.

The integration range is defined as proposed in [37]:

$$[a, b] := \left[\kappa_1 - \bar{L} \sqrt{\kappa_2 + \sqrt{\kappa_4}}, \kappa_1 + \bar{L} \sqrt{\kappa_2 + \sqrt{\kappa_4}} \right], \quad (4.75)$$

where κ_n is the n^{th} -order cumulant of the process used for the characteristic function and \bar{L} depending on the user-defined tolerance level, typically $\bar{L} \in [6, 12]$.

4.8 The Greeks with the COS method

A substantial advantage of the COS method is that the Greeks, described in Section 3.5.1, can be calculated at almost no additional computational complexity. The Greeks are found by differentiating the COS formula, where $v := v(t_0, S_{t_0})$, $S := S_{t_0}$ and $X := X_{t_0}$, respectively the option value at t_0 , the asset price and the underlying process used in the payoff and characteristic function:

$$\Delta := \frac{\partial v}{\partial S} = \frac{\partial v}{\partial X} \frac{\partial X}{\partial S}, \quad \Gamma := \frac{\partial^2 v}{\partial S^2} = \frac{\partial^2 v}{\partial X^2} \left(\frac{\partial X}{\partial S} \right)^2 + \frac{\partial v}{\partial X} \frac{\partial^2 X}{\partial S^2}, \quad \nu := \frac{\partial v}{\partial \sigma}. \quad (4.76)$$

Note that the general COS formula for the various options is defined as:

$$v \approx e^{-r\Delta t} \sum_{k=0}^{N-1} \text{Re} \left\{ \phi \left(\frac{k\pi}{b-a} \middle| \Delta t, x \right) e^{ik\pi \frac{-a}{b-a}} \right\} V_k, \quad (4.77)$$

where the coefficients V_k are computed differently for the different options, i.e. (4.19), (4.42), (4.55) and (4.61) for respectively the European option, Bermudan option, Bermudan option with multiple early-exercise rights and the electricity storage contract.

It follows that the cosine series expansions of the Greeks Δ , Γ and ν are given by:

$$\begin{aligned} \hat{\Delta} &\approx \frac{\partial X}{\partial S} \cdot e^{-r\Delta t} \sum_{k=0}^{N-1} \text{Re} \left\{ \phi \left(\frac{k\pi}{b-a} \middle| \Delta t, x \right) e^{ik\pi \frac{-a}{b-a}} \frac{ik\pi}{b-a} \beta \right\} V_k, \\ \hat{\Gamma} &\approx \left(\frac{\partial X}{\partial S} \right)^2 \cdot e^{-r\Delta t} \sum_{k=0}^{N-1} \text{Re} \left\{ \phi \left(\frac{k\pi}{b-a} \middle| \Delta t, x \right) e^{ik\pi \frac{-a}{b-a}} \left(\frac{ik\pi}{b-a} \beta \right)^2 \right\} V_k \\ &\quad + \frac{\partial^2 X}{\partial S^2} \cdot e^{-r\Delta t} \sum_{k=0}^{N-1} \text{Re} \left\{ \phi \left(\frac{k\pi}{b-a} \middle| \Delta t, x \right) e^{ik\pi \frac{-a}{b-a}} \frac{ik\pi}{b-a} \beta \right\} V_k, \\ \hat{\nu} &\approx e^{-r\Delta t} \sum_{k=0}^{N-1} \text{Re} \left\{ \frac{\partial \phi \left(\frac{k\pi}{b-a} \middle| \Delta t, x \right)}{\partial \sigma} e^{ik\pi \frac{-a}{b-a}} \right\} V_k, \end{aligned} \quad (4.78)$$

where the characteristic function is defined as in Section 4.2.

Example 4.6. In this example the Greeks $\hat{\Delta}$ and $\hat{\Gamma}$ are derived for the second-order polynomial model, where the characteristic function of the underlying process is used. The asset prices generated with the second-order polynomial model are given by:

$$S_t = \Phi(X_t) = \frac{1-c}{2}X_t^2 + cX_t = CX_t^2 + cX_t.$$

The Greeks $\hat{\Delta}$ and $\hat{\Gamma}$ are obtained by taking the first and second derivative of the inverse $X_0 = \Phi^{-1}(S_0)$ with respect to the asset price S_0 and substitute those in the equations of (4.78).

The inverse of $S_t = \Phi(X_t)$ is given by:

$$X_t = \begin{cases} S_t, & \text{for } C = 0, \\ \frac{\sqrt{c^2+4CS_t-c}}{2C}, & \text{for } C \neq 0. \end{cases}$$

The first and second derivative of this function at initial time t_0 is computed as follows, where $S := S_{t_0}$ and $X := X_{t_0}$:

$$\frac{\partial X}{\partial S} = \begin{cases} 1, & \text{for } C = 0, \\ \frac{1}{\sqrt{c^2+4CS}}, & \text{for } C \neq 0, \end{cases} \quad \frac{\partial^2 X}{\partial S^2} = \begin{cases} 0, & \text{for } C = 0, \\ -\frac{2C}{(c^2+4CS)^{\frac{3}{2}}}, & \text{for } C \neq 0. \end{cases} \quad (4.79)$$

By substitution of these derivatives in (4.78) the COS method approximated Greeks $\hat{\Delta}$ and $\hat{\Gamma}$ are obtained.

Example 4.7. In this example the Greek $\hat{\nu}$ is derived, where the characteristic function of the OU process is used in the COS formula. The characteristic function of the OU process is defined by [43]:

$$\phi_{OU}(u|x, \Delta t) = \exp \left(iux e^{-\kappa\Delta t} + \frac{(e^{-2\kappa\Delta t} - e^{-\kappa\Delta t})(u^2\sigma^2 + ue^{\kappa\Delta t}(u\sigma^2 - 4i\kappa\theta))}{4\kappa} \right). \quad (4.80)$$

To compute the $\hat{\nu}$ it is necessary to differentiate the characteristic function with respect to the volatility parameter σ :

$$\frac{\partial \phi_{OU}(u|x, \Delta t)}{\partial \sigma} = \phi_{OU}(u|x, \Delta t) \cdot \frac{(e^{-2\kappa\Delta t} - e^{-\kappa\Delta t})(2u^2\sigma + 2u^2e^{\kappa\Delta t}\sigma)}{4\kappa}. \quad (4.81)$$

By substitution of (4.81) in $\hat{\nu}$ (4.78) the COS method to approximate the Greek ν is obtained.

5 The characteristic function approximation

In this section, various methods are discussed to approximate the characteristic function. In addition, we show that with a small modification in these approximations the FFT-based algorithm can be applied to compute the continuation value by means of the COS method in an efficient way, as mentioned in Remark 4.3.

The following approximations will be considered in this section:

- Approximation using the moments of the process.
- Approximation using the cumulants of the process.
- An empirical recovery of the characteristic function.
- Approximation with the adjoint expansion.

These numerical methods can be used for the approximation of the characteristic function of a variety of stochastic processes, including the polynomial model and the OU process. Moreover, the closed-form characteristic function of the process does not have to exist for these approximations.

5.1 Characteristic function approximation with moments

This approximation can be used for stochastic processes where the characteristic function is not available as a closed-form solution, but the moments can be generated for the process, e.g. the polynomial model.

The approximation with the moments is formed using the Maclaurin series expansion of the characteristic function. By the definition of the characteristic function and the MacLaurin series expansion of the exponent around zero, it holds for $t < T$:

$$\phi(u|X_t, \Delta t) = \mathbb{E}[e^{iuX_T} | \mathcal{F}_t] = \mathbb{E} \left[\sum_{j=0}^{\infty} \frac{(iuX_T)^j}{j!} \middle| \mathcal{F}_t \right] = \sum_{j=0}^{\infty} \mathbb{E}[X_T^j | \mathcal{F}_t] \frac{(iu)^j}{j!}, \quad (5.1)$$

where $\Delta t = T - t$.

By truncation of the series summation, the J^{th} -order approximation is given by:

$$\phi(u|X_t, \Delta t) \approx \hat{\phi}(u|X_t, \Delta t) = \sum_{j=0}^J \mathbb{E}[X_T^j | \mathcal{F}_t] \frac{(iu)^j}{j!}. \quad (5.2)$$

Due to the fact that the moments of a process are often known, this appears to be a good way to approach the characteristic function for a wide range of stochastic processes, e.g. the polynomial model. However, after testing, it turned out that hundreds of moments were needed to be accurate on a large interval, and not just around zero. This made this method to approximate the characteristic function inefficient. To show this an example is given, where this approximation (5.2) is used to approximate the characteristic function of the standard normal distribution.

Example 5.1. Let X be normally distributed with zero mean and variance one. The characteristic function and all the moments are known for this distribution. Note that the characteristic function of the standard normal distribution only has a real part. In Figure 3 different values of order J in formula (5.2) are used to evaluate the accuracy of the approximated characteristic function.

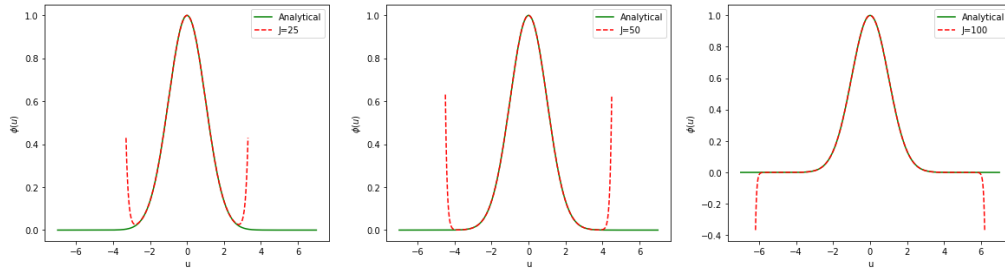


Figure 3: The approximated characteristic function (5.2) for various J compared to the closed-form characteristic function of the standard normal distribution.

As can be seen in Figure 3, the approximated characteristic function is accurate around zero, but at a larger interval the approximated characteristic function diverges from the closed-form characteristic function. The more moments that are used, the larger the interval that is accurate.

5.2 Characteristic function approximation with cumulants

In this section the characteristic function is approximated in terms of its cumulants. The cumulants are closely related to the moments of a stochastic process, i.e. any two processes with identical moments will have identical cumulants as well. Moreover, the cumulants of a process can be recovered by its moments, and vice versa.

The n^{th} -order cumulant κ_n of a stochastic process X_T conditional on X_t , for $t \leq T$, is defined by the cumulant generating function $K_{X_T|X_t}(u)$:

$$K_{X_T|X_t}(u) = \log \mathbb{E} [e^{uX_T} | \mathcal{F}_t],$$

$$\kappa_n = \left. \frac{\partial^n}{\partial u^n} K_{X_T|X_t}(u) \right|_{u=0}.$$

Note that the moment generating function is the exponential of the cumulant generating function. Furthermore, the cumulants can be recovered by the moments with the following relation:

$$\kappa_n = \mathbb{E} [X_T^n | \mathcal{F}_t] - \sum_{m=1}^{n-1} \binom{n-1}{m-1} \kappa_m \mathbb{E} [X_T^{n-m} | \mathcal{F}_t].$$

Hence, the first- and second-order cumulant of a stochastic process is equal to respectively the mean and variance of that process.

Now that the cumulants have been defined, we can approximate the characteristic function with them. In a similar manner as with the approximation with the moments,

the approximation with the cumulants is formed by using the Maclaurin series. By the definition of the cumulants, the characteristic function and the MacLaurin series expansion of the cumulant generating function around zero, it holds that [45]:

$$\phi(u|X_t, \Delta t) = \mathbb{E}[e^{iuX_T} | \mathcal{F}_t] = \exp\left(\sum_{j=1}^{\infty} \kappa_j \frac{(iu)^j}{j!}\right). \quad (5.3)$$

By truncation of the series summation, the J^{th} -order approximation of the characteristic function is given by:

$$\phi(u|X_t, \Delta t) \approx \hat{\phi}(u|\Delta t, X_t) = \exp\left(\sum_{j=1}^J \kappa_j \frac{(iu)^j}{j!}\right). \quad (5.4)$$

We expect the cumulant approximation of the characteristic function to be more accurate than the moment approximation in section 5.1, because we do not expand the exponential function itself. However, similar as with the approximation with the moments, the obtained approximation of the characteristic function can be inaccurate on some intervals, this is due to the fact that the series is obtained as a Taylor series around zero.

Example 5.2. In this example the cumulants are used to approximate the characteristic function of the OU process, defined in Appendix A.2, with parameters set as follows:

$$\kappa = 0.5, \quad \theta = 10, \quad \sigma = 1, \quad X_0 = 10, \quad T = 1, \quad t_0 = 0. \quad (5.5)$$

Because the OU process is normally distributed with mean $X_0 e^{-\kappa T} + \theta(1 - e^{-\kappa T})$ and variance $\frac{\sigma^2}{2\kappa}(1 - e^{-2\kappa T})$, the cumulants κ_n for $n > 2$ are zero. Therefore, it is expected that the approximated characteristic function, $\phi(u|X_0, \Delta t)$, is similar to the closed-form characteristic function for $J = 2$. The results of the imaginary and real parts of the characteristic function of the OU process approximated with the cumulants is given in Figure 4.

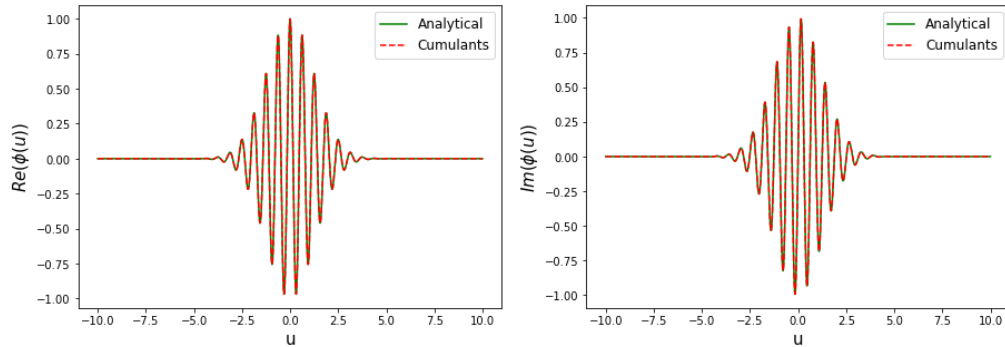


Figure 4: The characteristic function of the OU process approximated by its cumulants (5.4) for $J = 2$ in comparison to the closed-form characteristic function of the OU process.

Example 5.3. In this example the cumulant approximation will be applied to a second-order polynomial model, with an OU process as underlying process. The increasing second-order polynomial map and the parameters of the OU process are defined in respectively (3.27) and (5.5). The polynomial model is not normally distributed, so the cumulants κ_n are not zero for $n > 2$. Figure 5 shows the real part of the cumulant approximation of the characteristic function (5.4) of the second-order polynomial model for various approximation orders J and in addition the absolute differences. The differences of the imaginary part of the characteristic function approximations are of the same order of magnitude as the real part.

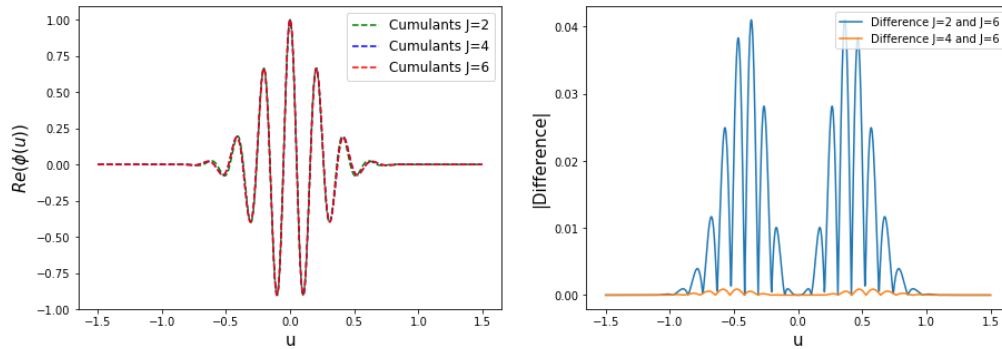


Figure 5: The characteristic function and absolute differences of the second-order polynomial model approximated with the cumulants (5.4) for various J .

5.3 Empirical characteristic function approximation

If the dynamics of a stochastic process are known, the characteristic function can be approximated with its samples. The justification for the empirical characteristic function approximation is that there is a direct relation between the cumulative distribution function (CDF) and the characteristic function. That is to say, the characteristic function is the Fourier–Stieltjes transform of the CDF. As a consequence, all the information of the empirical characteristic function is contained in the samples. The empirical characteristic function is defined as follows:

$$\phi(u|X_t, \Delta t) \approx \hat{\phi}_{ECF}(u|\mathbf{X}_T, \Delta t) = \int e^{iu x_T} dF_N(x_T) = \frac{1}{N} \sum_{j=1}^N e^{iu X_{j,T}}, \quad (5.6)$$

where $\mathbf{X}_T = \{X_{1,T}, \dots, X_{N,T}\}$ are iid samples of a process at time T which started at time t and $F_N(x_T)$ the empirical CDF.

The disadvantage of this approximation is that the calculation takes a relatively long CPU time compared to approximating the characteristic function with the moments or cumulants of a process, which is done respectively in sections 5.1 and 5.2.

Example 5.4. Let $X_{j,T}$ be the j^{th} trajectory of the OU process at time T , with the parameters as defined in (5.5) and $j \in \{1, 2, \dots, N\}$. In Figure 6 the real part of the empirical characteristic function of the OU process are compared with the closed-form ones,

$\phi(u|X_0, \Delta t)$, where different numbers of samples are used for the empirical characteristic function. The errors of the imaginary part of the characteristic function approximations are of the same order of magnitude as the real part.

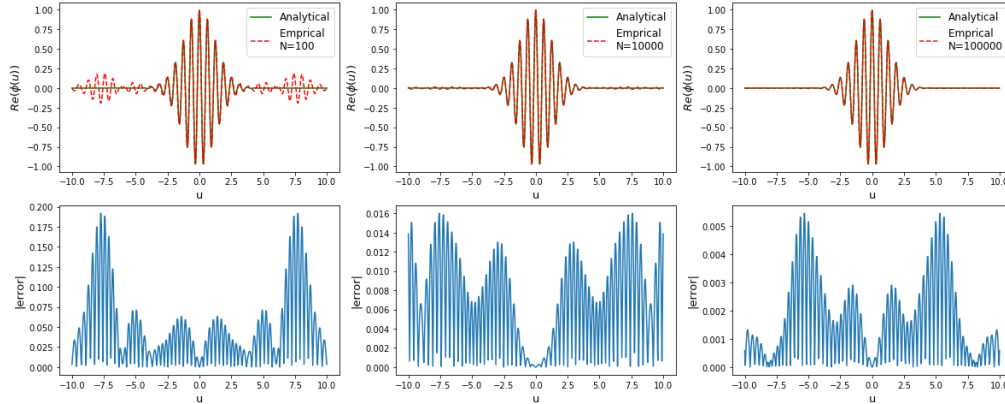


Figure 6: The empirical characteristic function (5.6) and absolute error for various number of samples N compared to the closed-form characteristic function of the OU process.

In the results of Example 5.4 it can be seen that the characteristic function approximation around zero is accurate, but that it has a fluctuating error when moving away from zero, especially when using a small number of samples. This development, of a fluctuating error, is called the Gibb's phenomenon. When valuating options by means of the COS method, there are methods to filter this Gibb's phenomenon, see e.g. [46].

5.4 Characteristic function approximation with the adjoint expansion

In this section the characteristic function is approximated with the adjoint expansion method, introduced in [47]. With the adjoint expansion method the characteristic function of the general class of local Lévy processes is approximated by a Taylor-based expansion in a way that it exhibits a convenient form for the pricing of options:

$$e^{iux} \sum_{k=0}^n (x - \bar{x})^k \hat{g}_{n,k}(u|t, T), \quad (5.7)$$

where $\hat{g}_{n,k}$ does not depend on x . Thus the approximation of the characteristic function can be written as a sum of products depending on u and functions that are a linear combination of $e^{iux}(x - \bar{x})^k$, $k \in \mathbb{N}$. This form has the advantage that it exhibits properties so that the FFT-based algorithm can be used to price the continuation values of options/contracts, [48]-[49].

5.4.1 General framework of the adjoint expansion method

Consider the local Lévy model with the following risk-neutral dynamics:

$$dX_t = \mu(t, X_t)dt + \sigma(t, X_t)dW_t^{\mathbb{Q}}, \quad (5.8)$$

where the discounted asset price $\tilde{X}_t := e^{-rt}X_t$ has the martingale property under the risk-neutral measure \mathbb{Q} .

It is known by the Feynman-Kac theorem that the price of a European option with maturity T and payoff function $g(T, X_T)$ is computed as [37]:

$$v(t, X_t) = e^{-r(T-t)}\mathbb{E}_{\mathbb{Q}}[g(T, X_T)|\mathcal{F}_t]. \quad (5.9)$$

To compute this option price the following function needs to be considered:

$$\bar{u}(t, X_t) = \mathbb{E}_{\mathbb{Q}}[g(T, X_T)|\mathcal{F}_t]. \quad (5.10)$$

Furthermore, $\bar{u}(t, X_t)$ can be computed as a solution of the following Cauchy problem:

$$\begin{cases} L\bar{u}(t, x) = 0, & t \in [0, T), x \in \mathbb{R}, \\ \bar{u}(T, x) = g(T, X), & x \in \mathbb{R}, \end{cases} \quad (5.11)$$

where L is the following differential operator:

$$L\bar{u}(t, x) = \partial_t \bar{u}(t, x) + \mu(t, x)\partial_x \bar{u}(t, x) + \frac{\sigma^2(t, x)}{2}\partial_{xx} \bar{u}(t, x). \quad (5.12)$$

This operator is also called the Kolmogorov backward operator (KBO). Moreover, the function $\bar{u}(t, x)$ in (5.10) can be written as an integral:

$$\bar{u}(t, x) = \int_{\mathbb{R}} g(T, y)f(y|T, t, x)dy, \quad (5.13)$$

where $f(y|T, t, x)$ is defined as the probability density of y at time T given x at time $t < T$. Note that f is the fundamental solution of the operator (5.12).

The probability density and its characteristic function form a Fourier pair. The characteristic function for u of the variable x , $\phi(u|T, t, x)$, is given by the following Fourier transform:

$$\phi(u|T, t, x) = \mathbb{F}(f(y|T, t, \cdot))(u) = \int_{\mathbb{R}} e^{iuy} f(y|T, t, x)dy. \quad (5.14)$$

5.4.2 Adjoint expansion for the OU process

In this section the characteristic function of the OU process is approximated by the adjoint expansion. The main idea is to consider the approximation of the drift and the volatility variables of a Lévy process (5.8) with a Taylor expansion.

Remember the OU process as described in Appendix A.2. The drift and the volatility parameters are given as follows:

$$\begin{aligned}\mu(t, x) &= \kappa(\theta - x), \\ \sigma(t, x) &= \sigma.\end{aligned}\tag{5.15}$$

Note that the volatility parameter is constant for the OU process, thus only the drift will be approximated. The n^{th} -order Taylor polynomial of $\mu(t, x)$ around \bar{x} is given by:

$$\mu(t, x) \approx \mu_0 + \sum_{k=1}^n \mu_k (x - \bar{x})^k,\tag{5.16}$$

where

$$\begin{aligned}\mu_0 &= \mu(t, \bar{x}), \\ \mu_k &= \left. \frac{\partial^k \mu(t, x)}{\partial x^k} \frac{1}{k!} \right|_{x=\bar{x}}.\end{aligned}$$

The coefficients of the Taylor approximation are as follows:

$$\mu_0 = \kappa(\theta - \bar{x}) \quad \text{and} \quad \mu_1 = -\kappa.\tag{5.17}$$

Note that this is the highest-order approximation, because $\mu_k = 0$ for all $k > 1$.

By substituting the Taylor approximation (5.16) in the differential operator (5.12) the n^{th} -order approximation L is introduced, $\forall n \geq 1$:

$$\begin{aligned}L_n &:= L_0 + \sum_{k=1}^n \mu_k (x - \bar{x})^k \partial_x \\ &= L_0 - \mu_1 (x - \bar{x}) \partial_x,\end{aligned}\tag{5.18}$$

where

$$L_0 = \partial_t + \mu_0 \partial_x + \frac{\sigma^2}{2} \partial_{xx}.$$

The n^{th} -order approximation of the probability density used in (5.13) is defined by:

$$f^{(n)}(y|T, t, x) = \sum_{k=0}^n \bar{G}^k(t, x; T, y),\tag{5.19}$$

where the first term \bar{G}^0 is the fundamental solution of the following Cauchy problem:

$$\begin{cases} L_0 \bar{G}^0(t, x; T, y) = 0, & t \in [0, T), x \in \mathbb{R}, \\ \bar{G}^0(T, x; T, y) = \delta_y(x), & x \in \mathbb{R}, \end{cases}\tag{5.20}$$

where $\delta_y(x)$ is the delta function. The following terms \bar{G}^k , for $k \geq 1$, are defined recursively with the following Cauchy problems:

$$\begin{cases} L_0 \bar{G}^k(t, x; T, y) = -\sum_{h=1}^k (L_h - L_{h-1}) \bar{G}^{k-h}(t, x; T, y), & t \in [0, T), x \in \mathbb{R}, \\ \bar{G}^k(T, x; T, y) = 0, & x \in \mathbb{R}, \end{cases} \quad (5.21)$$

where $\forall h = 1, \dots, k$:

$$L_h - L_{h-1} = \mu_h (x - \bar{x})^h \partial_x. \quad (5.22)$$

To obtain the n^{th} -order approximation of the characteristic function $\phi^{(n)}$, the Fourier transform with respect to y of the approximated density function $f^{(n)}$ (5.19) is taken:

$$\phi^{(n)}(u|T, t, x) = \sum_{k=0}^n \mathbb{F}(\bar{G}^k(t, x; T, \cdot))(u) = \sum_{k=0}^n \hat{G}^k(t, x; T, u). \quad (5.23)$$

Notice that the operator L acts on (t, x) while the characteristic function is a Fourier transform with respect to y . To utilize this transformation the terms \bar{G}^k will be characterized as solutions of the adjoint operator \tilde{L} of L , which acts on (T, y) , after which a Fourier transformation takes place to obtain the terms \hat{G}^k .

The adjoint operator \tilde{L} of an operator L is defined by:

$$\int_{\mathbb{R}^2} u(t, x) L v(t, x) dx dt = \int_{\mathbb{R}^2} v(t, x) \tilde{L} u(t, x) dx dt.$$

The adjoint of the differential operator L (5.12) is called the Kolmogorov forward operator (KFO). This adjoint of the operator can be approximated in the same way with a Taylor expansion as the operator (5.12). Furthermore, the fundamental solutions of \bar{G}^k are characterized as the following adjoint Cauchy problems:

$$\begin{cases} \tilde{L}_0 \bar{G}^0(t, x; T, y) = 0, & T > t, y \in \mathbb{R}, \\ \bar{G}^k(T, x; T, y) = \delta_x(y), & y \in \mathbb{R}, \end{cases} \quad (5.24)$$

where

$$\tilde{L}_0 = -\partial_T - \mu_0 \partial_y + \frac{1}{2} \sigma^2 \partial_{yy}.$$

Moreover, the terms \bar{G}^k , for $k \geq 1$, are defined recursively as:

$$\begin{cases} \tilde{L}_0 \bar{G}^k(t, x; T, y) = -\sum_{h=1}^k (\tilde{L}_h - \tilde{L}_{h-1}) \bar{G}^{k-h}(t, x; T, y), & t \in [0, T), x \in \mathbb{R}, \\ \bar{G}^k(T, x; T, y) = 0, & x \in \mathbb{R}, \end{cases} \quad (5.25)$$

where $\forall h = 1, \dots, k$:

$$\tilde{L}_h - \tilde{L}_{h-1} = -\mu_h (y - \bar{x})^h \partial_y - \mu_h h (y - \bar{x})^{h-1}.$$

Remark that the adjoint Cauchy problems, (5.24) and (5.25), have a solution in the Fourier space. Thus to find the terms \hat{G}^k in (5.23) the Fourier transform is taken and the problem is solved explicitly in the Fourier space. The Fourier transform of $\tilde{L}_0 \bar{G}^k(t, x; T, y)$, for all $k \geq 0$, with respect to y is computed as follows:

$$\begin{aligned} \mathbf{F}(\tilde{L}_0 \bar{G}^k(t, x; T, \cdot))(u) &= -\partial_T \hat{G}^k(t, x; T, u) + \mu_0 i u \hat{G}^k(t, x; T, u) - \frac{1}{2} \sigma^2 u^2 \hat{G}^k(t, x; T, u) \\ &= -\partial_T \hat{G}^k(t, x; T, u) + \psi(u) \hat{G}^k(t, x; T, u), \end{aligned} \quad (5.26)$$

where

$$\psi(u) = \mu_0 i u - \frac{1}{2} \sigma^2 u^2. \quad (5.27)$$

This results in the following problems in the Fourier space:

$$\begin{cases} \partial_T \hat{G}^0(t, x; T, u) = \hat{G}^0(t, x; T, u) \psi(u), & T > t, \\ \hat{G}^0(t, x; t, u) = e^{iux}, & x \in \mathbb{R}, \end{cases} \quad (5.28)$$

and for $k > 0$:

$$\begin{cases} \partial_T \hat{G}^k(t, x; T, u) = \psi(u) \hat{G}^k(t, x; T, u) + \sum_{h=1}^k \mathbf{F}(\tilde{L}_h - \tilde{L}_{h-1}) \hat{G}^{k-h}(t, x; T, u), & T > t, \\ \hat{G}^k(t, x; t, u) = 0, \end{cases} \quad (5.29)$$

where the Fourier transform $\mathbf{F}(\tilde{L}_h - \tilde{L}_{h-1})$ is as follows, $\forall h = 1, \dots, k$:

$$\begin{aligned} \mathbf{F}(\tilde{L}_h - \tilde{L}_{h-1}) &= \mathbf{F}(-\mu_h (y - \bar{x})^h \partial_y - \mu_h h (y - \bar{x})^{h-1}) \\ &= \mu_h (-i \partial_u - \bar{x})^h i u - \mu_h h (-i \partial_u - \bar{x})^{h-1}. \end{aligned} \quad (5.30)$$

The solutions of the ordinary differential equations (5.28) and (5.29) are given by:

$$\begin{cases} \hat{G}^0(t, x; T, u) = e^{iux + (T-t)\psi(u)}, \\ \hat{G}^k(t, x; T, u) = \int_t^T e^{\psi(u)(T-s)} \sum_{h=1}^k \mathbf{F}(\tilde{L}_h - \tilde{L}_{h-1}) \hat{G}^{k-h}(t, x; s, u) ds, & k \geq 1. \end{cases} \quad (5.31)$$

Now for $k = 1$ we obtain:

$$\begin{aligned} \hat{G}^1(t, x; T, u) &= \int_t^T e^{\psi(u)(T-s)} \left[\left(\mu_1 (-i \partial_u - \bar{x}) i u - \mu_1 \right) \hat{G}^0(t, x; s, u) \right] ds \\ &= \int_t^T e^{\psi(u)(T-s)} \mu_1 \left(\partial_u u \hat{G}^0(t, x; s, u) - \bar{x} i u \hat{G}^0(t, x; s, u) - \hat{G}^0(t, x; s, u) \right) ds \\ &\stackrel{(*)}{=} \int_t^T e^{\psi(u)(T-s)} \hat{G}^0(t, x; s, u) \mu_1 \left(u (ix + (s-t)\psi'(u)) e^{iux + (s-t)\psi(u)} - \bar{x} i u \right) ds \\ &= \hat{G}^0(t, x; T, u) \mu_1 \int_t^T \left(u (ix + (s-t)\psi'(u)) e^{iux + (s-t)\psi(u)} - \bar{x} i u \right) ds \\ &= \hat{G}^0(t, x; T, u) \mu_1 \left(\frac{1}{2} u \psi'(u) (T-t)^2 + i u (x - \bar{x}) (T-t) \right), \end{aligned} \quad (5.32)$$

with $\psi(u)$ as in (5.48), $\psi'(u) = \mu_0 i - \sigma^2 u$ and at (*) it is used that:

$$\partial_u \left(u \hat{G}^0(t, x; s, u) \right) = \hat{G}^0(t, x; s, u) + u (ix + (s-t)\psi'(u)) e^{iux + (s-t)\psi(u)}.$$

Thus the first-order approximation of the characteristic function (5.23) is given by:

$$\begin{aligned} \phi^{(1)}(u|T, t, x) &= \hat{G}^0(t, x; T, u) + \hat{G}^1(t, x; T, u) \\ &= e^{iux + \psi(u)(T-t)} \left(1 + \mu_1 \left(\frac{1}{2} u \psi'(u) (T-t)^2 + iu(x - \bar{x})(T-t) \right) \right). \end{aligned} \quad (5.33)$$

For $k = 2$ a similar straightforward computation is done, which results in:

$$\hat{G}^2(t, x; T, u) = \hat{G}^0(t, x; T, u) \sum_{j=0}^2 \hat{g}_j^{(2)}(T-t, u) (x - \bar{x})^j, \quad (5.34)$$

where

$$\begin{aligned} \hat{g}_0^{(2)}(T-t, u) &= \mu_1^2 u (T-t)^3 \left(\frac{1}{8} (T-t) u \psi'(u)^2 + \frac{1}{6} u \psi''(u) + \frac{1}{6} \psi'(u) \right) \\ &\quad + \mu_2 (T-t)^2 \left(-\frac{1}{3} u i (T-t) \psi'(u) - \frac{1}{2} u \psi''(u) \right), \\ \hat{g}_1^{(2)}(T-t, u) &= \mu_1^2 u (T-t)^2 \left(\frac{1}{2} (T-t) i u \psi'(u) + \frac{1}{2} i \right) + \mu_2 u (T-t)^2 \psi'(u), \\ \hat{g}_2^{(2)}(T-t, u) &= -\frac{1}{2} \mu_1^2 (T-t)^2 u^2 + \mu_2 i u (T-t). \end{aligned} \quad (5.35)$$

Resulting in the second-order approximation of the characteristic function (5.23):

$$\phi^{(2)}(u|T, t, x) = \hat{G}^0(t, x; T, u) + \hat{G}^1(t, x; T, u) + \hat{G}^2(t, x; T, u). \quad (5.36)$$

The first- and second-order approximation of the characteristic function, respectively (5.33) and (5.36), can be written in the form (5.7), for which the FFT-based algorithm can be used to compute the continuation value by means of the COS method in an efficient way.

5.4.3 Adjoint expansion for the second-order polynomial model

The adjoint expansion for the polynomial model is done in a similar way as the adjoint expansion for the OU process. However, the polynomial model does not have a constant volatility parameter, therefore it has an additional Taylor approximation term compared to the adjoint expansion for the OU process. In this section a second-order polynomial model will be considered, the adjoint expansion of higher-order polynomial models can be determined in the same way.

Consider the following second-order polynomial model, where X_t follows an OU process:

$$\begin{cases} S_t &= C X_t^2 + c X_t, \\ dX_t &= \kappa(\theta - X_t) dt + \sigma dW_t, \\ C &= \frac{1-c}{2}. \end{cases} \quad (5.37)$$

With Ito's lemma and the substitution of $X_t = \Phi^{-1}(S_t)$ the following SDE is obtained for this model:

$$dS_t = \tilde{\mu}(t, S_t)dt + \tilde{\sigma}(t, S_t)dW_t, \quad (5.38)$$

where for $C \neq 0$:

$$\begin{aligned} \tilde{\mu}(t, S_t) &= \kappa \left(\theta - \frac{\sqrt{c^2 + 4CS_t} - c}{2C} \right) \left(\sqrt{c^2 + 4CS_t} \right) + 2C\sigma^2, \\ \tilde{\sigma}(t, S_t) &= \sigma \left(\sqrt{c^2 + 4CS_t} \right). \end{aligned} \quad (5.39)$$

To obtain the approximation of the characteristic function we develop a Taylor expansion around \bar{x} for coefficients in the differential operator L (5.12):

$$a(t, x) := \frac{\tilde{\sigma}^2(t, x)}{2} \quad \text{and} \quad \tilde{\mu}(t, x).$$

The n^{th} -order approximation of L is defined as follows:

$$L_n := L_0 + \sum_{k=1}^n \left[\mu_k(x - \bar{x})^k \partial_x + a_k(x - \bar{x})^k \partial_{xx} \right], \quad (5.40)$$

where

$$L_0 = \partial_t + \mu_0 \partial_x + a_0 \partial_{xx},$$

and

$$\mu_n = \frac{\partial^n \mu(t, x)}{\partial x^n} \frac{1}{n!} \Big|_{x=\bar{x}} \quad \text{and} \quad a_n = \frac{\partial^n a(t, x)}{\partial x^n} \frac{1}{n!} \Big|_{x=\bar{x}}.$$

This gives us the following coefficients μ_n and a_n for $n \in \{0, 1\}$:

$$\begin{aligned} \mu_0 &= \kappa \left(\theta - \frac{\sqrt{c^2 + 4C\bar{x}} - c}{2C} \right) \cdot \left(\sqrt{c^2 + 4C\bar{x}} \right) + 2C\sigma^2, & a_0 &= \frac{1}{2}\sigma^2 (c^2 + 4C\bar{x}), \\ \mu_1 &= \frac{\kappa (-2\sqrt{c^2 + 4C\bar{x}} + c + 2C\theta)}{\sqrt{c^2 + 4C\bar{x}}}, & a_1 &= 2C\sigma^2 \end{aligned} \quad (5.41)$$

Remember that the n^{th} -order approximation of the density f is given by:

$$f^{(n)}(y|T, t, x) = \sum_{k=0}^n \bar{G}^k(t, x; T, y). \quad (5.42)$$

The fundamental solutions of the terms \bar{G}^k , $k \geq 0$, have the same Cauchy problems as described in (5.20) and (5.21), except $L_h - L_{h-1}$ (5.22) is different, $\forall h = 1, \dots, k$:

$$L_h - L_{h-1} = \mu_h(x - \bar{x})^h \partial_x + a_h(x - \bar{x})^h \partial_{xx}. \quad (5.43)$$

Remember also that the n^{th} -order approximation of the characteristic function is given by the Fourier transform of $f^{(n)}$ (5.42):

$$\phi^{(n)}(u|T, t, x) = \sum_{k=0}^n \mathbb{F}(\bar{G}^k(t, x; T, \cdot))(u) = \sum_{k=0}^n \hat{G}^k(t, x; T, u). \quad (5.44)$$

Furthermore, due to the fact that the operator L acts on (t, x) and the approximated characteristic function $\phi^{(n)}$ is a Fourier transform with respect to y , the adjoint operator of L will be used, acting on (T, y) . The adjoint Cauchy problems are as follows:

$$\begin{cases} \tilde{L}_0 \bar{G}^0(t, x; T, y) = 0, & T > t, y \in \mathbb{R}, \\ \bar{G}^k(T, x; T, y) = \delta_x(y), & y \in \mathbb{R}, \end{cases} \quad (5.45)$$

where

$$\tilde{L}_0 = -\partial_T - \mu_0 \partial_y + a_0 \partial_{yy}.$$

Moreover, the terms \bar{G}^k , for $k \geq 1$, are defined recursively as:

$$\begin{cases} \tilde{L}_0 \bar{G}^k(t, x; T, y) = -\sum_{h=1}^k (\tilde{L}_h - \tilde{L}_{h-1}) \bar{G}^{k-h}(t, x; T, y), & t \in [0, T), x \in \mathbb{R}, \\ \bar{G}^k(T, x; T, y) = 0, & x \in \mathbb{R}, \end{cases} \quad (5.46)$$

where $\forall h = 1, \dots, k$:

$$\begin{aligned} \tilde{L}_h - \tilde{L}_{h-1} = & -\mu_h(y - \bar{x})^h \partial_y - \mu_h h(y - \bar{x})^{h-1} + a_h h(h-1)(y - \bar{x})^{h-2} \\ & + 2a_h h(y - \bar{x})^{h-1} \partial_y + a_h (y - \bar{x})^h \partial_{yy}. \end{aligned}$$

In order to compute the terms \hat{G}^k , the Fourier transforms of the adjoint Cauchy problems (5.45) and (5.46) are taken. First we see that the Fourier transform of $\tilde{L}_0 \bar{G}^k(t, x; T, y)$, for all $k \geq 0$, w.r.t. y is given by:

$$\mathbb{F}(\tilde{L}_0 \bar{G}^k(t, x; T, \cdot))(u) = -\partial_T \hat{G}^k(t, x; T, u) + \psi(u) \hat{G}^k(t, x; T, u), \quad (5.47)$$

where

$$\psi(u) = \mu_0 i u - a_0 u^2. \quad (5.48)$$

Furthermore, the Fourier transform $\mathbb{F}(\tilde{L}_h - \tilde{L}_{h-1})$ is as follows, $\forall h = 1, \dots, k$:

$$\begin{aligned} \mathbb{F}(\tilde{L}_h - \tilde{L}_{h-1}) = & \mu_h (-i\partial_u - \bar{x})^h i u - \mu_h h (-i\partial_u - \bar{x})^{h-1} + a_h h(h-1) (-i\partial_u - \bar{x})^{h-2} \\ & - 2a_h h (-i\partial_u - \bar{x})^{h-1} i u - a_h (-i\partial_u - \bar{x})^h u^2. \end{aligned} \quad (5.49)$$

Hence, the Cauchy problems (5.45) and (5.46) have the following solution in the Fourier space:

$$\begin{cases} \hat{G}^0(t, x; T, u) = e^{iux + (T-t)\psi(u)}, \\ \hat{G}^k(t, x; T, u) = \int_t^T e^{\psi(u)(T-s)} \sum_{h=1}^k \mathbb{F}(\tilde{L}_h - \tilde{L}_{h-1}) \hat{G}^{k-h}(t, x; s, u) ds \quad k \geq 1. \end{cases} \quad (5.50)$$

For $k = 1$ we obtain:

$$\begin{aligned}
\hat{G}^1(t, x; T, u) &= \int_t^T e^{\psi(u)(T-s)} \left[\left(\mu_1(-i\partial_u - \bar{x})iu - \mu_1 - 2a_1iu \right. \right. \\
&\quad \left. \left. + a_1(-i\partial_u - \bar{x})(-u)^2 \right) \hat{G}^0(t, x; s, u) \right] ds \\
&= \int_t^T e^{\psi(u)(T-s)} \left[\left(\mu_1(-i\partial_u - \bar{x})iu - \mu_1 \right) \hat{G}^0(t, x; s, u) \right] ds \\
&\quad + \int_t^T e^{\psi(u)(T-s)} \left[\left(-2a_1iu + a_1(-i\partial_u - \bar{x})(-u)^2 \right) \hat{G}^0(t, x; s, u) \right] ds \\
&\stackrel{(5.32)}{=} \hat{G}^0(t, x; T, u) \mu_1 \left(\frac{1}{2} u \psi'(u) (T-t)^2 + iu(x - \bar{x})(T-t) \right) \\
&\quad + \hat{G}^0(t, x; T, u) \int_t^T a_1 i u^2 (ix + (s-t)\psi(u)) + a_1 \bar{x} u^2 ds \\
&= \hat{G}^0(t, x; T, u) \left(\mu_1 \frac{1}{2} u \psi'(u) (T-t)^2 + \mu_1 i u (x - \bar{x})(T-t) \right) \\
&\quad + \frac{1}{2} a_1 i u^2 \psi'(u) (T-t)^2 - a_1 u^2 (x - \bar{x})(T-t).
\end{aligned} \tag{5.51}$$

The first-order adjoint expansion approximation of the characteristic function of the second-order polynomial model is therefore:

$$\phi^{(1)}(u|T, t, x) = \hat{G}^0(t, x; T, u) + \hat{G}^1(t, x; T, u), \tag{5.52}$$

where $\hat{G}^0(t, x; T, u)$ and $\hat{G}^1(t, x; T, u)$ are respectively defined in (5.50) and (5.51). This can be written in the form (5.7), for which the FFT-based algorithm can be used to compute the continuation values by means of the COS method.

Remark 5.5. Most commonly used in practice is to expand the coefficients around $x = \bar{x}$, which simplifies the obtained approximations of the characteristic function significantly. In this way, the characteristic function approximation is just e^{iux} multiplied by a sum of terms that depend only on t , T and u . This has the same form as described in (4.15) with $\beta = 1$ and therefore the FFT-based algorithm can be used for the computation of the continuation values as mentioned in Remark 4.3.

If $x \neq \bar{x}$ then a FFT-based algorithm can still be used, for this we refer to section 3.2 of [48].

Example 5.6. In this example the first- and second-order adjoint expansion is used to approximate the characteristic function of the OU process with the parameters defined in (5.5). Figure 7 shows the real part of the approximation of the characteristic function of the OU process with the adjoint expansion and the absolute error of these approximations. The imaginary part of the characteristic function approximations has an error of the same order of magnitude as the real part.

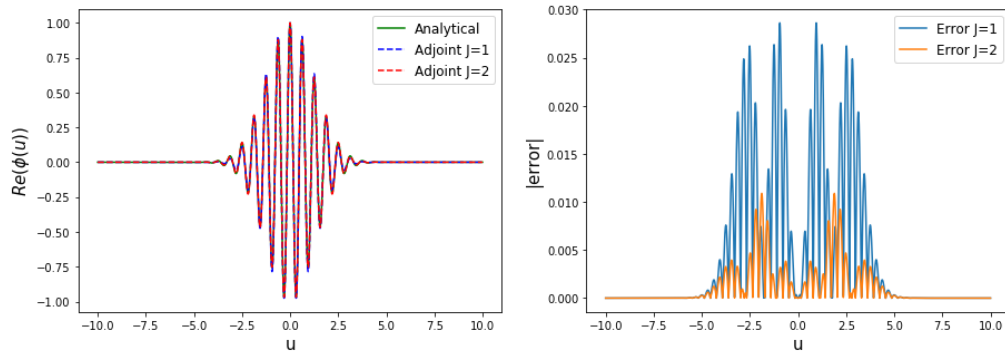


Figure 7: The approximation and absolute error of the characteristic function of the OU process with the adjoint expansion for $J = 1$ and $J = 2$, respectively (5.33) and (5.36).

5.5 An efficient characteristic function approximation for the COS method

In this section we introduce an adjustment to the characteristic function approximation with the cumulants, defined in Section 5.2, so that it can be used to efficiently compute the continuation values by means of the COS method with the FFT-based algorithm. The approximation with the cumulants is used because after testing the various approximations, the cumulant approximation was the most accurate and takes relatively little computation time (although these adjustments can also be applied to approximations with the moments and the empirical method, respectively Section 5.1 and 5.3).

The approximation with the adjoint expansion is also quite accurate and takes little computation time and the FFT-based algorithm can be directly applied without the adjustments introduced in this section, see Remark 5.5.

As mentioned in Section 4.2 and Remark 4.3, the efficient FFT-based algorithm can be used if the characteristic function can be written in the following form with $\beta = 1$:

$$\phi(u|x, \Delta t) = e^{iu\beta x} \phi(u|\Delta t) \stackrel{\beta=1}{=} e^{iu x} \phi(u|\Delta t), \quad (5.53)$$

where $\phi(u|\Delta t)$ does not depend on x .

The method suggested here uses the following two consecutive approximations on the closed-form characteristic function:

1. Approximate the closed-form characteristic function of a process with its cumulants, described in Section 5.2:

$$\hat{\phi}_1(u|x, \Delta t) = \exp \left(\sum_{j=1}^J \kappa_j \frac{(iu)^j}{j!} \right). \quad (5.54)$$

This approximation has the following relation with the closed-form characteristic function:

$$\begin{aligned} \hat{\phi}_1(u|x, \Delta t) &= \phi(u|x, \Delta t) \cdot e^{-iu \sum_{j=J+1}^{\infty} \kappa_j \frac{(iu)^{j-1}}{j!}} \\ &= \phi(u|x, \Delta t) \cdot e^{iu\hat{\epsilon}_1}, \end{aligned} \quad (5.55)$$

where

$$\hat{\epsilon}_1 = - \sum_{j=J+1}^{\infty} \kappa_j \frac{(iu)^{j-1}}{j!}. \quad (5.56)$$

However the value of the stochastic process at time t , denoted as x , is not known for $t > 0$, due to the fact that the asset/electricity prices are simulated from time $t = 0$. Therefore we use $\mathbb{E}[x|\mathcal{F}_0]$ instead of x in our approximation of the characteristic function. This results in the following approximation of the characteristic function $\phi(u|\Delta t, x) = \int_{-\infty}^{\infty} e^{iuy} f(y|\Delta t, x) dy$:

$$\tilde{\phi}_1(u|x, \Delta t) = \exp \left(\sum_{j=1}^J \tilde{\kappa}_j \frac{(iu)^j}{j!} \right), \quad (5.57)$$

where $\tilde{\kappa}_j$ is the j^{th} order cumulant of y conditional on $\mathbb{E}[x|\mathcal{F}_0]$ and $\Delta t = T - t$.

The approximation (5.57) has the following relation with the closed-form characteristic function:

$$\begin{aligned} \tilde{\phi}_1(u|x, \Delta t) &= \phi(u|\mathbb{E}[x|\mathcal{F}_0], \Delta t) \cdot e^{-iu \sum_{j=J+1}^{\infty} \tilde{\kappa}_j \frac{(iu)^{j-1}}{j!}} \\ &= e^{iu\beta\mathbb{E}[x|\mathcal{F}_0]} \phi(u|\Delta t) \cdot e^{-iu \sum_{j=J+1}^{\infty} \tilde{\kappa}_j \frac{(iu)^{j-1}}{j!}} \\ &= \phi(u|x, \Delta t) \cdot e^{iu\beta(\mathbb{E}[x|\mathcal{F}_0] - x)} \cdot e^{-iu \sum_{j=J+1}^{\infty} \tilde{\kappa}_j \frac{(iu)^{j-1}}{j!}} \\ &= \phi(u|x, \Delta t) \cdot e^{iu\tilde{\epsilon}_1}, \end{aligned} \quad (5.58)$$

where

$$\tilde{\epsilon}_1 = \beta (\mathbb{E}[x|\mathcal{F}_0] - x) - \sum_{j=J+1}^{\infty} \tilde{\kappa}_j \frac{(iu)^{j-1}}{j!}. \quad (5.59)$$

2. Approximate the characteristic function so that the FFT-based algorithm can be applied, which is the case when $\beta = 1$. This can be accomplished by the following approximation of the general characteristic function [43]:

$$\tilde{\phi}_2(u|x, \Delta t) = \phi(u|\mathbb{E}[x|\mathcal{F}_0], \Delta t) e^{iux} e^{-iu\mathbb{E}[x|\mathcal{F}_0]}. \quad (5.60)$$

It has the following connection with the closed-form characteristic function:

$$\begin{aligned} \tilde{\phi}_2(u|x, \Delta t) &= \phi(u|\mathbb{E}[x|\mathcal{F}_0], \Delta t) e^{iux} e^{-iu\mathbb{E}[x|\mathcal{F}_0]} \\ &= e^{iu\beta\mathbb{E}[x|\mathcal{F}_0]} \phi(u|\Delta t) e^{iux} e^{-iu\mathbb{E}[x|\mathcal{F}_0]} \\ &= e^{iu\beta\mathbb{E}[x|\mathcal{F}_0]} \phi(u|\Delta t) e^{iux} e^{-iu\mathbb{E}[x|\mathcal{F}_0]} e^{iu\beta x} e^{-iu\beta x} \\ &= e^{iu\beta x} \phi(u|\Delta t) e^{iux} e^{-iu\mathbb{E}[x|\mathcal{F}_0]} e^{iu\beta\mathbb{E}[x|\mathcal{F}_0]} e^{-iu\beta x} \\ &= \phi(u|x, \Delta t) \cdot e^{iu(1-\beta)(x - \mathbb{E}[x|\mathcal{F}_0])} \\ &= \phi(u|x, \Delta t) \cdot e^{iu\tilde{\epsilon}_2}, \end{aligned} \quad (5.61)$$

where $\tilde{\epsilon}_2$ is defined by:

$$\tilde{\epsilon}_2 = (1 - \beta)(x - \mathbb{E}[x|\mathcal{F}_0]). \quad (5.62)$$

These two approximation methods can be combined, which results in the following approximation of the characteristic function:

$$\tilde{\phi}(u|x, \Delta t) = \tilde{\phi}_1(u|x, \Delta t) \cdot e^{iux} e^{-iu\mathbb{E}[X_t|\mathcal{F}_0]}. \quad (5.63)$$

This approximation has the following relation with the closed-form characteristic function:

$$\begin{aligned} \tilde{\phi}(u|x, \Delta t) &= \tilde{\phi}_1(u|x, \Delta t) \cdot e^{iux} \cdot e^{-iu\mathbb{E}[x|\mathcal{F}_0]} \\ &\stackrel{(5.58)}{=} \phi(u|\mathbb{E}[x|\mathcal{F}_0], \Delta t) \cdot e^{-iu \sum_{j=J+1}^{\infty} \tilde{\kappa}_j \frac{(iu)^{j-1}}{j!}} \cdot e^{iux} \cdot e^{-iu\mathbb{E}[x|\mathcal{F}_0]} \\ &\stackrel{(5.61)}{=} \phi(u|x, \Delta t) \cdot e^{iu(1-\beta)(x-\mathbb{E}[x|\mathcal{F}_0])} \cdot e^{-iu \sum_{j=J+1}^{\infty} \tilde{\kappa}_j \frac{(iu)^{j-1}}{j!}} \\ &= \phi(u|x, \Delta t) \cdot e^{iu\epsilon_3}, \end{aligned} \quad (5.64)$$

where ϵ_3 is defined as follows:

$$\epsilon_3 = (1 - \beta)(x - \mathbb{E}[x|\mathcal{F}_0]) - \sum_{j=J+1}^{\infty} \tilde{\kappa}_j \frac{(iu)^{j-1}}{j!}. \quad (5.65)$$

5.6 Error analysis for COS method with approximated characteristic function

This section shows the error of using the approximated characteristic function as defined in (5.63) for the valuation of a Bermudan option with the COS method. In this error analysis we follow the analysis from [43] applied to our approximation of the characteristic function. The error is described as the difference between the Bermudan option value obtained with the closed-form characteristic function and obtained with the approximated characteristic function. There is also an error using the COS method itself, this error and its convergence are described in [39]. Furthermore, the error of using the adjoint expansion for valuation of Bermudan options is specified in Section 4 of [48].

For the error analysis the following errors are considered:

- ϵ_3 : The error by approximating the characteristic function as in (5.64).
- $\epsilon_c(x, t)$: The error in the continuation value at time t .
- $\epsilon_x(t)$: The error in the early-exercise point x_t^* at exercise moment t .
- $\epsilon_v(t)$: The error in the coefficients $V_k(t)$.

As earlier mentioned, the value of the Bermudan option is recovered in a backward manner. The error analysis is approached in the same way, first the error in the step from t_M to t_{M-1} is examined.

The error in the first step

In this step an error, due to the approximation of the characteristic function, is distinguished in the continuation value and in the computation of the early-exercise point $x_{t_{M-1}}^*$ with Newton's method. These errors are the origin of the error in the coefficients $V_k(t_{M-1})$, defined by $\epsilon_v(t_{M-1})$. For the other steps, $m = 1, \dots, M - 2$, the errors in the continuation value and the early-exercise point are not only related to the approximated characteristic function, but also to the error in the coefficients $V_k(t_{m+1})$.

The error in the continuation value in the first step is given in the Lemma 5.7.

Lemma 5.7. The error in the continuation value is given by

$$\epsilon_c(x, t_{M-1}) = \hat{c}(x + \beta^{-1}\epsilon_3, t_{M-1}) - \hat{c}(x, t_{M-1}), \quad (5.66)$$

where $\hat{c}(x, t)$ is from the COS formula for the continuation value, defined in (4.39), and ϵ_3 is defined in (5.65).

Proof. In (5.64) the relation between the approximated and the closed-form characteristic functions is defined. By rewriting we get:

$$\begin{aligned} \tilde{\phi}(u|x, \Delta t) &= \phi(u|x, \Delta t) \cdot e^{iu\epsilon_3} \\ &= e^{iu\beta x} \phi(u|\Delta t) \cdot e^{iu\epsilon_3} \\ &= e^{iu\beta(x + \beta^{-1}\epsilon_3)} \phi(u|\Delta t) \\ &= \phi(u|x + \beta^{-1}\epsilon_3, \Delta t). \end{aligned} \quad (5.67)$$

By inserting this into the COS formula for the continuation value $\hat{c}(x, t_{M-1})$, (4.39), the following is obtained:

$$\tilde{c}(x, t_{M-1}) := \hat{c}(x + \beta^{-1}\epsilon_3, t_{M-1}). \quad (5.68)$$

Therefore the error in the continuation value, due to the use of the approximated characteristic function, is as follows:

$$\epsilon_c(x, t_{M-1}) = \tilde{c}(x, t_{M-1}) - \hat{c}(x, t_{M-1}) = \hat{c}(x + \beta^{-1}\epsilon_3, t_{M-1}) - \hat{c}(x, t_{M-1}).$$

□

Next a corollary is presented, which explains how the positivity/negativity of the error of the characteristic function affects the positivity/negativity of the error of the continuation value and early-exercise point.

Corollary 5.8. For put options it holds that if $\beta^{-1}\epsilon_3 > 0$, then $\epsilon_c(x, t_{M-1}) < 0 \forall x$ and subsequently $\epsilon_x(t_{M-1}) > 0$. To the contrary, if $\beta^{-1}\epsilon_3 < 0$, then $\epsilon_c(x, t_{M-1}) > 0 \forall x$ and subsequently $\epsilon_x(t_{M-1}) < 0$.

Proof. The continuation value is a decreasing function for put options, which implies that for $\beta^{-1}\epsilon_3 > 0$ and $\forall x$:

$$\hat{c}(x + \beta^{-1}\epsilon_3, t_{M-1}) < \hat{c}(x, t_{M-1}). \quad (5.69)$$

Thus it holds according to lemma 5.7 that:

$$\epsilon_c(x, t_{M-1}) = \hat{c}(x + \beta^{-1}\epsilon_3, t_{M-1}) - \hat{c}(x, t_{M-1}) < 0.$$

Now it is shown that $\epsilon_x(t_{M-1}) > 0$. It is known that the early-exercise point x^* is the point where the continuation value is equal to the payoff function. So for the early exercise point, obtained by the closed-form characteristic function, we have:

$$\hat{c}(x_{t_{M-1}}^*, t_{M-1}) = g(x_{t_{M-1}}^*, t_{M-1}).$$

As a result and by the fact that the continuation value is a decreasing function it holds that:

$$\tilde{c}(x_{t_{M-1}}^*, t_{M-1}) = \hat{c}(x_{t_{M-1}}^* + \beta^{-1}\epsilon_3, t_{M-1}) < \hat{c}(x_{t_{M-1}}^*, t_{M-1}) = g(x_{t_{M-1}}^*, t_{M-1}), \quad (5.70)$$

where equation (5.68) is used.

So the continuation value obtained with the approximated characteristic function, $\tilde{c}(x_{t_{M-1}}^*, t_{M-1})$, is less than the payoff function, $g(x_{t_{M-1}}^*, t_{M-1})$. Consequently the early-exercise point obtained by the approximated characteristic function must be larger than the early-exercise point obtained by the closed-form characteristic function and thus $\epsilon_x(t_{M-1}) > 0$.

The proof that if $\beta^{-1}\epsilon_3 < 0$ then $\epsilon_c(x, t_{M-1}) > 0 \forall x$ and subsequently $\epsilon_x(t_{M-1}) < 0$ is similar. \square

The next lemma shows the upper bounds of the absolute errors $|\epsilon_c(x, t_{M-1})|$ and $|\epsilon_x(t_{M-1})|$.

Lemma 5.9. $\forall x \in [a, b]$ and $\forall t$, we have that:

$$|\hat{c}(x + \beta^{-1}\epsilon_3, t) - \hat{c}(x, t)| \leq \Theta \cdot |\beta^{-1}\epsilon_3| =: \tilde{\epsilon}_c, \quad (5.71)$$

where Θ is based on the underlying process X_t being used for the characteristic function and subsequent on the terms which are represented in the payoff function of the put option:

$$\Theta = \begin{cases} Ke^a, & \text{for } S_t = Ke^{X_t}, \\ e^a, & \text{for } S_t = e^{X_t}, \\ 1, & \text{for } S_t = X_t, \\ \left. \frac{\partial}{\partial x} \Phi(x) \right|_{x=a}, & \text{for } S_t = \Phi(X_t). \end{cases} \quad (5.72)$$

The bound (5.71) implies that $\forall x \in [a, b]$:

$$|\epsilon_c(x, t_{M-1})| \leq \tilde{\epsilon}_c, \quad (5.73)$$

Furthermore, the error $|\epsilon_x(t_{M-1})|$ is bounded by:

$$|\epsilon_x(t_{M-1})| \leq \frac{\tilde{\epsilon}_c}{|h'(\bar{\delta}, t_{M-1})|}, \quad (5.74)$$

for some $\bar{\delta} \in (x_{t_{M-1}}^*, x_{t_{M-1}}^* + \epsilon_x(t_{M-1}))$ and $h'(x, t) = \frac{\partial}{\partial x} h(x, t) = \frac{\partial}{\partial x} (g(x, t) - \hat{c}(x, t))$.

Proof. This is the proof for the polynomial model $S_t = \Phi(X_t)$ where the characteristic function of the underlying process X_t is used. The differences in the proof for other processes will be indicated in brackets.

First the Lagrange's mean value theorem is applied:

$$|\hat{c}(x + \beta^{-1}\epsilon_3, t) - \hat{c}(x, t)| = |\beta^{-1}\epsilon_3| \left| \left[\frac{\partial}{\partial x} c(x, t) \right]_{x=\delta_0} \right|, \quad (5.75)$$

where $\delta_0 \in (x, x + \beta^{-1}\epsilon_3)$. Note that for a Bermudan put option it holds that $\frac{\partial c(x, t)}{\partial x}$ is a non-positive and non-decreasing function for $x \geq \Phi^{-1}(K)$ (With $S_t = X_t$ it holds for $x \geq K$, with $S_t = e^{X_t}$ for $x \geq \log(K)$ and with $S_t = Ke^{X_t}$ for $x \geq 0$). Furthermore, $\frac{\partial c(x, t)}{\partial x}$ goes to zero as x goes to infinity. Therefore, if $a \geq \Phi^{-1}(K)$ we have:

$$\max_{x \in [a, b]} \left| \frac{\partial c(x, t)}{\partial x} \right| = \left| \left[\frac{\partial c(x, t)}{\partial x} \right]_{x=a} \right|. \quad (5.76)$$

This derivative of the continuation value at $x = a$ is denoted by $c'(a, t)$. Now (5.75) can be bounded by:

$$|\hat{c}(x + \beta^{-1}\epsilon_3, t) - \hat{c}(x, t)| \leq |\beta^{-1}\epsilon_3| |c'(a, t)|.$$

If $a < \Phi^{-1}(K)$, the equation (5.76) does not hold. However, this upper bound is still valid, because otherwise the error can be overestimated [43], e.g. when x is very small the payoff function is used instead of the continuation value over the integration range $[a, b]$ and thus the error will be zero.

Thus, it holds that for each time step that $|c'(x, t)| \leq |g'(x, t)|$ for $x < \Phi^{-1}(K)$. So, for $a < \Phi^{-1}(K)$ we have:

$$|c'(a, t)| \leq |g'(a, t)| = \Phi'(a).$$

For $a \geq \Phi^{-1}(K)$ it holds that:

$$|c'(a, t)| \leq |c'(\Phi^{-1}(K), t)| \leq |g'(\Phi^{-1}(K), t)| = \Phi'(\Phi^{-1}(K)) \leq \Phi'(a).$$

Thus for all cases we have:

$$|c'(a, t)| \leq \Phi'(a). \quad (5.77)$$

Similar derivations can be done for $S_t = Ke^{X_t}$, $S_t = e^{X_t}$ and $S_t = X_t$, which results in:

$$|c'(a, t)| \leq \begin{cases} Ke^a, & \text{for } S_t = Ke^{X_t}, \\ e^a, & \text{for } S_t = e^{X_t}, \\ 1, & \text{for } S_t = X_t, \\ \left. \frac{\partial}{\partial x} \Phi(x) \right|_{x=a}, & \text{for } S_t = \Phi(X_t). \end{cases} \quad (5.78)$$

By substitution of (5.78) in (5.76) the following boundary is obtained $\forall x \in [a, b]$ and $\forall t$:

$$|\hat{c}(x + \beta^{-1}\epsilon_3, t) - \hat{c}(x, t)| \leq \Theta \cdot |\beta^{-1}\epsilon_3| =: \tilde{\epsilon}_c,$$

where Θ is defined in (5.72). Thus it holds that:

$$|\epsilon_c(x, t_{M-1})| \leq \tilde{\epsilon}_c.$$

Now we take a look at the error in the early-exercise point at time t_{M-1} . Assume $x_{t_{M-1}}^*$ and $x_{t_{M-1}}^* + \epsilon_x(t_{M-1})$ are the early-exercise points obtained by the closed-form and approximated characteristic function, respectively. We have:

$$\begin{aligned}\hat{c}(x_{t_{M-1}}^*, t_{M-1}) &= g(x_{t_{M-1}}^*, t_{M-1}), \\ \tilde{c}(x_{t_{M-1}}^* + \epsilon_x(t_{M-1}), t_{M-1}) &= g(x_{t_{M-1}}^* + \epsilon_x(t_{M-1}), t_{M-1}).\end{aligned}\tag{5.79}$$

Therefore:

$$\begin{aligned}g(x_{t_{M-1}}^* + \epsilon_x(t_{M-1}), t_{M-1}) - \hat{c}(x_{t_{M-1}}^* + \epsilon_x(t_{M-1}), t_{M-1}) \\ = \tilde{c}(x_{t_{M-1}}^* + \epsilon_x(t_{M-1}), t_{M-1}) - \hat{c}(x_{t_{M-1}}^* + \epsilon_x(t_{M-1}), t_{M-1}) \\ = \hat{c}(x_{t_{M-1}}^* + \epsilon_x(t_{M-1}) + \epsilon_x(t_{M-1}), t_{M-1}) - \hat{c}(x_{t_{M-1}}^* + \epsilon_x(t_{M-1}), t_{M-1}) \\ =: \epsilon_c(x_{t_{M-1}}^* + \epsilon_x(t_{M-1}), t_{M-1}),\end{aligned}\tag{5.80}$$

using equation (5.68).

We define the following function: $h(x, t) := g(x, t) - \hat{c}(x, t)$. Due to (5.79) and (5.80) it holds respectively:

$$\begin{aligned}h(x_{t_{M-1}}^*, t_{M-1}) &= 0, \\ h(x_{t_{M-1}}^* + \epsilon_x(t_{M-1}), t_{M-1}) &= \epsilon_c(x_{t_{M-1}}^* + \epsilon_x(t_{M-1}), t_{M-1}).\end{aligned}\tag{5.81}$$

By (5.81) and because we already saw that $|\epsilon_c(x, t_{M-1})| \leq \Theta|\beta^{-1}\epsilon_3| \forall x$, it holds that:

$$|h(x_{t_{M-1}}^* + \epsilon_x(t_{M-1}), t_{M-1}) - h(x_{t_{M-1}}^*, t_{M-1})| = |\epsilon_c(x_{t_{M-1}}^* + \epsilon_x(t_{M-1}), t_{M-1})| \leq \Theta|\beta^{-1}\epsilon_3|.$$

By the Lagrange mean value theory we obtain:

$$|\epsilon_x(t_{M-1})| \left| \left[\frac{\partial h(x, t_{M-1})}{\partial x} \right]_{x=\bar{\delta}} \right| \leq \Theta|\beta^{-1}\epsilon_3|,$$

where $\bar{\delta} \in (x_{t_{M-1}}^*, x_{t_{M-1}}^* + \epsilon_x(t_{M-1}))$.

Due to the fact that the early-exercise point x^* is unique for Bermudan put options it holds that:

$$|h(x_{t_{M-1}}^* + \epsilon_x(t_{M-1}), t_{M-1}) - h(x_{t_{M-1}}^*, t_{M-1})| > 0.$$

Therefore if $\epsilon_x(t_{M-1}) \neq 0$ we have $|h'(\bar{\delta}, t_{M-1})| > 0$ and thus:

$$|\epsilon_x(t_{M-1})| \leq \frac{\Theta|\beta^{-1}\epsilon_3|}{|h'(\bar{\delta}, t_{M-1})|}.$$

□

As shown in Lemma 5.9, the upper bound for the error in the early-exercise points can be determined by the error of the continuation value. If the error of the continuation value goes to zero, the error of the early-exercise points also goes to zero.

In the next lemma the error of the coefficients $V_k(t_{M-1})$, defined in (4.42), is examined.

Lemma 5.10. For $\epsilon_x(t_{M-1}) > 0$, there exists two points, $\delta_1 \in (x_{t_{M-1}}^* + \epsilon_x(t_{M-1}), b)$ and $\delta_2 \in (x_{t_{M-1}}^*, x_{t_{M-1}}^* + \epsilon_x(t_{M-1}))$, so that:

$$\begin{aligned} \epsilon_v(t_{M-1}) = & \epsilon_c(\delta_1, t_{M-1}) I_k(x_{t_{M-1}}^* + \epsilon_x(t_{M-1}), b) \\ & + (g(\delta_2, t_{M-1}) - \hat{c}(\delta_2, t_{M-1})) I_k(x_{t_{M-1}}^*, x_{t_{M-1}}^* + \epsilon_x(t_{M-1})), \end{aligned} \quad (5.82)$$

where

$$I_k(x_1, x_2) = \frac{2}{b-a} \int_{x_1}^{x_2} \cos\left(k\pi \frac{x-a}{b-a}\right) dx.$$

Moreover, there is an upper bound for the terms in front of the integral I_k :

$$|\epsilon_c(\delta_1, t_{M-1})| \leq \tilde{\epsilon}_c \quad \text{and} \quad |(g(\delta_2, t_{M-1}) - \hat{c}(\delta_2, t_{M-1}))| \leq \tilde{\epsilon}_c.$$

Proof. See Lemma 4.3 of [43]. □

Remark 5.11. The proof where $\epsilon_x(t_{M-1}) < 0$ goes similar and gives the following results. There exists two points, $\delta_1 \in (x_{t_{M-1}}^*, b)$ and $\delta_2 \in (x_{t_{M-1}}^* + \epsilon_x(t_{M-1}), x_{t_{M-1}}^*)$, so that:

$$\begin{aligned} \epsilon_v(t_{M-1}) = & \epsilon_c(\delta_1, t_{M-1}) I_k(x_{t_{M-1}}^*, b) \\ & + (g(\delta_2, t_{M-1}) - \hat{c}(\delta_2, t_{M-1})) I_k(x_{t_{M-1}}^* + \epsilon_x(t_{M-1}), x_{t_{M-1}}^*). \end{aligned} \quad (5.83)$$

Moreover, $|\epsilon_c(\delta_1, t_{M-1})| \leq \tilde{\epsilon}_c$ and $|(g(\delta_2, t_{M-1}) - \hat{c}(\delta_2, t_{M-1}))| \leq \tilde{\epsilon}_c$.

Remark 5.12. As described in (4.44), the coefficient $V_k(t)$ can be split in two parts, in one part the continuation value is considered and in the other part the payoff function. The error $\epsilon_v(t_{M-1})$, for $\epsilon_x(t_{M-1}) > 0$, also consists of two parts:

1. $\epsilon_c(\delta_1, t_{M-1}) I_k(x_{t_{M-1}}^* + \epsilon_x(t_{M-1}), b)$.
2. $(g(\delta_2, t_{M-1}) - \hat{c}(\delta_2, t_{M-1})) I_k(x_{t_{M-1}}^*, x_{t_{M-1}}^* + \epsilon_x(t_{M-1}))$.

The two parts of the error refer to the split in the coefficient $V_k(t)$. The first error occurs because the continuation value is taken between $x^* + \epsilon_x$ and b instead of between x^* and b . The second error because the payoff function is taken between a and $x^* + \epsilon_x$ instead of between a and x^* . A similar statement can be made about $\epsilon_x(t_{M-1}) < 0$.

The error in the other steps

The error in the steps $m \in \{M-2, \dots, 1\}$ will be determined with a backward induction proof. The main idea is to find an upper bound for $\epsilon_c(x, t_0)$, because as earlier mentioned it holds that the value of a Bermudan option at initial time t_0 is equal to the continuation value at time t_0 , $v(x, t_0) = c(x, t_0)$. First the error at exercise moment $t = t_{M-2}$ will be analysed:

Lemma 5.13. $\forall x \in [a, b]$ it holds that:

$$|\epsilon_c(x, t_{M-2})| \leq \tilde{\epsilon}_c \cdot (1 + e^{-r\Delta t}),$$

where $\Delta t = \frac{T}{M}$ and $\tilde{\epsilon}_c$ defined in (5.71).

Proof. See Lemma 4.4 of [43]. □

With induction the error in the continuation value at t_0 is obtained as follows:

Theorem 5.14. $\forall x \in [a, b]$, $j \in \{1, \dots, M - 1\}$ and where the induction assumption is:

$$|\epsilon_c(x, t_{M-j})| \leq \tilde{\epsilon}_c \sum_{l=1}^j e^{-r(l-1)\Delta t}.$$

Then it follows that, $\forall x$,

$$|\epsilon_c(x, t_{M-j-1})| \leq \tilde{\epsilon}_c \sum_{l=1}^{j+1} e^{-r(l-1)\Delta t}.$$

Proof. See Theorem 4.1 and Remark 4.2 of [43]. □

Remark 5.15. The error in the Bermudan option value at initial time t_0 is equal to the error of the continuation value at time t_0 and therefore can be bounded according to Theorem 5.14 by:

$$|\epsilon_c(x, t_0)| \leq \tilde{\epsilon}_c \sum_{l=1}^M e^{-r(l-1)\Delta t},$$

where $\Delta t = \frac{T}{M}$ and $\tilde{\epsilon}_c$ defined in (5.71).

6 The Least Squares Monte Carlo method

In this section the Least Squares Monte Carlo method (LSMC) is discussed, developed by Longstaff and Schwartz [50]. Remember that the values of the Bermudan option, the Bermudan option with multiple early-exercise rights and the electricity storage contract are obtained by computing the continuation values. Therefore it is important for the valuation of these financial derivatives to determine the continuation value as accurate as possible. In Section 4 the COS method is used to obtain an approximation of the continuation values. The LSMC is another method to approximate these continuation values, based on simulations of the asset price.

This method presents a simple, intuitive, yet powerful approximation to value the Bermudan option, the Bermudan option with multiple early-exercise rights and the electricity storage contract. The main insight behind LSMC is that the conditional expectation to compute the continuation value can be approximated by the use of least squares regression as a function of the simulated price process.

An advantage of the LSMC is that it is not model dependent, a multi-factor pricing model can be valued just as easily as a simpler model. In addition, the method is easy to implement, since only a least squares regression is needed on the simulations of the pricing model. However, the COS method generally has less CPU time, jumps in the price process are easy to add with the COS method and the Greeks can be determined without additional computational costs.

6.1 LSMC for Bermudan options

The LSMC for Bermudan options uses least squares regression to compute the continuation value at the M exercise moments, t_1, \dots, t_M . This is done for each simulated asset price path. Recall that the continuation value is computed in a backward manner, as described in the backward induction algorithm (3.10).

Before explaining the backward algorithm of the LSMC method, the following notations are defined:

- S_m^i : the asset price of trajectory i at time t_m .
- $PO_m^i := g(t_m, S_m^i)$, where $g(t, S)$ is the payoff function of asset S at time t .
- $CV_m^i := c(t_m, S_m^i)$, where $c(t, S)$ is the continuation value of asset S at time t .
- CF_m^i : The cash flow of the asset trajectory i at time t_m . Note that for each trajectory i there is at most one exercise moment $t_m \in \{t_1, \dots, t_M\}$ where the cash flow $CF_m^i > 0$, since the Bermudan option has only one exercise right.
- $DCF_m^i := \sum_{k>m} e^{-r(k-m)\Delta t} CF_k^i$, is the discounted cash flow.

With the LSMC method we start at the last exercise moment t_M and work backward in time. At time t_M the continuation values of all the trajectories are equal to zero, since it is the last moment to exercise. Therefore at time t_M the cash flow equals the payoff, \forall trajectories i :

$$CF_M^i = PO_M^i,$$

where for a Bermudan put option the payoff is defined by $PO_m^i := \max(K - S_m^i, 0)$.

For the next step, at exercise moment t_{M-1} , the option is exercised iff the payoff at time t_{M-1} exceeds the continuation value, i.e. the value of exercising exceeds the value if you do not exercise.

The LSMC method uses least squares regression of the discounted cash flows DCF_{M-1}^i onto the basis functions of the asset price of all the trajectories that are in the money at time t_{M-1} to approximate the continuation value. Only in the money asset trajectories are considered since the exercise decision is only relevant if the option is in the money, otherwise you will not exercise. The approximation of the continuation value with the LSMC is defined as follows, for all trajectories i that are in the money at time t_{M-1} :

$$CV_{M-1}^i \approx \sum_{p=1}^P a_p^{M-1} B_p(S_{M-1}^i), \quad (6.1)$$

where B_p is the set of basis functions of the asset price S_{M-1}^i and a_p^{M-1} the regression coefficients at time t_{M-1} . For example if a third-order polynomial is used for the regression then: $CV_{M-1}^i \approx a_1 + a_2 S_{M-1}^i + a_3 (S_{M-1}^i)^2 + a_4 (S_{M-1}^i)^3$. Finding the regression coefficient a_p^{M-1} boils down to regressing the discounted cash flows, DCF_{M-1} , on the asset prices, S_{M-1} , such that the coefficients fit the cross-sectional data best in least squares sense.

Now that the continuation value is approximated, the exercise decision at time t_{M-1} can be updated. The holder of the option will perform the early-exercise of trajectory i at time t_{M-1} if the payoff function exceeds the continuation value, $PO_{M-1}^i > CV_{M-1}^i$. The cash flow values for each trajectory are now updated as follows:

$$CF_{M-1}^i = \begin{cases} PO_{M-1}^i & , \text{if } PO_{M-1}^i > CV_{M-1}^i, \\ 0 & , \text{otherwise.} \end{cases} \quad (6.2)$$

Note that when the trajectory is exercised at time t_{M-1} and thus the cash flow CF_{M-1}^i is set to the payoff function, the cash flow at time t_M is set to zero, because a Bermudan option has only one exercise right.

For the other iterations backward in time, $m \in \{M-2, \dots, 1\}$, the same steps can be taken to obtain the cash flow CF_m^i of each trajectory i . So the cash flow is set to the payoff function if $PO_m^i > CV_m^i$, where the continuation value is approximated by (6.1) applied to t_m instead of t_{M-1} . Again note that the cash flow CF_k^i for $k > m$ is set to zero if the holder exercises at time t_m , because the Bermudan option can only be exercised once.

At the end, when all the cash flows CF_m^i are known for all trajectories $i \in \{1, \dots, N\}$ and all time steps $m \in \{1, \dots, M\}$, the approximation of the Bermudan option value is given by the arithmetic average of the discounted cash flows:

$$v(t_0, S_0) \approx \frac{1}{N} \sum_{i=1}^N DCF_0^i = \frac{1}{N} \sum_{i=1}^N \sum_{m=1}^M e^{-r \cdot m \Delta t} CF_m^i. \quad (6.3)$$

The pseudocode of the LSMC method for pricing the Bermudan option is given in Algorithm 1 in Appendix B.

6.2 LSMC for Bermudan options with multiple early-exercise rights

In this section the LSMC method for Bermudan options is extended to have multiple early-exercise rights. This extension is introduced by Dörr [51].

The LSMC method for multiple early-exercise rights works in a similar way as for the Bermudan options, where the holder can only exercise once - described in Section 6.1. However, now the number of early-exercise rights left must be taken into account. Therefore, in the notation of Section 6.1 a superscript j is added for the variables affected by the number of early-exercise rights left:

- $CV_m^{i,j} := c^j(t_m, S_m^i)$, where $c^j(t_m, S_m^i)$ is the continuation value of the option with $j \in \mathcal{R}$ rights left at time t_m with the underlying asset S_m^i .
- $CF_m^{i,j}$: The cash flow of the asset trajectory i at time t_m with $j \in \mathcal{R}$ rights left.
- $DCF_m^{i,j} := \sum_{k>m} e^{-r(k-m)\Delta t} CF_k^{i,j}$ is the discounted cash flow if there are $j \in \mathcal{R}$ rights left.

For the asset price and the payoff of trajectory i at time t_m the same notation is used as in section 6.1, respectively S_m^i and PO_m^i .

The main difference between the LSMC method for one early-exercise right and for multiple early-exercise rights is that the value of exercising the option is not only equal to the payoff but equal to the payoff plus the continuation value with one right less. Therefore least squares regression needs to be done to approximate the continuation value for all the number of exercise rights $j \in \mathcal{R}$. Furthermore, due to the fact that the holder has more than one early-exercise right the cash flow for trajectory i can be positive for more than one exercise moment, in contrast with the LSMC method for the Bermudan option.

Now the backward LSMC algorithm for the Bermudan option with multiple early-exercise rights will be elaborated. The algorithm has the same two settings/steps as described in Section 3.3:

1. The LSMC algorithm starts with the initialization for all the level of rights $j \in \mathcal{R}$, i.e. when the number of exercise rights is equal to the number of exercise moments. Note that in this initialization there is no need to compute the continuation value, because the holder will exercise at each exercise moment if the value is positive. Therefore the cash flow at these exercise moments equals the payoff. Thus the cash flow with j rights left is as follows, for all trajectories i :

$$CF_m^{i,j} = PO_m^i, \quad \text{for } m \in M, \dots, M - j + 1.$$

2. Now the cash flows are described for the setting when there are less exercise rights than exercise moments. Here the holder has to make the decision if he/she wants to exercise the option early and continue with one right less or to not exercise and continue with the same amount of rights. So in contrast to the initialization step, the continuation value needs to be computed $\forall j \in \mathcal{R}$ to make this decision.

The approximation of the continuation value is done with least squares regression in a similar way as with the LSMC method for the Bermudan option. For each number of

rights $j \in \mathcal{R}$, which is less than the number of exercise moments left, the continuation value at time t_m is approximated separately for each j by least squares regression of the cash flow discounted to t_m onto the basis functions of the asset price trajectories at time t_m . In the regression only the trajectories with positive payoff are considered, as discussed in Section 6.1.

After the approximation of the continuation values, the decision can be made if the holder should use the early-exercise right or continue with the same amount of rights. The holder of the option prefers the choice that has the most value at that time. Therefore the right to exercise early is used if and only if $PO_m^i + CV_m^{i,j-1} > CV_m^{i,j}$ for $m \in \{M-j, \dots, 1\}$. This results in the following cash flow with $j \in \mathcal{R}$ rights at time t_m for each trajectory i , for $m \in \{M-j, \dots, 1\}$:

$$CF_m^{i,j} = \begin{cases} PO_m^i & , \text{if } PO_m^i + CV_m^{i,j-1} > CV_m^{i,j}, \\ 0 & , \text{otherwise.} \end{cases} \quad (6.4)$$

If the option of trajectory i is exercised early at time t_m the cash flow needs to be updated: The cash flow at time t_m equals the payoff function at that time, $CF_m^{i,j} = PO_m^i$. In addition, it is important that the cash flows for the exercise moments $k > m$ for this trajectory i are replaced by the cash flows at those exercise moments with one right less, $CF_k^{i,j} = CF_k^{i,j-1}$. This replacement is important in the algorithm so that the holder can not use more early-exercise rights than he/she is entitled to.

When all the cash flows for all the trajectories $i \in \{1, \dots, N\}$ are computed, the approximation of the Bermudan option value with R early-exercise rights and M exercise moments is given by the arithmetic average of the discounted cash flows:

$$v^R(t_0, S(t_0)) \approx \frac{1}{N} \sum_{i=1}^N DCF_0^{i,R} = \frac{1}{N} \sum_{i=1}^N \sum_{m=1}^M e^{-r \cdot m \Delta t} CF_m^{i,R}. \quad (6.5)$$

The pseudocode of the LSMC method for pricing the Bermudan option with multiple early-exercise rights is given in Algorithm 2 in Appendix B.

Remark 6.1. For the valuation with the LSMC method of the Bermudan option with R early-exercise rights, the cash flow and continuation value for every number of rights $j \in \mathcal{R} = \{1, \dots, R\}$ is computed. Therefore you can directly obtain the values of the Bermudan option with $r < R$ early-exercise rights without extra computation costs by taking the arithmetic average of the discounted cash flows for r early-exercise rights.

6.3 LSMC for electricity storage contracts

In this section the LSMC method for Bermudan options with multiple early-exercise rights is extended so that it can be used for the valuation of electricity storage contracts.

The LSMC method for electricity storage contracts works similarly as for the Bermudan option with multiple early-exercise rights. However, instead of keeping track of the amount of early-exercise rights left, it keeps track of the energy level in storage. In addition, for each energy level the accumulated value of the cash flows of the optimal actions taken in the future are kept track of. Furthermore, the penalty function and limitations of the contract are taken into account. Therefore, the notation of Section 6.2 is adjusted for the electricity storage contract, where $e \in E$ indicates the electricity level in the storage and $i \in \{1, \dots, N\}$ the trajectory:

- $CV_m^{i,e}$: The continuation value with $e \in E$ electricity level in storage after action $\Delta e \in \mathcal{A}$ is taken at time t_m .
- $CF_m^{i,e}$: The cash flow at time t_m with $e \in E$ energy level in storage.
- $ACF_m^{i,e}$: The accumulated value of the cash flows for the optimal actions realised for moments t_k , $k \in \{m, \dots, M+1\}$, with energy level $e \in E$.
- $DACF_m^{i,e} := e^{-r\Delta t} ACF_{m+1}^{i,e}$, the discounted accumulated value of cash flows with $e \in E$ energy in storage.
- $Q_m^{\Delta e} := q_b(\Delta e)$, the penalty function, which is imposed if an action $\Delta e \in \mathcal{A}(t_m, e) \setminus \mathcal{D}(t_m, e)$ is taken.
- $PO_m^{i,\Delta e} := g(t_m, S_m^i, \Delta e)$, the payoff function if action $\Delta e \in \mathcal{A}$ is taken, as defined in formula (3.11).

In contrast with the Bermudan option with multiple early-exercise rights, where the LSMC method starts at moment t_M , the LSMC method for the electricity contract starts at t_{M+1} and works back in time to get the contract value at initial time t_0 .

At time t_{M+1} the contract is settled and no action can be taken. Therefore, the cash flow at settlement time equals the penalty function for all energy levels $e \in E$:

$$CF_{M+1}^{i,e} = q_s(t_{M+1}, S_{M+1}^i, e), \quad \forall e \in E. \quad (6.6)$$

Due to the fact that no cash flows occur after moment t_{M+1} , the accumulated value of cash flows is equal to the cash flow at this moment:

$$ACF_{M+1}^{i,e} = CF_{M+1}^{i,e}, \quad \forall e \in E. \quad (6.7)$$

Note that this cash flow is a penalty and therefore either negative or zero.

At moments t_m , $m \in \{M, \dots, 1\}$, with energy level $e \in E$ in storage, the holder of the contract has to choose between different actions $\Delta e \in \mathcal{A}(t_m, e)$. The holder will choose the action that results in the highest value. In order to make this decision, the continuation values are required.

The continuation values $CV_m^{i,e}$ are approximated using least squares regression of the discounted accumulated cash flows $DACF_m^{i,e}$ onto the basis functions of the asset prices S_m^i , in a similar way as for the Bermudan type options. The regression is done separately for each allowed energy level $e \in E$. Note that for Bermudan-type options only trajectories with positive payoff are considered for the regression. This consideration does not work with a storage contract, because injecting energy naturally generates negative payoffs.

After the continuation values have been determined, the holder can choose an optimal action $\Delta e^* \in \mathcal{A}(t_m, e)$ for each individual energy level $e \in E$, which results in the highest ultimate value. The optimal action with energy level $e \in E$ in storage for trajectory i is defined by:

$$\Delta e^* =_{\Delta e \in \mathcal{A}(t_m, e)} \left\{ PO_m^{i, \Delta e} + CV_m^{i, e + \Delta e} + Q^{\Delta e} \right\}, \quad \forall e \in E. \quad (6.8)$$

With this decision the cash flow at time t_m is computed for each trajectory i and energy level $e \in E$:

$$CF_m^{i,e} = PO_m^{i, \Delta e^*} + Q^{\Delta e^*}, \quad \forall e \in E, \quad (6.9)$$

and the accumulated value of cash flows is updated:

$$ACF_m^{i,e} = CF_m^{i,e} + e^{-r\Delta t} ACF_{m+1}^{i, e + \Delta e^*}, \quad \forall e \in E. \quad (6.10)$$

Ultimately, at initial time t_0 , when all the accumulated values of the cash flows are computed for all trajectories $i \in \{1, \dots, N\}$ and energy levels $e \in E$ at each time step $t_m \in \{t_1, \dots, t_{M+1}\}$, the approximation of the value of the electricity contract is given by the arithmetic average of the accumulated cash flows discounted to t_0 :

$$v(t_0, S(t_0), e(t_0)) \approx \frac{1}{N} \sum_{i=1}^N DACF_0^{i, e(t_0)} = \frac{1}{N} \sum_{i=1}^N e^{-r\Delta t} ACF_1^{i, e(t_0)}. \quad (6.11)$$

The pseudocode of the LSMC method for pricing the electricity storage contract is described in Algorithm 3 in Appendix B.

7 Numerical results of the options

In this section numerical experiments are done to see how well the COS method works for pricing options where the electricity/asset price follows the polynomial model. In addition, the implementations of the pricing methods have been verified by doing similar experiments as in validated papers and comparing our results, in these experiments the asset price follows the well-known GBM.

All the experiments with the COS method have been done for both the closed-form characteristic function as well as the cumulants approximated characteristic function, defined in Section 5.5. In addition, the 95% confidence intervals (c.i.) of the option values are given, derived with the LSMC method.

For the COS method we set $N = 256$ terms in the Fourier series expansion and $\bar{L} = 10$ to make the integration interval. Moreover, for the LSMC method 100 000 paths are taken with 5000 time steps each (unless otherwise stated). Furthermore, the 95% confidence intervals are computed by repeating the LSMC method ten times. After the ten repetitions, the confidence interval is constructed as follows:

$$\text{Confidence Interval} = \left[\bar{V} - z_{\alpha/2} \left(\frac{\bar{\sigma}}{\sqrt{10}} \right), \bar{V} + z_{\alpha/2} \left(\frac{\bar{\sigma}}{\sqrt{10}} \right) \right], \quad (7.1)$$

where \bar{V} is the sample mean of the ten experiments, $\bar{\sigma}$ the standard deviation and $z_{\alpha/2}$ the critical Z-value ($z_{\alpha/2} = 1.96$ for a 95% confidence interval).

For all numerical experiments Python 3.7.1 is used and the CPU is an Intel(R) Core(TM) i7-8750H CPU (2.20GHz, 2208 Mhz, 6 Cores, 12 Logical Processors).

7.1 Verification of the COS and LSMC method

This section examines whether the COS method and the LSMC have been properly implemented. Furthermore, the results of the COS method where the closed-form characteristic function is used are compared to the results where the characteristic function approximation with the cumulants is used.

7.1.1 The European and Bermudan option

In this test the European and Bermudan put option values are computed with the COS method and (LS)MC method, where the asset price process is driven by the GBM. The value of the European option is analytically known. Furthermore, to verify if the methods for the Bermudan option are implemented correctly, the same test has been conducted as in [42]. The parameters of this test are given in Table 1 of [42]:

$$S_0 = 100, \quad K = 110, \quad T = 1, \quad \sigma = 0.2, \quad \mu = r = 0.1.$$

The reference values for the European option and the Bermudan option with $M = 10$ exercise moments are respectively 7.715179... and 10.479520... . The numerical results obtained with the COS method and LSMC method are given in Table 2.

Pricing method	(LS)MC 95% c.i.	the COS method	
Characteristic function	-	Closed-form	Approximation with cumulants
European option	[7.7017 , 7.7286]	7.5152	7.5152
Bermudan option	[10.4693 , 10.4860]	10.4795	10.4795

Table 2: The European option value and the Bermudan option value with $M = 10$ exercise moments obtained with the COS method and the LSMC method.

The results in Table 2 are similar as the reference values, this shows that the COS method and (LS)MC for European options and Bermudan options have been correctly implemented.

Furthermore, the results show that the European and Bermudan option values obtained with the COS method where an approximated characteristic function of the GBM is used are identical to the values obtained with the closed-form characteristic function. Remark that the closed-form characteristic function of the GBM is already in the FFT-form ($\beta = 1$), described in Section 4.2, which explains the accurate results obtained with the approximated characteristic function.

7.1.2 The Bermudan option with multiple early-exercise rights

To demonstrate that the COS method and LSMC method for a Bermudan option with multiple early-exercise rights are well implemented, the same experiment is performed as in the validated paper [52] and the results are compared. In this experiment the Bermudan option is valued for up to $R = 6$ early-exercise rights and $M = 12$ exercise moments, where the asset price follows a GBM with the following parameters from [52]:

$$S_0 = 35, \quad K = 40, \quad T = 0.5, \quad \sigma = 0.25, \quad \mu = r = 0.0488.$$

The results of this experiment with the COS method and LSMC are stated in Table 3.

Pricing method	LSMC 95% c.i.	The COS method	
Characteristic function	-	Closed-form	Approximation with cumulants
R=1	[5.3720 , 5.3847]	5.3816	5.3816
R=2	[10.6783 , 10.7089]	10.6956	10.6956
R=3	[15.9132 , 15.9609]	15.9407	15.9407
R=4	[21.0826 , 21.1436]	21.1157	21.1157
R=5	[26.1814 , 26.2537]	26.2187	26.2187
R=6	[31.2041 , 31.2904]	31.2474	31.2474

Table 3: The values of the Bermudan option with multiple early-exercise rights where the price follows the GBM computed with the LSMC method and the COS method.

The results from [52], which are shown in Table 3.1 of the paper, are all in the 95% LSMC confidence interval given in Table 3. In addition, the values obtained with the COS method are close to these results. For other parameter combinations and results in Table 3.1 from [52] the same is concluded. This suggests that the COS method and the LSMC method for Bermudan options with multiple early-exercise rights are correctly implemented and work well.

7.2 The Bermudan option

In this section the Bermudan option is evaluated where the asset price is generated by the second-order polynomial model with an underlying Ornstein-Uhlenbeck process. This second-order polynomial model is given by:

$$\begin{aligned} S_t &= \Phi(X_t) = \frac{1-c}{2}X_t^2 + cX_t = CX_t^2 + cX_t, \\ dX_t &= \kappa(\theta - X_t)dt + \sigma dW_t. \end{aligned} \quad (7.2)$$

The following parameters of the model are reviewed and analysed on how much they affect the error that occurs when using the approximated characteristic function:

- The coefficient c .
- The number of exercise moments M .
- The maturity time T .
- The parameters κ and σ .

The other parameters of the OU process are set as follows:

$$\theta = 11, \quad X_0 = 10, \quad K = 50, \quad S_0 = \Phi(X_0), \quad (7.3)$$

and the risk-free interest rate $r = 0.05$.

The COS method for this model can be determined with the characteristic function of the polynomial model, S_t , or with the characteristic function of the underlying OU process, X_t . In the following experiments, both characteristic functions are approximated with its cumulants, as described in Section 5, to examine which approach is most accurate in pricing the options using the efficient FFT-based algorithm. These results obtained with the approximations are compared with the COS method where the closed-form characteristic function of the OU process is used, denoted by analytical COS method. Note that the closed-form characteristic function of the polynomial model does not exist, it can be approximated.

Furthermore, to better analyse the polynomial model, the SDE of the process is considered. With Ito's lemma the following SDE is obtained of the polynomial model (7.2):

$$dS_t = \tilde{\mu}(t, X_t)dt + \tilde{\sigma}(t, X_t)dW_t, \quad (7.4)$$

where the drift and volatility variables are given by

$$\begin{aligned} \tilde{\mu}(t, X_t) &= \kappa(\theta - X_t)(2CX_t + c) + 2C\sigma^2, \\ \tilde{\sigma}(t, X_t) &= \sigma(2CX_t + c). \end{aligned} \quad (7.5)$$

Moreover, in Figure 8 six asset paths are simulated for various c .

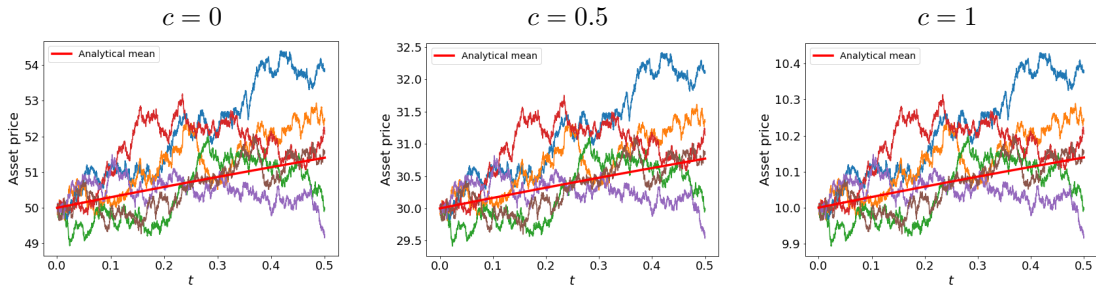


Figure 8: The simulation of six asset paths with dynamics (7.4) for various c and $\sigma = \kappa = 0.3$ and other parameters set as in (7.3).

The simulations in Figure 8 show that the asset paths exhibit larger price differences for a smaller coefficient c , resulting in a higher variance. Note that for $c = 1$ a normal OU process is simulated and for $c = 0$ the square of the OU process.

The influence of the coefficient c

The drift and the volatility variables in (7.5) show that the coefficient c has an influence on the process. To measure the impact of the coefficient c on the option valuation, we compute the option values with the COS method and the LSMC method for various c and $\sigma \in \{0.3, 0.9\}$. In addition, it is examined how well the COS method with an approximated characteristic function can determine the value of the Bermudan option with the efficient FFT-based algorithm and how large the impact of the coefficient c is on the accuracy. Furthermore, it is verified whether the values obtained with the COS method lie within the 95% confidence interval acquired with the LSMC method.

In Figure 9 and Table 4 the Bermudan option with $M = 10$ exercise moments is priced with the LSMC method and the COS method for various c .

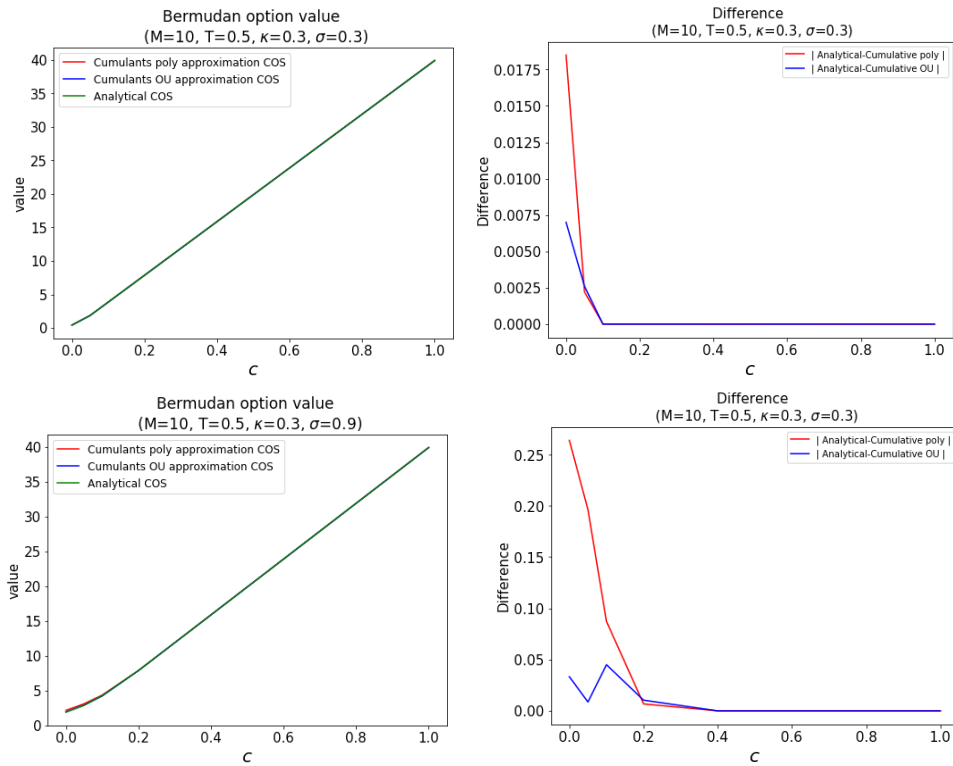


Figure 9: The values and differences of the Bermudan option obtained with the COS method with closed-form and approximated characteristic function for various c and $\sigma \in \{0.3, 0.9\}$ and the other parameters set.

$\sigma = 0.3 \quad \kappa = 0.3 \quad T = 0.5$				
Pricing method	LSMC 95% c.i.	The COS method		
Characteristic function	-	Closed-form	Approximation polynomial with cumulants	Approximation OU with cumulants
$c=0$	[0.4183, 0.4207]	0.4191	0.4377	0.4262
$c=0.1$	[3.8514, 3.8539]	3.8528	3.8528	3.8528
$c=0.5$	[19.8664, 19.8779]	19.8672	19.8672	19.8672
$c=0.9$	[35.8814, 35.8819]	35.8817	35.8817	35.8817
$c=1$	[39.8851, 39.8853]	39.8853	39.8853	39.8853
CPU time	529 sec	18.3 sec	0.078 sec	0.060 sec

$\sigma = 0.9, \quad \kappa = 0.3, \quad T = 0.5.$				
Pricing method	LSMC 95% c.i.	The COS method		
Characteristic function	-	Closed-form	Approximation polynomial with cumulants	Approximation OU with cumulants
c=0	[1.8668, 1.8768]	1.8724	2.1364	1.9057
c=0.1	[4.2363, 4.2477]	4.2439	4.3312	4.1989
c=0.5	[19.8577, 19.8633]	19.8584	19.8584	19.8584
c=0.9	[35.8797, 35.8816]	35.8799	35.8799	35.8799
c=1	[39.8847, 39.8856]	39.8853	39.8853	39.8853
CPU time	535 sec	18.0 sec	0.062 sec	0.052 sec

Table 4: The Bermudan option values with 10 early-exercise moments obtained with the COS method and the LSMC method for various coefficients c and the other parameters set.

Table 4 shows that the values obtained with COS method where the closed-form characteristic function is used always lie within the 95% LSMC confidence interval. Furthermore, the values derived with the approximated characteristic functions are close to the closed-form results and almost always within the LSMC confidence interval. The only values that are not within the boundaries of the interval are the values for $c = 0$ for both σ 's and for $c = 0.1$ for $\sigma = 0.9$.

The results from Figure 9 and Table 4 suggest that for a higher coefficient c the COS method where the characteristic function is approximated is closer to the values obtained with the closed-form characteristic function. Moreover, the accuracy is higher for a smaller σ . Furthermore, the values obtained by means of the COS method with the approximated characteristic function of the underlying OU process with the cumulants are more accurate than with the approximated characteristic function of the polynomial model with the cumulants for the examined parameter combinations.

The influence of the number of exercise moments M

In Figure 10 and Table 5 the Bermudan option value is computed with the LSMC method and the COS method for different numbers of early-exercise moments before expiry, while the other parameters are set.

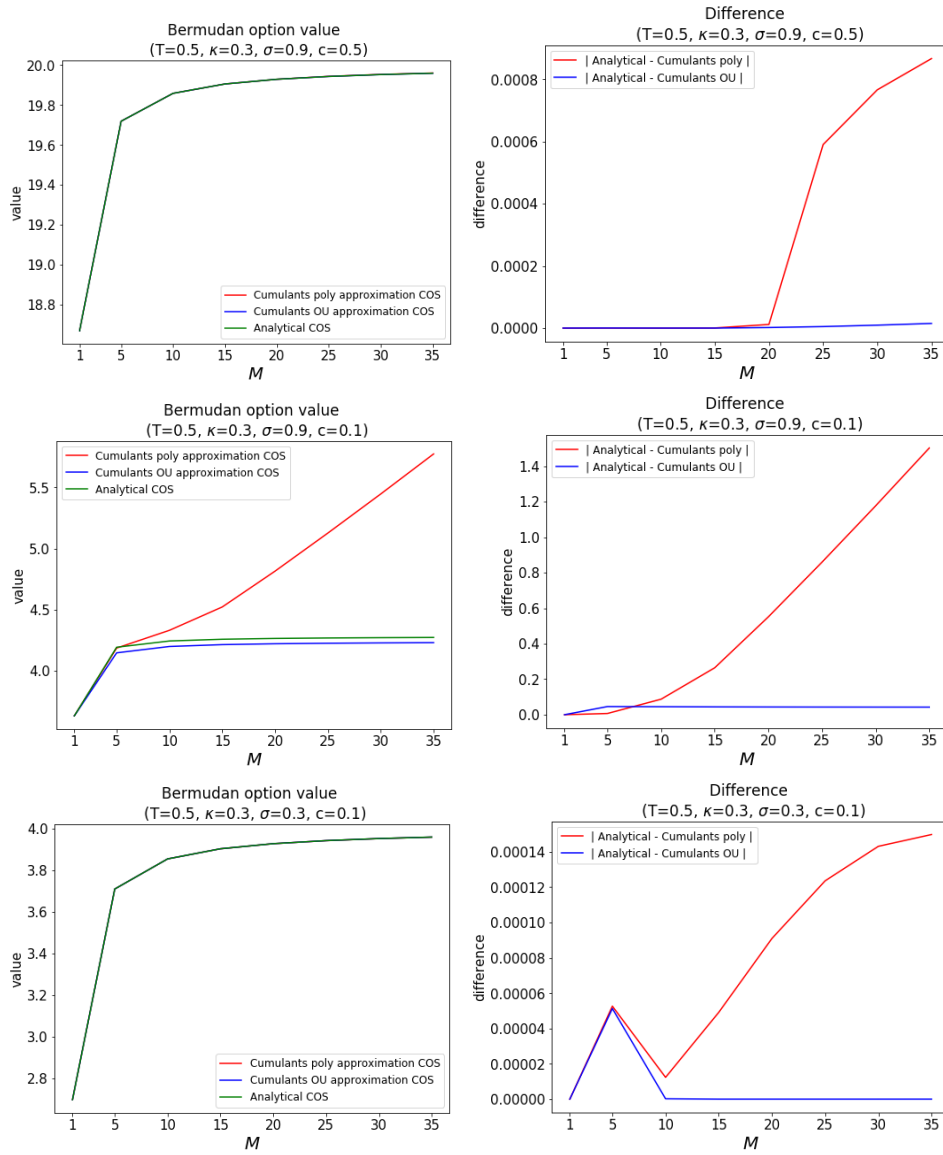


Figure 10: The values and differences of the Bermudan option obtained with the COS method for various number of early-exercise moments M and the other parameters set.

$\sigma = 0.9 \quad c = 0.5, \quad \kappa = 0.3, \quad T = 0.5.$				
Pricing method	LSMC 95% c.i.	The COS method		
Characteristic function	-	Closed-form	Approximation polynomial with cumulants	Approximation OU with cumulants
M=1	[18.6662 , 18.6773]	18.6690	18.6690	18.6690
M=5	[19.7165 , 19.7194]	19.7187	19.7187	19.7187
M=10	[19.8576 , 19.8608]	19.8584	19.8584	19.8584
M=15	[19.9033 , 19.9058]	19.9054	19.9054	19.9054

$\sigma = 0.9 \quad c = 0.1 \quad \kappa = 0.3 \quad T = 0.5$				
Pricing method	LSMC 95% c.i.	The COS method		
Characteristic function	-	Closed-form	Approximation polynomial with cumulants	Approximation OU with cumulants
M=1	[3.6182 , 3.6407]	3.6315	3.6315	3.6315
M=5	[4.1822 , 4.1960]	4.1927	4.1859	4.1468
M=10	[4.2368 , 4.2510]	4.2439	4.3313	4.1989
M=15	[4.2501 , 4.2626]	4.2582	4.5225	4.2141

$\sigma = 0.3 \quad c = 0.1 \quad \kappa = 0.3 \quad T = 0.5$				
Pricing method	LSMC 95% c.i.	The COS method		
Characteristic function	-	Closed-form	Approximation polynomial with cumulants	Approximation OU with cumulants
M=1	[2.6961 , 2.7030]	2.6962	2.6962	2.6962
M=5	[3.7070 , 3.7109]	3.7082	3.7082	3.7082
M=10	[3.8514 , 3.8539]	3.8528	3.8528	3.8528
M=15	[3.8997 , 3.9017]	3.9016	3.9015	3.9016

Table 5: The Bermudan option values computed with the COS method and the LSMC method for various number of early-exercise moments M and the other parameters set.

The Bermudan option value increases when there are more exercise moments, due to the fact that the option holder has more possible moments to exercise the option for the strike price K if the asset price is low. Furthermore, Table 5 shows that the values obtained with the closed-form characteristic function by means of the COS method for all chosen parameters and number of early-exercise moments M lie within the 95% confidence interval obtained with the LSMC method.

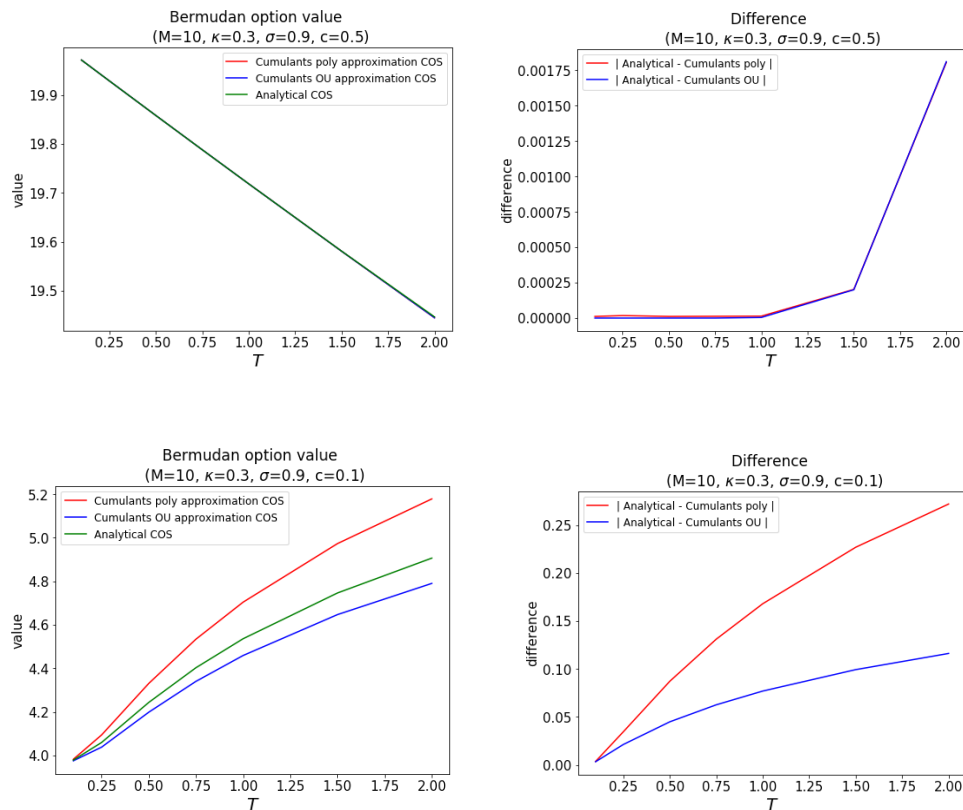
Figure 10 clearly shows that the error obtained by using the characteristic function approximation of the polynomial model with its cumulants increases as more early-exercise moments occur, while this is not the case if the approximation of the OU process with its cumulants is used. In general, the COS method is more accurate using the approximated characteristic function of the OU process with the cumulants than of the polynomial model with the cumulants for pricing the Bermudan option for the different choices of the number of exercise moments M . Moreover, the errors for both approximations remain lowest for a large value of coefficient c and a low value for σ .

Pricing method	LSMC 95% c.i.	The COS method		
Characteristic function	-	Closed-form	Approximation polynomial with cumulants	Approximation OU with cumulants
M=1	480 sec	0.001 sec	0.006 sec	0.002 sec
M=5	490 sec	7.8 sec	0.041 sec	0.021 sec
M=10	530 sec	17.6 sec	0.060 sec	0.045 sec
M=15	570 sec	27.4 sec	0.071 sec	0.058 sec

Table 6: The average CPU time of 10 runs for various number of early-exercise moments M before expiry, $T = 0.5$ and $\Delta t = T/5000$ the time step size used for the LSMC simulations.

The influence of the maturity time T

The maturity time T has substantial impact on the accuracy of the LSMC method and the COS method. The numerical results of these two pricing methods for different maturity times is shown in Figure 11 and Table 7. Furthermore, for the LSMC method the step size $\Delta t = 1/2500$ is taken for all T for the simulation of the 100 000 asset paths.



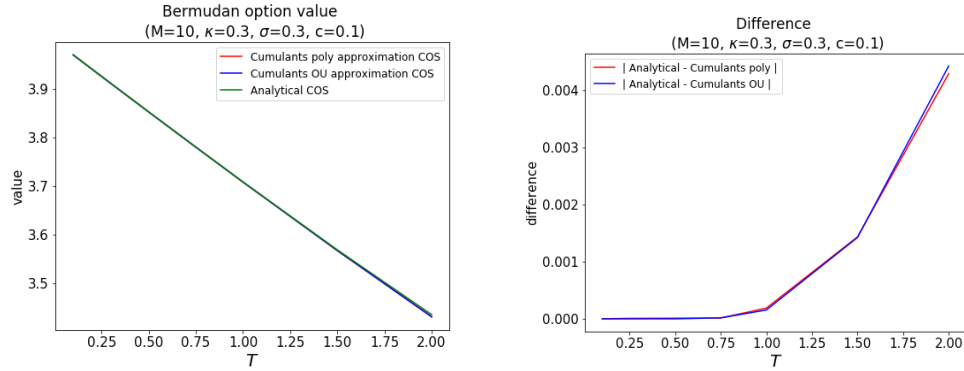


Figure 11: The values and differences of the Bermudan option obtained with the COS method for various T and the other parameters set.

$\sigma = 0.9 \quad \kappa = 0.3 \quad c = 0.5$				
Pricing method	LSMC 95% c.i.	The COS method		
Characteristic function	-	Closed-form	Approximation polynomial with cumulants	Approximation OU with cumulants
T=0.1	[19.9713 , 19.9729]	19.9715	19.9715	19.9715
T=0.5	[19.8573 , 19.8601]	19.8584	19.8584	19.8584
T=1	[19.7173 , 19.7214]	19.7187	19.7188	19.7187
T=2	[19.4457 , 19.4549]	19.4471	19.4453	19.4453

$\sigma = 0.9 \quad \kappa = 0.3 \quad c = 0.1$				
Pricing method	LSMC 95% c.i.	The COS method		
Characteristic function	-	Closed-form	Approximation polynomial with cumulants	Approximation OU with cumulants
T=0.1	[3.9768 , 3.9793]	3.9790	3.9827	3.9757
T=0.5	[4.2400 , 4.2462]	4.2439	4.3312	4.1989
T=1	[4.5272 , 4.5409]	4.5364	4.7044	4.4594
T=2	[4.9034 , 4.9190]	4.9067	5.1785	4.7905

Table 7: The Bermudan option values computed with the COS method and the LSMC method for various maturity times T and the other parameters set.

The results in Table 7 show that if the maturity time gets higher the range of the LSMC confidence interval increases in size. Moreover, the values obtained by means of the COS method with the closed-form characteristic function all lie within the 95% LSMC confidence interval.

From Figure 11 it can be concluded that the lower the maturity time T , the lower the error caused by the use of the approximated characteristic function. Furthermore, it is clear to see from the figures that the parameters c and σ have a major impact on the numerical results obtained with the COS method where the approximated characteristic function is used.

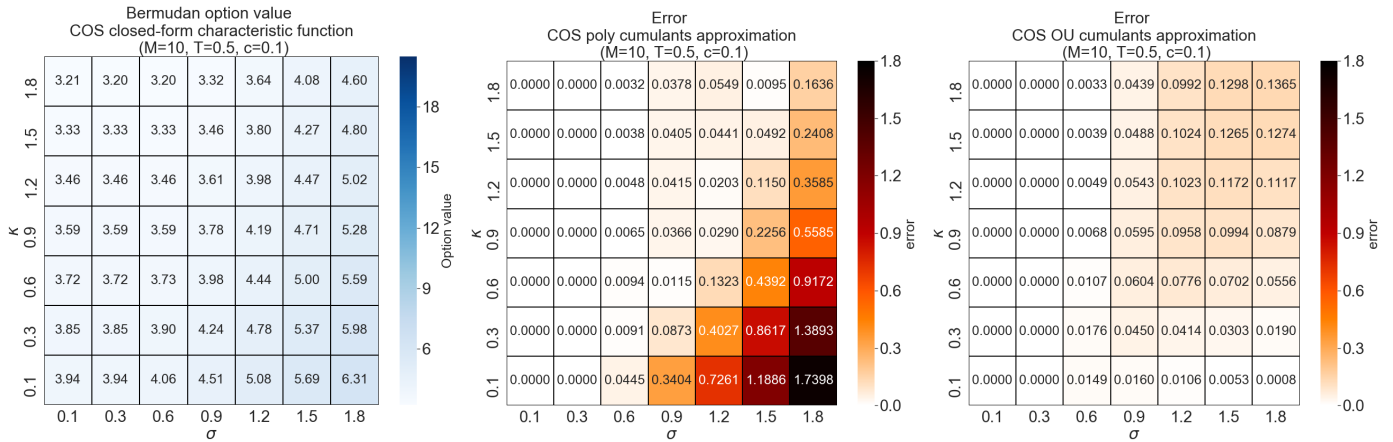
Pricing method	LSMC 95% c.i.	The COS method		
		Closed-form	Approximation polynomial with cumulants	Approximation OU with cumulants
Characteristic function	-			
T=0.1	28.6 sec	18.0 sec	0.059 sec	0.050 sec
T=0.5	117.2 sec	17.3 sec	0.063 sec	0.042 sec
T=1	245.0 sec	17.5 sec	0.067 sec	0.042 sec
T=2	570.0 sec	17.3 sec	0.060 sec	0.043 sec

Table 8: The average CPU time of 10 runs for various maturity times T and $\Delta t = 1/2500$ the time step size used for the LSMC simulations.

The influence of the parameters κ and σ

Previous analyses of the influence of the parameters on the error by using the approximated characteristic function in the COS method indicate that parameter σ has a substantial effect on the error. In addition, it is expected that κ will also have a significant effect on the error, because $\beta = e^{-\kappa\Delta t}$ in the characteristic function of the OU process, which is set equal to $\beta = 1$ with a transformation to be able to use the efficient FFT-based algorithm. Therefore the error is analysed for various combinations of κ and σ to get a better understanding on how it affects the error.

First the value of the Bermudan option is given for the different parameter combinations, obtained with the COS method with the closed-form characteristic function. Thereafter, the error is given if an approximated characteristic function is used.



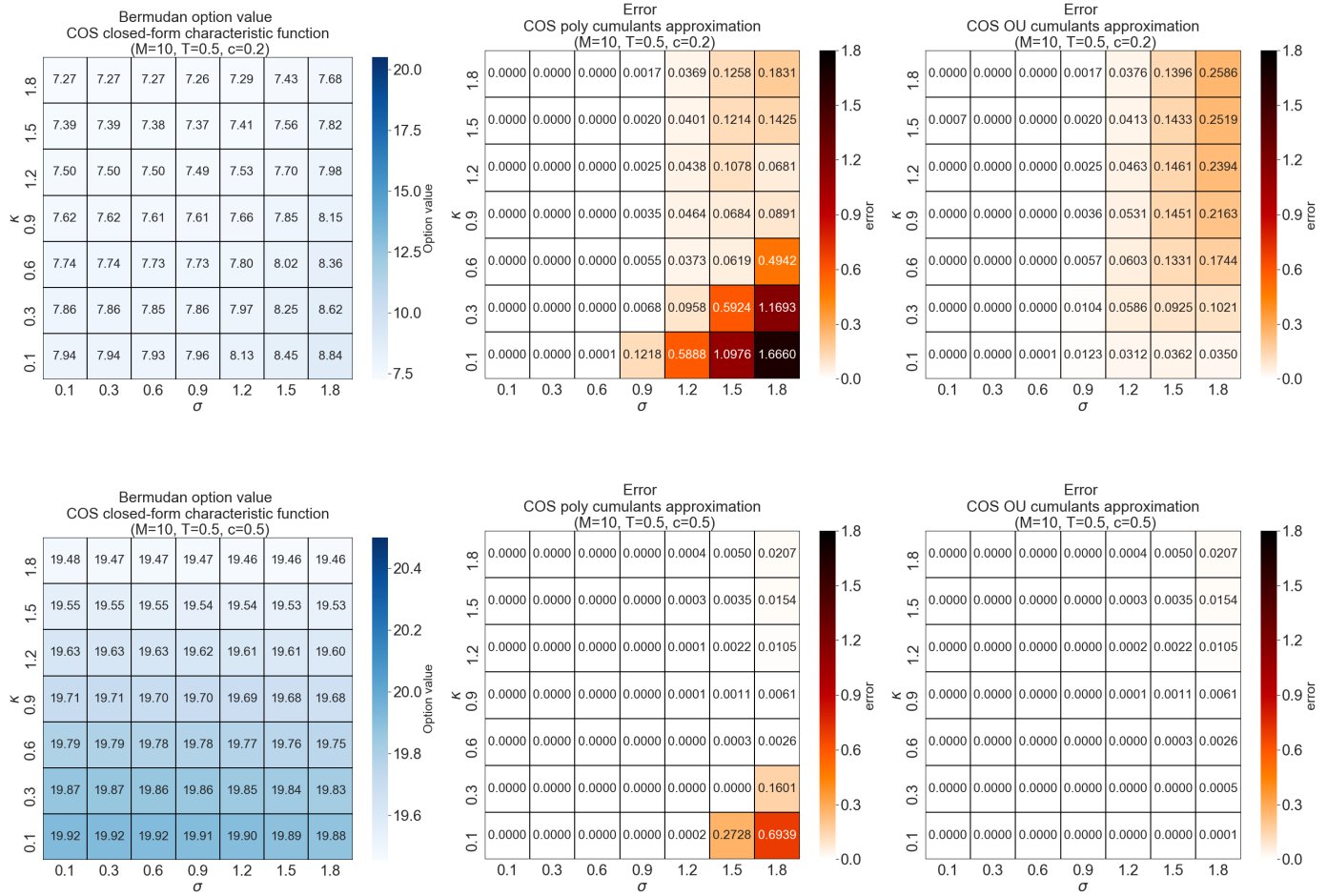


Figure 14: The values and errors of the Bermudan option obtained with the COS method for various κ and σ and the other parameters set.

The numerical results of Figure 14 show that the parameters κ and σ both have a significant influence on the error. In addition, it can be seen that changes in the parameters σ , κ and c affect the error more if the cumulants approximated characteristic function of the polynomial model is used than if the approximation with the cumulants of the OU process is used. For almost all parameter combinations, the values obtained with the approximated characteristic function of the OU process with the cumulants are more accurate than the values obtained with the approximation of the characteristic function of the polynomial model with the cumulants.

7.3 The Bermudan option with multiple early-exercise rights

This section shows the numerical results of the valuation of the Bermudan option with multiple early-exercise rights by means of the COS method and LSMC method where the price process follows the second-order polynomial model with an underlying OU process (7.2). The same parameters (7.3) are used as in the valuation of the Bermudan option.

	$\sigma = 0.3 \quad \kappa = 0.3 \quad c = 0.1 \quad M = 10$			
Pricing method	LSMC c.i.	The COS method		
Characteristic function	-	Closed-form	Approximation polynomial with cumulants	Approximation OU with cumulants
R=1	[3.8522 , 3.8548]	3.8528	3.8528	3.8528
R=2	[7.5595 , 7.5654]	7.5610	7.5629	7.5609
R=3	[11.1267 , 11.1356]	11.1281	11.1352	11.1275
R=4	[14.5566 , 14.5680]	14.5581	14.5756	14.5565
R=5	[17.8529 , 17.8674]	17.8553	17.8903	17.8529
CPU time	605 sec	118.2 sec	0.141 sec	0.100 sec

	$\sigma = 0.3 \quad \kappa = 0.3 \quad c = 0.5 \quad M = 10$			
Pricing method	LSMC c.i.	The COS method		
Characteristic function	-	Closed-form	Approximation polynomial with cumulants	Approximation OU with cumulants
R=1	[19.8672 , 19.8683]	19.8672	19.8672	19.8672
R=2	[39.6025 , 39.6050]	39.6033	39.6044	39.6033
R=3	[59.2086 , 59.2128]	59.2100	59.2143	59.2099
R=4	[78.6865 , 78.6925]	78.6889	78.6994	78.6885
R=5	[98.0382 , 98.0468]	98.0414	98.0623	98.0409
CPU time	609 sec	117.0 sec	0.139 sec	0.110 sec

	$\sigma = 0.3 \quad \kappa = 0.3 \quad c = 0.8 \quad M = 10$			
Pricing method	LSMC c.i.	The COS method		
Characteristic function	-	Closed-form	Approximation polynomial with cumulants	Approximation OU with cumulants
R=1	[31.878 , 31.8786]	31.8781	31.8781	31.8781
R=2	[63.6347 , 63.6360]	63.6352	63.6356	63.6351
R=3	[95.2716 , 95.2737]	95.2723	95.2740	95.2722
R=4	[126.7892 , 126.7923]	126.7904	126.7946	126.7903
R=5	[158.1889 , 158.1932]	158.1905	158.1989	158.1903
CPU time	615 sec	117.8 sec	0.139 sec	0.111 sec

	$\sigma = 0.9 \quad \kappa = 0.3 \quad c = 0.1 \quad M = 10$			
Pricing method	LSMC c.i.	The COS method		
Characteristic function	-	Closed-form	Approximation polynomial with cumulants	Approximation OU with cumulants
R=1	[4.2392 , 4.2466]	4.2439	4.3312	4.1989
R=2	[8.3813 , 8.3917]	8.3874	8.5725	8.3138
R=3	[12.4136 , 12.4311]	12.4244	12.7256	12.3405
R=4	[16.334 , 16.3559]	16.3496	16.7919	16.2748
R=5	[20.1364 , 20.1644]	20.1568	20.7717	20.1119
CPU time	599 sec	119.9 sec	0.134 sec	0.103 sec

	$\sigma = 0.9 \quad \kappa = 0.3 \quad c = 0.5 \quad M = 10$			
Pricing method	LSMC c.i.	The COS method		
Characteristic function	-	Closed-form	Approximation polynomial with cumulants	Approximation OU with cumulants
R=1	[19.8562 , 19.8605]	19.8584	19.8584	19.8584
R=2	[39.5706 , 39.5816]	39.5771	39.5867	39.5768
R=3	[59.1482 , 59.1616]	59.1582	59.1963	59.157
R=4	[78.5898 , 78.6068]	78.6035	78.698	78.6005
R=5	[97.8953 , 97.9183]	97.9149	98.1022	97.9091
CPU time	611 sec	121.1 sec	0.129 sec	0.112 sec

	$\sigma = 0.9 \quad \kappa = 0.3 \quad c = 0.8 \quad M = 10$			
Pricing method	LSMC c.i.	The COS method		
Characteristic function	-	Closed-form	Approximation polynomial with cumulants	Approximation OU with cumulants
R=1	[31.8734 , 31.8756]	31.8745	31.8745	31.8745
R=2	[63.6213 , 63.6269]	63.6247	63.6285	63.6245
R=3	[95.2464 , 95.2533]	95.2516	95.2668	95.2511
R=4	[126.7492 , 126.7580]	126.7563	126.7941	126.7551
R=5	[158.1298 , 158.1416]	158.1399	158.2148	158.1376
CPU time	609 sec	120.2 sec	0.140 sec	0.119 sec

Table 9: The Bermudan option with R early-exercise rights values computed with the COS method and the LSMC method for various σ and coefficients c and the other parameters set.

The Bermudan option value with multiple early-exercise rights increases when the holder gets more rights to early-exercise, which makes sense because he/she has the right to sell the asset for the strike price K more often. Moreover, the values obtained by means of the COS method with the closed-form characteristic function all lie within the LSMC 95% confidence interval.

The approximated characteristic function of the OU process with the cumulants performs better than the characteristic function approximation of the polynomial model. Furthermore, Table 9 and additional experiments with various parameter settings show that the approximation of the characteristic function of the OU process with its cumulants works well for the same parameters where the approximation works well for the Bermudan option. Although it can be seen that the values become somewhat less accurate if there are more early-exercise rights. The reason for this inaccuracy is that the continuation value must be calculated more often and if the continuation value is computed with the approximated characteristic function by means of the COS method an error occurs, as shown in the error analysis in Section 5.6.

7.4 Implications of the numerical results

The COS method with the closed-form characteristic function of the OU process works well for pricing the options and the obtained option values always lie within the LSMC 95% confidence interval. Furthermore, the computation for determining the value of the financial derivatives is in general a lot faster with the COS method compared to the LSMC method.

Moreover, it has been shown that with the approximation of the characteristic function of the (underlying) price process with the cumulants, the efficient FFT-based algorithm can be used, so that the computation time of the COS method decreases significantly. For many parameter settings, the values obtained with the approximation are close to the values obtained with the closed-form characteristic function and lie within the LSMC 95% confidence interval. Furthermore, after testing various parameter settings, it can be concluded that the option values obtained with the cumulants approximation of the characteristic function of the underlying OU process is more accurate than the cumulants approximation of the characteristic function of the polynomial model.

The same parameter settings that work well when pricing the Bermudan option by means of the COS method with the approximated characteristic function of the OU process also work well when pricing the Bermudan option with multiple early-exercise rights. Although it can be seen that the price becomes slightly less accurate if there are more early-exercise rights, the reason for this is that the continuation value must be calculated more often. Namely, when the continuation value is calculated, an error occurs when using the approximated characteristic function, as shown in Section 5.6.

In general, the option values, where the asset price follows a second-order polynomial model with an underlying OU process, obtained by means of the COS method with the approximated characteristic function of the OU process are most accurate for low values of σ , κ and maturity time T and a high value for coefficient c . For the number of exercise moments M , the accuracy is indifferent.

Remark 7.1. The experiments are also performed with the adjoint expansion approximation of the characteristic function of the OU process, which gave essentially the same numerical results as with the approximation of the characteristic function of the OU process with the cumulants. However, the advantage of the cumulative approximation is that it is a simpler and more tractable approach.

8 Numerical results electricity contract

In this section, several different electricity storage contracts are valued by means of the COS method where the closed-form characteristic function is used and compared with the values obtained where the approximated characteristic function is used. In addition, using the LSMC method, the 95% confidence intervals of the contract values are determined and the average energy level in storage for each contract over time is given. The confidence intervals are computed in the same way as defined in (7.1).

Python 3.7.1 is used for all the numerical experiments and the CPU is an Intel(R) Core(TM) i7-8750H CPU (2.20GHz, 2208 Mhz, 6 Cores, 12 Logical Processors).

For pricing the various electricity storage contracts, the electricity price is modeled according to the second-order polynomial model:

$$S_t = \Phi(X_t) = \frac{1-c}{2}X_t^2 + cX_t, \quad (8.1)$$

where the underlying process X_t follows an OU process:

$$dX_t = \kappa(\theta - X_t)dt + \sigma dW_t.$$

The parameters for this model are chosen as follows:

$$c = 0.5, \quad \kappa = 0.3, \quad \theta = 11, \quad \sigma \in \{0.3, 0.6, 0.9, 1.2\}, \quad X_0 = 10, \quad S_0 = \Phi(X_0). \quad (8.2)$$

The valuation of the electricity storage contract is done for $\sigma = 0.3$ (low volatility), $\sigma = 0.6$ (mid-low volatility), $\sigma = 0.9$ (mid-high volatility) and $\sigma = 1.2$ (high volatility). Note that for a stock market these are all fairly high volatility parameters, however the electricity market is much more volatile than the stock market. In Figure 15, six simulations of the electricity price process trajectory S_t are shown for each volatility parameter.

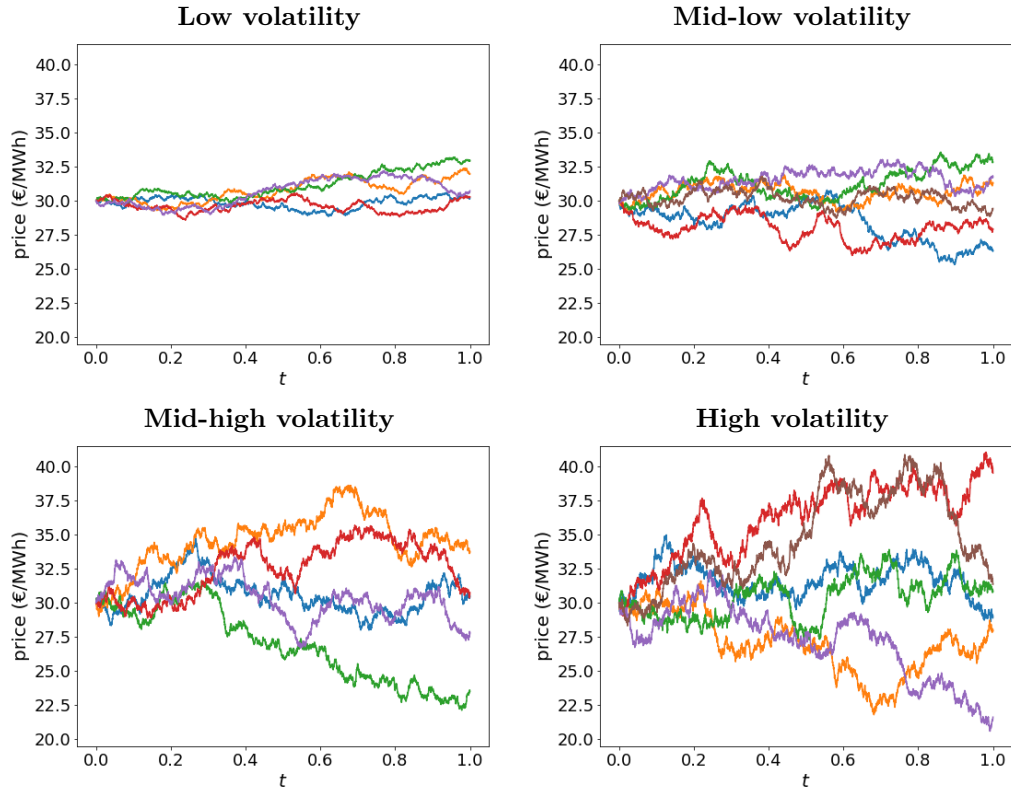


Figure 15: Six simulations of the electricity price process simulated by the second-order polynomial model (8.1) with parameters defined in (8.2).

8.1 The electricity storage contracts

This section is focused on five different electricity storage contracts. There are many different technologies for large scale electricity storage systems and each technology has its own technical characteristics. Each contract is based on these technical characteristics. In addition, expected improvements of the characteristics and new concepts to store electricity are considered, such as higher battery efficiency and the concept of the Car-Park as Power Plant [10].

Some of the electricity storage contract characteristics will be the same for each contract, these are shown in Table 10. The other contract characteristics will differ per contract. The five contracts and their characteristics are defined in the remainder of this section.

Start date	t_0	0
Time to maturity	T	1
Number of exercise moments	M	50
Time between exercise moments	Δt	1/50
Required min. injection in market	i_{market}^{min}	-0.1 MWh [10]

Table 10: The general electricity storage parameters, used for each discussed contract.

Contract 1: Standard electricity storage

The most widely used electricity storage system is the rechargeable battery. The current rechargeable battery storage facilities often have capacities between 0.25-50 MWh and an output of 0.1-20 MW, depending on the battery [53]. Furthermore, rechargeable batteries can have an efficiency up to $\sim 95\%$ [5]. In addition, charging and discharging a rechargeable battery too rapidly reduces the battery lifetime, so there is a penalty $q_b(\Delta e) < 0$ for this. Moreover, the settlement penalty of -350 euro is activated when the energy level in the battery is lower than when the contract started.

The characteristics for contract 1 are given in Table 11.

Start energy level	$e(t_0)$	7	MWh
Min. capacity	e^{min}	0	MWh
Max. capacity	e^{max}	15	MWh
Min. energy level change	i_{op}^{min}	-2	MWh
Max. energy level change	i_{op}^{max}	2	MWh
Min. energy level change without penalty	i_b^{min}	-1	MWh
Max. energy level change without penalty	i_b^{max}	1	MWh
Efficiency of the battery	η	95	%
Penalty of charging/discharging too rapidly	$q_b(\Delta e)$ for $\Delta e \in \mathcal{A} \setminus \mathcal{D}$	-3	€
Penalty at settlement date	$q_s(e)$ for $e < e(t_0)$	-350	€

Table 11: The electricity storage characteristics for contract 1.

Contract 2: Highly efficient electricity storage

In this contract a highly efficient electricity storage is considered, with an efficiency of 100%. Batteries of $\sim 100\%$ efficiency already exist, but due to the high manufacturing costs, they are not yet used for electricity storage [6].

The contract characteristics for contract 2 are the same as for contract 1 (Table 11), only the efficiency of the electricity storage is increased to $\eta = 100\%$.

Contract 3: Fast charging/discharging electricity storage

Contract 3 is a contract for an electricity storage that can charge/discharge faster compared to the standard contract 1. Therefore, higher energy changes can take place in the storage at each exercise moment.

The characteristics of this contract are defined in Table 12.

Start energy level	$e(t_0)$	7	MWh
Min. capacity	e^{min}	0	MWh
Max. capacity	e^{max}	15	MWh
Min. energy level change	i_{op}^{min}	-6	MWh
Max. energy level change	i_{op}^{max}	6	MWh
Min. energy level change without penalty	i_b^{min}	-4	MWh
Max. energy level change without penalty	i_b^{max}	4	MWh
Efficiency of the battery	η	95	%
Penalty of charging/discharging too rapidly	$q_b(\Delta e)$ for $\Delta e \in \mathcal{A} \setminus \mathcal{D}$	-3	€
Penalty at settlement date	$q_s(e)$ for $e < e(t_0)$	-350	€

Table 12: The electricity storage characteristics for contract 3.

Contract 4: Highly efficient and fast charging/discharging electricity storage

This contract considers an electricity storage facility that combines the added characteristics described in contracts 2 and 3, a fast charging/discharging electricity storage facility with high efficiency.

The characteristics of this contract are given in Table 13.

Start energy level	$e(t_0)$	7	MWh
Min. capacity	e^{min}	0	MWh
Max. capacity	e^{max}	15	MWh
Min. energy level change	i_{op}^{min}	-6	MWh
Max. energy level change	i_{op}^{max}	6	MWh
Min. energy level change without penalty	i_b^{min}	-4	MWh
Max. energy level change without penalty	i_b^{max}	4	MWh
Efficiency of the battery	η	100	%
Penalty of charging/discharging too rapidly	$q_b(\Delta e)$ for $\Delta e \in \mathcal{A} \setminus \mathcal{D}$	-3	€
Penalty at settlement date	$q_s(e)$ for $e < e(t_0)$	-350	€

Table 13: The electricity storage characteristics for contract 4.

Contract 5: Car-Park as Power Plant (CPPP)

The Car-Park as Power Plant is a concept that is seen as a solution for the high variable output of renewable energy sources. Cars are parked for an average of 96% of the time [54], therefore there is a lot of potential in using the battery of an electric vehicle for electricity storage. However, a single car cannot work on the electricity market because there are minimal injection rules of 100 KWh while a full electric car has an average of 80 KWh. In addition, a single car may not be available continuously, while the presence of a large number of cars is highly predictable [55]. That is why we consider multiple electric vehicles at the same time that are seen as one storage, e.g. a car park can be used [10].

For this contract, a car park is assumed with 150 electric vehicles and an average of 80 KWh capacity and 90% efficiency per electric vehicle [10]. At each exercise moment, the vehicles can change 25% of its energy level without getting a penalty. This results in a total capacity of 12 MWh and an energy change without penalty of 3 MWh.

At the end of the contract, the owner of the car must be able to drive away, which is why there is a high penalty if there is not enough energy in the car.

Start energy level	$e(t_0)$	6	MWh
Min. capacity	e^{min}	0	MWh
Max. capacity	e^{max}	12	MWh
Min. energy level change	i_{op}^{min}	-4	MWh
Max. energy level change	i_{op}^{max}	4	MWh
Min. energy level change without penalty	i_b^{min}	-3	MWh
Max. energy level change without penalty	i_b^{max}	3	MWh
Efficiency of the battery	η	90	%
Penalty of charging/discharging too rapidly	$q_b(\Delta e)$ for $\Delta e \in \mathcal{A} \setminus \mathcal{D}$	-10	€
Penalty at settlement date	$q_s(e)$ for $e < e(t_0)$	-2000	€

Table 14: The electricity storage characteristics for contract 5.

8.2 The numerical contract values

This section shows the numerical results of the values of the storage contracts, which are defined in Section 8.1, obtained with the COS method, for both the closed-form characteristic function and the characteristic function approximated with the cumulants of the OU process. Moreover, the 95% confidence intervals of the contract values are given, derived with the LSMC method.

Furthermore, the average energy level and the 95% confidence interval of the energy level in the storage is shown, obtained with the LSMC method. The average energy level gives an indication to the holder of a contract which energy levels must be maintained to get maximum profit. Additionally, the maximum and minimum energy levels of all the trajectories used in the LSMC method are given.

For the COS method we set $N = 128$ terms in the Fourier series expansion and $\bar{L} = 10$ to make the integration interval. Moreover, the resulting confidence intervals are computed by ten runs with the LSMC method of 50 000 trajectories. In addition, the maximum and minimum energy levels at each exercise moments are taken over all the trajectories of the ten runs of the LSMC method.

Contract 1: Standard electricity storage

Table 15 shows the numerical results of the values of contract 1, with characteristics defined in Table 11. In addition, in Figure 16 the average energy levels in storage are given, together with the 95% confidence interval. Figure 17 gives a closer look at the average energy levels of Figure 16. Note that the y-axes in Figure 17 are not scaled equally.

Pricing method	LSMC 95% c.i.	COS	
Characteristic function	-	Closed-form	Approximated
σ	N=50000	N=128	N=128
0.3	[0.0000 , 0.0000]	0.0000	-0.0049
0.6	[-0.0001 , 0.0008]	0.0002	0.0006
0.9	[0.0014 , 0.0107]	0.0065	0.0035
1.2	[0.1084 , 0.1370]	0.1222	0.0985

Table 15: The values of contract 1 obtained with the COS method and the LSMC method.

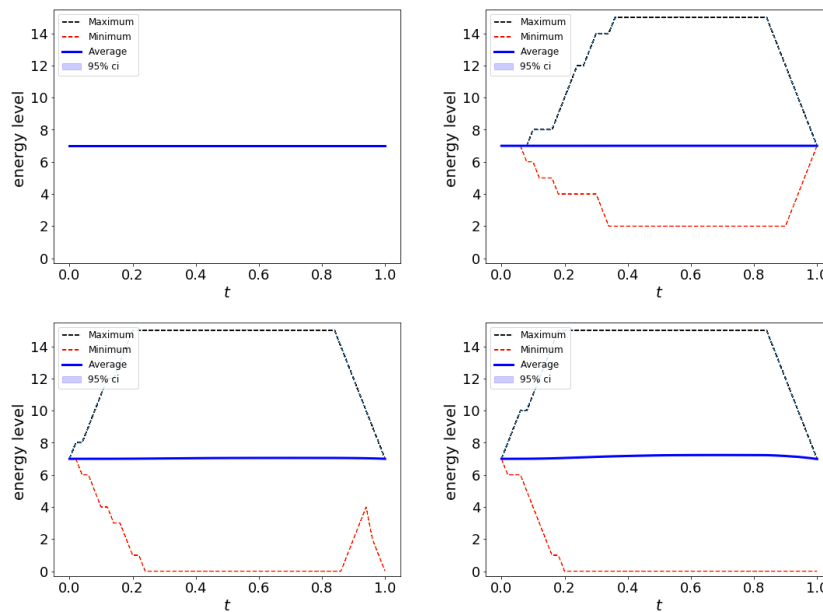


Figure 16: The average energy level in storage for, respectively from left to right, low volatility, mid-low volatility, mid-high volatility and high volatility obtained with the LSMC method.

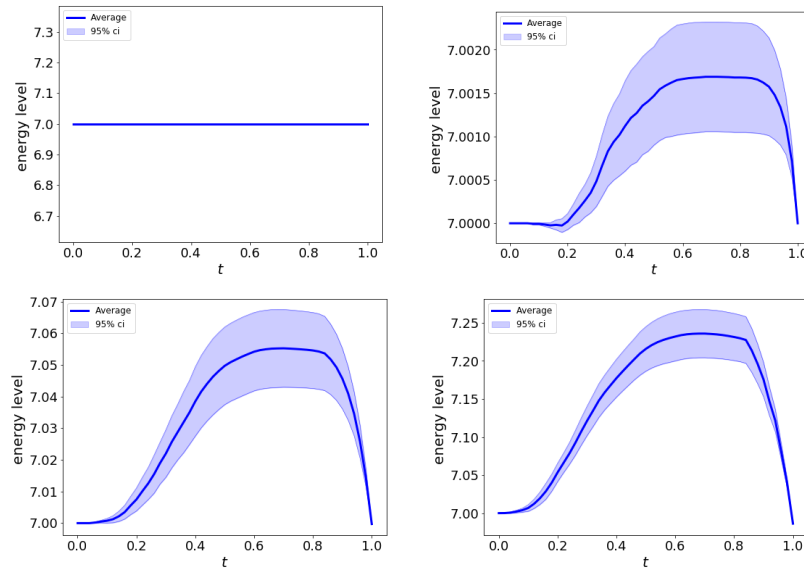


Figure 17: A zoom in at the average energy levels in Figure 16.

Table 15 shows that the values obtained with the COS method with the closed-form characteristic function are always in the 95% LSMC confidence interval. Most of the COS values obtained with the approximated characteristic function also lie in the confidence interval, however due to the relatively low contract values, there is still a high error in percentage terms compared to the COS values obtained with the closed-form characteristic function.

As seen in Table 11, the values of contract 1 are relatively low, especially for less volatile price processes. The reason for this is that the efficiency of the electricity storage is 95%, so the discounted electricity price must have increased by $(1/0.95 - 1)\%$ to make a profit. This price change happens more often when the volatility of the price is higher, with the low volatility price process ($\sigma = 0.3$) this did not occur, as shown in Figures 16-17.

Although there is little energy change taking place, Figures 16-17 show that the strategy is to slowly start storing electricity around $t = 0.1$ in the battery if this is expected to yield a profit. In the end, the energy is usually sold until the starting energy level is reached to avoid being fined 350 euros at the settlement date. However, with mid-high and high volatility levels, all energy is sometimes sold from the battery even if a penalty has to be paid, because this strategy yields more profit.

The computation time of the methods is as follows. The LSMC method took ± 26 minutes to compute a contract value. The CPU time of the COS method with the closed-form characteristic function is ± 28 minutes, however the valuation with the mid-high volatility parameter took only ± 20 minutes. This lower CPU time is because at each exercise moment the integration range is split into fewer parts compared to the computations with the other volatility parameters and therefore the continuation value had to be calculated less often. Furthermore, the COS method with the approximated characteristic function took only ± 14 seconds.

Contract 2: Highly efficient electricity storage

Table 16 and Figures 18-19 state the numerical results of contract 2.

Pricing method	LSMC 95% c.i.	COS	
Characteristic function	-	Closed-form	Approximated
σ	N=50000	N=128	N=128
0.3	[1.5543 , 1.6054]	1.5918	0.6690
0.6	[2.9985 , 3.0658]	3.0370	0.6488
0.9	[4.5021 , 4.6516]	4.5905	0.9508
1.2	[6.1667 , 6.3611]	6.2705	1.8628

Table 16: The values of contract 2 obtained with the COS method and LSMC method.

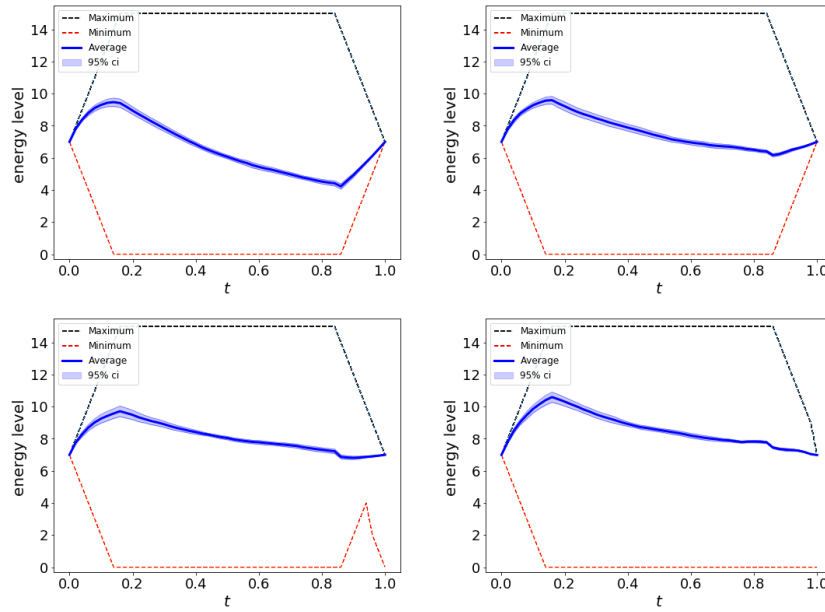


Figure 18: The average energy level in storage for contract 2, respectively from left to right, low volatility, mid-low volatility, mid-high volatility and high volatility obtained with the LSMC method.

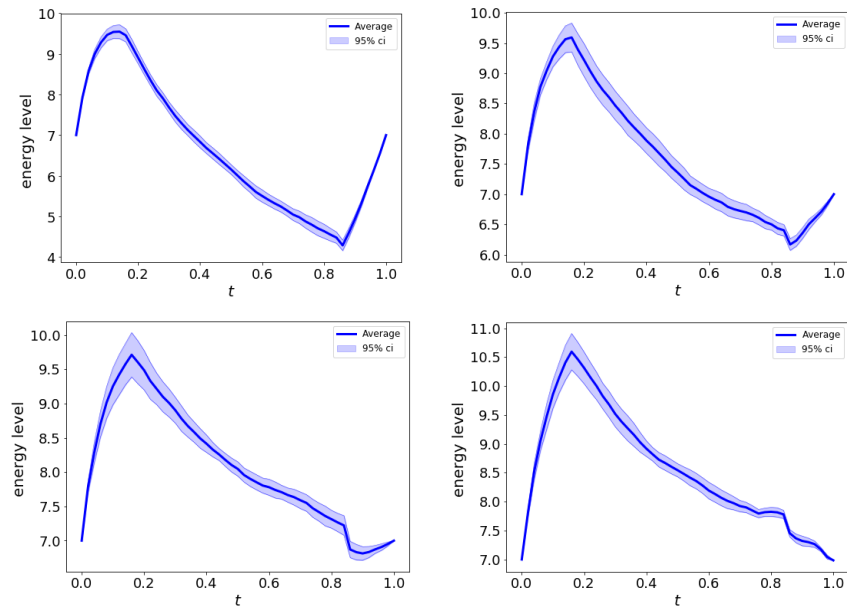


Figure 19: A zoom in at the average energy levels in Figure 18, note that the scale of the y-axes are not equal.

As shown in Table 16, the values obtained with the COS method with the closed-form characteristic function are all within the 95% LSMC confidence interval, however the values obtained with the approximated characteristic function by means of the COS method are not. This is partly because at each exercise moment the integral is divided into many parts in order to take the maximum of all actions, and at each split the approximated characteristic function is used to determine the continuation value resulting in an error.

The values of contract 2 are a lot higher than of contract 1, this is because the 100% efficiency allows greater use to be made of smaller fluctuations in the price process.

The strategy is also different compared to contract 1, a lot of electricity is immediately stored at the start of the contract and then it is withdrawn slowly. As the settlement date approaches, it is ensured that the energy level returns to the starting energy level to avoid a penalty. Although, the maximum and minimum energy levels in figure 18 show that at mid-high and high volatility electricity price processes all energy is sometimes sold and a penalty is accepted.

The CPU times of the various valuation methods for contract 2 are as follows. The LSMC method took ± 28 minutes, the COS method with closed-form characteristic function ± 37 minutes and the COS method with approximated characteristic function ± 15 seconds. Again, the COS method with the closed-form characteristic function where the mid-high volatility parameter is used took less computation time, namely ± 25 minutes.

Contract 3: Fast charging electricity storage

The numerical results of contract 3 are shown in Table 17 and Figures 20-21. The characteristics of contract 3 are defined in Table 12.

Pricing method	LSMC 95% c.i.	COS	
Characteristic function	-	Closed-form	Approximated
σ	N=50000	N=128	N=128
0.3	[0.0000 , 0.0000]	0.0000	0.0022
0.6	[-0.0010 , 0.0023]	0.0003	0.0007
0.9	[0.0055 , 0.0200]	0.0144	0.0059
1.2	[0.1935 , 0.2434]	0.2094	0.1307

Table 17: The values of contract 3 obtained with the COS method and the LSMC method.

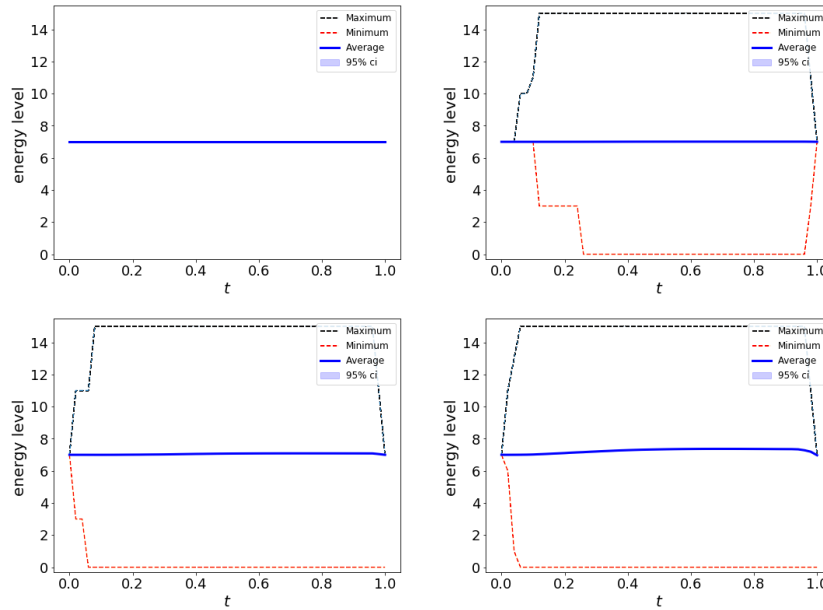


Figure 20: The average energy level in storage for contract 3, respectively from left to right, low volatility, mid-low volatility, mid-high volatility and high volatility obtained with the LSMC method.

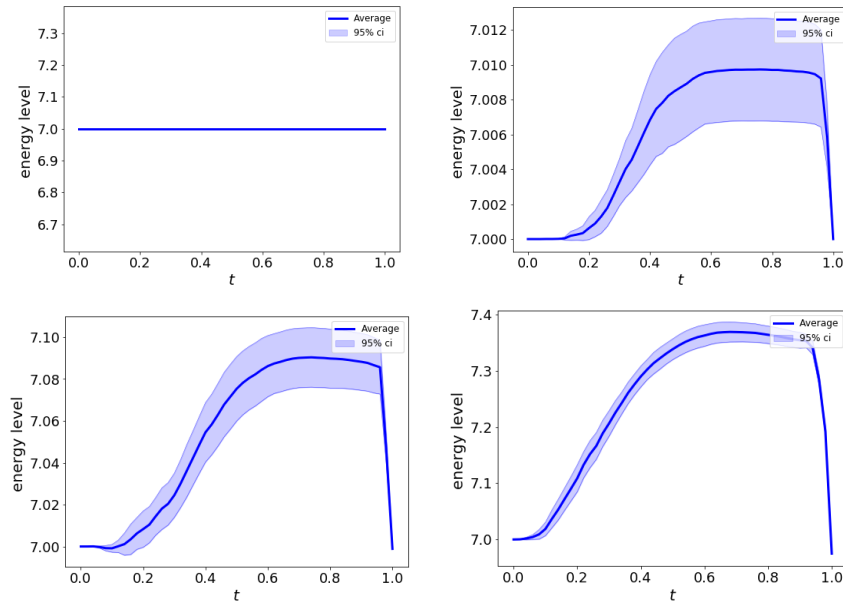


Figure 21: A zoom in at the average energy levels in Figure 20, note that the scale of the y-axis is not equal.

There are more actions possible at each exercise moment with this contract in comparison to contracts 1 and 2, the other characteristics are the same as in contract 1. The extra actions allow the holder of the contract to make better use of price fluctuations, which increases the value of the contract, as shown in Table 17.

The values obtained with the COS method where the closed-form characteristic function is used lie within the 95% confidence interval. Moreover, the values derived with the COS method where the approximated characteristic function is used have a relatively large difference compared to the COS values derived with the closed-form characteristic function, due to the error obtained when calculating the continuation value for each split part of the integration interval at each exercise moment.

The strategy is comparable to contract 1, first electricity is gradually stored, after which all the electricity up to the starting energy level is sold just before the settlement date to maximize the profit.

The CPU time is as follows. The LSMC method took ± 53 minutes, the COS method with closed-form characteristic function ± 52 minutes and the COS method with approximated characteristic function ± 22 seconds. The COS method where the mid-high volatility parameter is used took only ± 32 min. The computation time for each method took longer with this contract, compared to contracts 1 and 2, because more actions need to be considered at each exercise moment.

Contract 4: Highly efficient and fast charging/discharging electricity storage

The numerical results of the fast charging/discharging electricity storage with highly efficiency are stated in Table 18 and Figures 22-23.

Pricing method	LSMC 95% c.i.	COS	
Characteristic function	-	Closed-form	Approximated
σ	N=50000	N=128	N=128
0.3	[1.9703 , 2.0255]	1.9756	0.8691
0.6	[3.7016 , 3.8055]	3.7518	0.8546
0.9	[5.5749 , 5.8276]	5.6629	1.1898
1.2	[7.5772 , 7.7689]	7.7270	2.2016

Table 18: The values of contract 4 obtained with the COS method and the LSMC method.

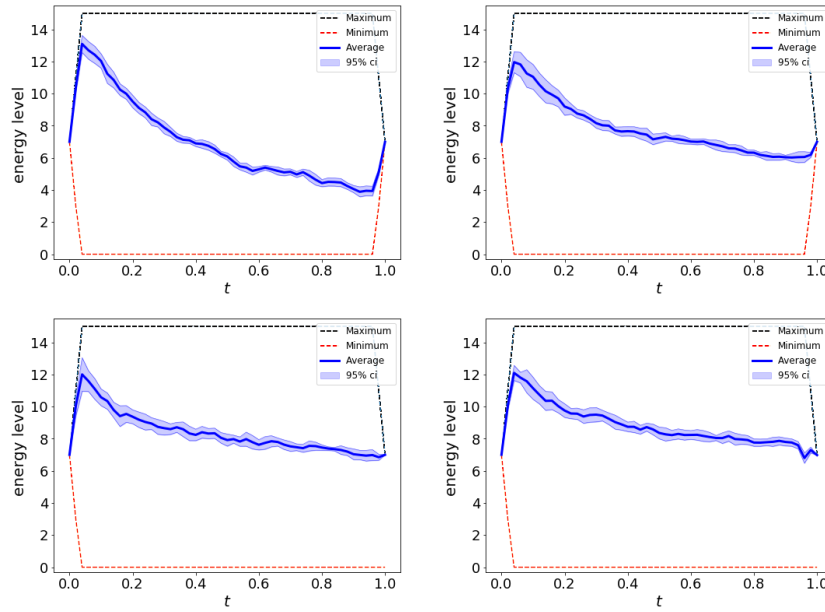


Figure 22: The average energy level in storage for contract 4, respectively from left to right, low volatility, mid-low volatility, mid-high volatility and high volatility obtained with the LSMC method.

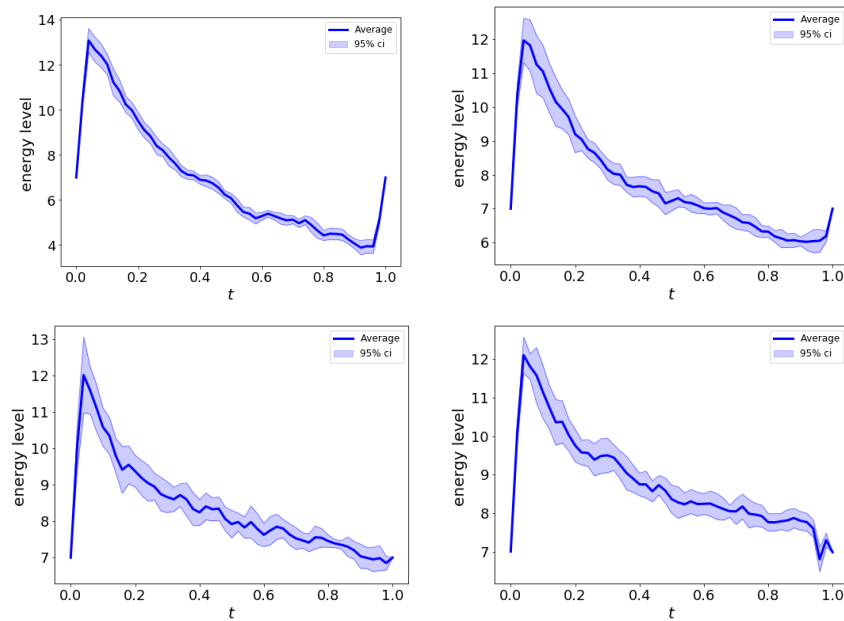


Figure 23: A zoom in at the average energy levels in Figure 22, note that the scale of the y-axis is not equal.

Contract 4 has the advantages of both contract 2 and contract 3, that is to say, fast charging/discharging and a 100% efficient electricity storage. Therefore, it is possible for the holder to make maximum use of the fluctuations in the price process, resulting in a higher contract value, as shown in Table 18.

Moreover, it can be seen that the contract values calculated by means of the COS method with closed-form characteristic function for all price processes are within the 95% LSMC confidence intervals. The values obtained with the COS method where the approximated characteristic function is used lie far outside the confidence intervals.

The strategy is the same as in contract 2, however it is possible to inject/withdraw more energy per exercise moment, therefore higher energy levels are achieved in storage. Furthermore, the low volatility electricity price processes achieve a higher average energy level in the beginning, this can be explained by the upward drift in the price process, a process with low volatility is more dependent on this.

The CPU time is as follows. The LSMC method took ± 55 minutes, the COS method with closed-form characteristic function ± 59 minutes and the COS method with approximated characteristic function ± 23 seconds. Again the CPU time for the COS method with closed-form characteristic function is less when the mid-high volatility parameter is used, namely ± 32 minutes.

Contract 5: Car-Park as Power Plant (CPPP)

In Table 14 and Figure 24 the numerical results are shown for contract 5, intended for the concept CPPP.

Pricing method	LSMC 95% c.i.	COS	
Characteristic function	-	Closed-form	Approximated
σ	N=50000	N=128	N=128
0.3	[0.0000 , 0.0000]	-0.0005	-0.0085
0.6	[0.0000 , 0.0000]	0.0000	0.0003
0.9	[-0.0007 , 0.0001]	0.0000	0.0000
1.2	[-0.0042 , 0.0018]	0.0004	-0.0007

Table 19: The values of contract 5 obtained with the COS method and the LSMC method.

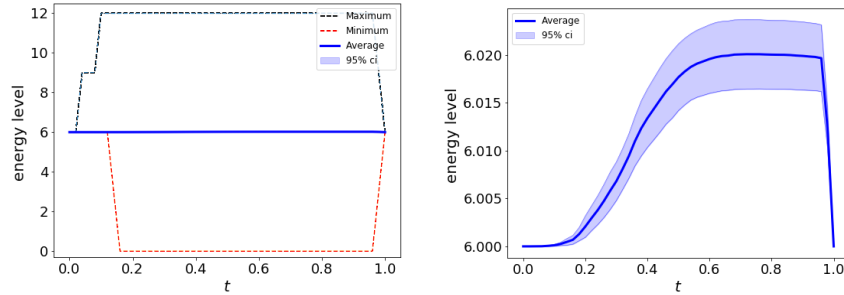


Figure 24: The average energy level in storage for contract 5 for high volatility obtained with the LSMC method.

Table 19 shows that the Car-Park as Power Plant has almost no profit by trading on the energy market, where the electricity prices are generated by the dynamics described in (8.1)-(8.2). The reason is that the efficiency is not high enough to make profitable use of the fluctuations of the electricity price (this can change due to technical improvements). Furthermore, an electricity storage consists of more value than obtained by trading on the electricity market, e.g. guaranteeing a more stable energy system.

In Figure 24 the average energy level in the storage is shown, where the high volatility price process is used. The strategy is the same as with contract 1 and contract 3, where the storage has an efficiency of 95%. A difference is that, due to the high penalty at the settlement date, there are no trajectories that sell all the energy in the end even if the penalty has to be paid.

The CPU time is as follows. The LSMC method took ± 34 minutes, the COS method with closed-form characteristic function ± 25 minutes and the COS method with approximated characteristic function ± 14 seconds.

8.3 The Greeks of the electricity storage contracts

An advantage of the COS method is that the Greeks can be calculated at almost no additional computation costs on top of the computation of the option value, unlike Monte Carlo methods. Tables 20 and 21 show the Greeks of the electricity contracts, with respectively an underlying low and mid-high volatility electricity price as described in (8.1)-(8.2), calculated by means of the COS method where the closed-form characteristic function is used.

	Contract 1	Contract 2	Contract 3	Contract 4	Contract 5
$\hat{\Delta}$	-0.0509	0.0523	-0.0607	-0.0579	-0.0408
$\hat{\Gamma}$	0.1263	1.5676	0.1512	1.5967	0.1015
$\hat{\nu}$	0.0229	0.2864	0.0274	0.2914	0.0184

Table 20: The Greeks of the electricity contracts, where low volatility ($\sigma = 0.3$) electricity prices are used, obtained with the COS method.

	Contract 1	Contract 2	Contract 3	Contract 4	Contract 5
$\hat{\Delta}$	-0.0054	-0.2254	-0.0104	-0.2929	-0.0001
$\hat{\Gamma}$	0.0092	0.4959	0.0169	0.5183	0.0006
$\hat{\nu}$	0.0050	0.2696	0.0091	0.2813	0.0003

Table 21: The Greeks of the electricity contracts, where mid-high volatility ($\sigma = 0.9$) electricity prices are used, obtained with the COS method.

The Delta $\hat{\Delta}$ measures the change in the contract value resulting from a change in the electricity price. Genuinely, put options have a negative Delta due to the negative relationship with the electricity price - so the value of a put option will increase if the asset price falls, and vice versa. Conversely, call options have a positive Delta - so the value of a call option will increase if the asset price increases, and vice versa. In general, the further away the Delta is from 0, the more likely the option will be in-the-money.

However with an electricity storage contract the electricity can be both bought and sold, and thus benefits from both price decreases and price increases, therefore Delta can be both positive and negative. With a positive Delta, such as with Contract 2 with a low volatility parameter, the contract benefits more from a price increase, and vice versa with a negative Delta. Moreover, as shown in Tables 20 and 21, most considered contracts benefit from a price decrease, especially highly efficient electricity storages where the price process has a high volatility parameter. In addition, the Delta becomes more extreme when the holder can make higher energy changes.

Furthermore, if the starting energy level is higher than the level for which the holder receives a penalty, we see that the Delta is rising strongly and is positive, i.e. $\hat{\Delta} \gg 0$. This makes sense because the holder will benefit from a high price because he/she can sell more than he/she has to buy in order not to receive a penalty at the settlement date. We see the opposite if the starting energy level is lower than the energy level for which a penalty is obtained, i.e. $\hat{\Delta} \ll 0$.

The Gamma $\hat{\Gamma}$ is a measure of the change of Delta resulting from a change in the electricity price. Since Delta values change continually with the electricity price, Gamma

is used to give an idea on how stable a contract is. For Gamma's far from zero, the Delta changes drastically when the price changes, making the contract behave differently after the next price change.

The contracts where a highly efficient storage is considered have a higher Gamma. In addition, the Gamma also becomes slightly higher if the holder has actions with high energy changes to choose from. However, the Gamma is the highest for contracts where highly efficient electricity storages are considered and high volatility price processes take place.

The Vega \hat{v} measures the impact of a change in the volatility parameter σ on the contract value. For the electricity contract, Vega is expected to be positive, because with a more fluctuating electricity price more profit can be made by buying the electricity at a low price and selling it at a high price.

The results show that with a lower volatility parameter a change in σ has more effect on the contract value than with a higher volatility parameter. Furthermore, the Greek Vega is the highest for the contracts that can make the most use of a high volatility, i.e. high efficiency and allowing bigger energy changes.

8.4 Implications of the numerical results

The numerical results of the contract value obtained with the COS method, where the closed-form characteristic function is used, are all within the LSMC 95% confidence interval. From this it can be implied that the COS method can accurately approximate the contract value. In addition, an advantage of the COS method is that the Greeks can be computed at almost no additional computational costs, in contrast to the LSMC method where the computation of the Greeks can be difficult and time consuming.

Although the contract value is accurately approximated by means of the COS method with the closed-form characteristic function, the CPU time is relatively high compared to pricing the other discussed financial derivatives with the COS method in Section 7. The reason for this is that when calculating the electricity storage contract, the integral is split into many parts to determine the maximum of all actions and the continuation value must be calculated for each split, which takes the most time.

Moreover, it is likely that splitting the integral, so that the continuation value has to be determined multiple times at each exercise moment, is also the reason why the contract values determined with the COS method where an approximated characteristic function is used has a relatively large error compared to the values determined for other options with this method. Namely, when computing the continuation value, there is an error when using the approximated characteristic function, as shown in Section 5.6. Therefore we do not recommend using the approximated characteristic function when pricing electricity storage contracts. The same conclusion is obtained when using the adjoint expansion for the approximation of the characteristic function.

Furthermore, the electricity price dynamics (8.1) have an impact on the electricity contract value. The larger the volatility parameter σ , the more the holder of the electricity storage contract can take advantage of the large price fluctuations, resulting in a higher contract value. It is also clearly visible in the Greek \hat{v} that the parameter σ of the underlying price process has a major influence on the contract value, see Tables 20 and 21. In addition, the rate of mean reversion parameter κ was also examined, which shows that the contract values typically decrease as κ increases, this is because for a higher κ

the price process goes to the mean faster and thus creates less volatility.

Additionally, the contract value depends on the electricity storage contract characteristics, defined in Tables 10-14. The numerical results clearly show that the efficiency has a major influence, this is because when the energy is bought the discounted price must increase by $(1/\eta - 1)\%$ in order not to make a loss. As a result, the price of the storage contract, which only takes into account trading on the electricity market by buying and selling electricity, is lower. In addition, the magnitude of electricity change per exercise moment is important for the value, the greater the permitted electricity change, the greater the value.

Besides the dependence on the contract values, the characteristics also have a major influence on the strategy of injecting/withdrawing energy at each exercise moment. When the characteristics of the contract change, the strategy can change completely, as can be seen by comparing the strategy of contract 3 and contract 4. Although the strategy depends more on the contract characteristics, the price dynamics also have an effect on this. Especially if there is low volatility, it can be seen that the confidence interval is a lot smaller and therefore the same strategy is more often applied to the trajectories.

9 Conclusions and outlook

In this thesis we have introduced the COS method to price European options, Bermudan options, Bermudan options with multiple early-exercise rights and electricity storage contracts, where the asset/electricity prices follow a structural model based on polynomial processes. In particular we focused on the well-known Ornstein-Uhlenbeck (OU) process as the underlying polynomial process. In addition, the Least Squares Monte Carlo (LSMC) method is presented to price the financial derivatives and validate the values obtained with the COS method. The numerical results show that the COS method, where the closed-form characteristic function is used, performs impressively and can price the discussed financial derivatives accurately.

We formalized a contract for storing electricity by trading on the electricity market, allowing the contract to be valued efficiently. An electricity storage contract deals with the physical limitations of an electricity storage, the operational constraints of the electricity grid and the subsequent actions that a holder of the contract can make. These features make it a more complex problem than standard Bermudan options or Bermudan options with multiple early-exercise rights.

Different types of electricity storage contracts are considered, where each discussed contract has its own characteristics (i.e. storage efficiency, charge/discharge rate, endurance of the storage). Moreover, we looked at the concept Car Park as Power Plant (CPPP), where the numerical results indicate that the efficiency of electric vehicle batteries is not yet high enough to make a profit with just trading on the electricity market.

For the valuation of the electricity storage contracts, the COS method with the closed-form characteristic function is competitive with the LSMC method in terms of computation time and accuracy. That is to say, while pricing the contracts accurately, either the LSMC method or the COS method with closed-form characteristic function can have faster computation times depending on the parameters of the price process and the electricity storage contract characteristics. An advantage of the COS method is that the Greeks can be computed at almost no additional computational costs, in contrast to the LSMC method where the calculation of the Greeks can be difficult and time consuming. However, if a general trading strategy based on the average energy level in storage is preferred over the Greeks, then the LSMC method should be used instead of the COS method.

Moreover, we investigated the COS method for pricing European options, Bermudan options and Bermudan options with multiple early-exercise rights, where the asset prices also follow the structural model based on polynomial processes. For these options, the COS method with the closed-form characteristic function outperforms the LSMC method. Both methods can accurately price the options, but the COS method requires significantly less computation time compared to the LSMC method.

Furthermore, we presented an approximation of the characteristic function which enables us to apply the Fast Fourier Transform (FFT) when pricing the discussed financial derivatives by means of the COS method, which significantly reduces the computation time of the valuation. In addition, this approximation can be used for (underlying) processes where the closed-form characteristic function is not available.

The numerical results show that the approximation of the characteristic function of the OU process performs well when pricing Bermudan-type options for most parameter combinations. For the Bermudan option and Bermudan option with multiple

early-exercise rights, where the underlying price process follows an OU process, the computation time is reduced from seconds to milliseconds while the results remain accurate. While the approximation works well for the Bermudan-type options, for electricity storage contracts there is an excessive pricing error when using the COS method with the approximated characteristic function and therefore the approximation is not recommended for pricing electricity storage contracts.

9.1 Outlook

As mentioned, the COS method for valuing the electricity storage contract does not perform well with the approximated characteristic function, so the FFT can not be applied to reduce the computation time. Therefore, we suggest parallelizing parts of the COS pricing algorithm to reduce the CPU time. Especially the parts where the Fourier coefficients of the continuation value are calculated, because this takes most of the computation time. For example, at each exercise moment, the Fourier coefficients of the continuation value can be calculated simultaneously for each energy level in storage. In addition, all elements of the matrices $\mathcal{M}_{k,l}^c$ and $\mathcal{M}_{k,l}^s$, defined in respectively (4.52) and (4.53), can also be computed simultaneously instead of per element of the $N \times N$ matrices.

We also suggest further research on the choice of \bar{L} used in the integration range of the COS method and the number of terms N in the Fourier cosine expansion. A smart choice of \bar{L} can ensure that less terms in the Fourier cosine expansion are needed to achieve the same accuracy while reducing the computation time.

In addition, it can be investigated whether our approach to approximate the characteristic function works well in valuing financial derivatives with the COS method when other stochastic models or higher-order polynomial models are used for the generation of the asset/electricity prices.

Moreover, the use of antithetic variates can be applied to the LSMC method to reduce the variance of the obtained results. This means that fewer trajectories need to be simulated to achieve the same accuracy with the LSMC method, resulting in higher computational efficiency.

Furthermore, due to the great potential of electricity storage, there are many different technologies for large-scale electricity storage and there is rapid technological progress in this area. Therefore it may be interesting to conduct more research into different electricity storage technologies and concepts that can be priced with the formalized electricity storage contract.

Appendices

A The dynamics of stochastic processes

In this appendix we present the dynamics of some stochastic processes used in this thesis.

A.1 Geometric Brownian Motion

The Geometric Brownian Motion (GBM) satisfies the following SDE:

$$dX_t = \mu X_t dt + \sigma X_t dW_t, \quad (\text{A.1})$$

where $t \geq 0$, $\mu > 0$ denotes the drift parameter, $\sigma > 0$ the percentage volatility parameter and W_t the Brownian motion under real-world measure \mathbb{P} .

By Ito's lemma it will be demonstrated that (A.1) has the lognormal distribution, i.e. that $\log(X_t)$ has the normal distribution. By setting $x(t) = \log(X_t)$ and applying Ito's lemma it gives:

$$dx_t = \left(\mu - \frac{1}{2}\sigma^2 \right) dt + \sigma dW_t. \quad (\text{A.2})$$

As the increments of the Brownian motion W_t are normally distributed with mean zero and variance dt , it shows that (A.2) has an expected value of $(\mu - \frac{1}{2}\sigma^2) dt$ and a variance of $\sigma^2 dt$. Because an integral can be regarded as an infinite sum, the variable x_t can be represented as the sum of the increments dx_t , such that $x_t = \log(X_t)$ is normally distributed:

$$x_t = \log(X_t) \sim N \left(\log(X_0) + \left(\mu - \frac{\sigma^2}{2} \right) (t - t_0), \sigma^2 (t - t_0) \right). \quad (\text{A.3})$$

Moreover, the right-hand side of the log-transformation dx_t (A.2) does not depend on x_t , and therefore can be simply integrated on both sides. Integration from t_0 to t results in the following solution:

$$x_t = x_{t_0} + \left(\mu - \frac{\sigma^2}{2} \right) (t - t_0) + \sigma (W_t - W_{t_0}). \quad (\text{A.4})$$

Now $X_t = e^{x_t}$ is obtained by taking the exponential on both sides of (A.4), which gives the following solution for X_t :

$$X_t = X_{t_0} \exp \left(\left(\mu - \frac{\sigma^2}{2} \right) (t - t_0) + \sigma (W_t - W_{t_0}) \right). \quad (\text{A.5})$$

When GBM is used for the risk-neutral valuation under the risk-neutral measure \mathbb{Q} , the drift term μ is set equal to the risk-free interest rate r to avoid arbitrage (i.e. $\mu = r$).

Furthermore, the characteristic function of the GBM is given by:

$$\phi(u|x, \Delta t) = e^{iu x + A(u, \Delta t)}, \quad (\text{A.6})$$

where

$$A(u, \Delta t) = iu \left(\mu - \frac{\sigma^2}{2} \right) \Delta t - \frac{1}{2} \sigma^2 u^2 \Delta t.$$

A.2 Ornstein-Uhlenbeck process

The Ornstein-Uhlenbeck (OU) process has the following SDE:

$$dX_t = \kappa(\theta - X_t)dt + \sigma dW_t, \quad (\text{A.7})$$

where $t \geq 0$, κ the rate of mean reversion, θ the long-run mean, σ the volatility of the process and W_t the Brownian motion under real-world measure \mathbb{P} .

Integration from t_0 to t on both sides of the SDE (A.7) yields the following solution of the OU process:

$$X_t = X_{t_0}e^{-\kappa(t-t_0)} + \theta \left(1 - e^{-\kappa(t-t_0)}\right) + \sigma e^{-\kappa(t-t_0)} \int_{t_0}^t e^{\kappa s} dW_s. \quad (\text{A.8})$$

By using a scaled time-transformed Brownian motion an analytical solution of the integral in equation (A.8) can be computed, see [56] for further details.

Moreover, the OU process is normally distributed, i.e. $X_t \sim N(\mathbb{E}[X_t], \text{Var}[X_t])$, where the expected value and variance are given by:

$$\begin{aligned} \mathbb{E}[X_t|\mathcal{F}_0] &= X_{t_0}e^{-\kappa(t-t_0)} + \theta(1 - e^{-\kappa(t-t_0)}), \\ \text{Var}[X_t|\mathcal{F}_0] &= \frac{\sigma^2}{2\kappa}(1 - e^{-2\kappa(t-t_0)}), \end{aligned} \quad (\text{A.9})$$

with initial position X_{t_0} .

Furthermore, the well-known characteristic function of the OU process is given by [43]:

$$\phi(u|x, \Delta t) = e^{iux e^{-\kappa\Delta t} + A(u, \Delta t)}, \quad (\text{A.10})$$

where

$$A(u, \Delta t) = \frac{1}{4\kappa} (e^{-2\kappa\Delta t} - e^{-\kappa\Delta t}) (u^2\sigma^2 + ue^{\kappa\Delta t} (u\sigma^2 - 4i\kappa\theta)).$$

B The LSMC algorithms

In this appendix the algorithms for the LSMC method are stated. Algorithm 1 and 2 are based on the algorithms in [57].

Algorithm 1 The LSMC algorithm for a Bermudan option.

```

1:  $PO_m^i = (K - S^i(t_m))^+ , \forall i = 1, \dots, N$  and  $\forall m = 1, \dots, M$ 
2:  $CF_M^i = PO_M^i , \forall i = 1, \dots, N$ 
3: for  $m = M - 1, \dots, 1$  do
4:    $X^i = S^i(t_m) , \forall i$  where  $PO_m^i > 0$ 
5:    $Y_m^i = DCF^i(t_m) = \sum_{k>m} e^{-r(k-t)\Delta t} CF_k^i , \forall i$  where  $PO_m^i > 0$ 
6:    $p = \text{polyfit}(X, Y, 3)$ 
7:    $CV_m = \text{polyval}(p, X_m^i) , \forall i$  where  $PO_m^i > 0$ 
8:   for  $i = 1, \dots, N$  do
9:     if  $CV_m^i < PO_m^i$  then
10:        $CF_m^i = PO_m^i$ 
11:        $CF_k^i = 0 , \forall k > m$ 
12:     end if
13:   end for
14: end for
15:  $v(t_0, S(t_0)) = \frac{1}{N} \sum_{i=1}^N DCF_0^i = \frac{1}{N} \sum_{i=1}^N \sum_{m=1}^M e^{-r \cdot m \Delta t} CF_m^i$ 

```

Algorithm 2 The LSMC algorithm for a Bermudan option with multiple early exercise rights.

```

1:  $PO_m^i = (K - S^i(t_m))^+ , \forall i = 1, \dots, N$  and  $\forall m = 1, \dots, M$ 
2: for  $j=1, \dots, R$  do
3:   for  $m=M, \dots, M-j+1$  do
4:      $CF_m^{i,j} = PO_m^i , \forall i = 1, \dots, N$ 
5:   end for
6: end for
7: for  $m = M - 1, \dots, 1$  do
8:    $X^i = S^i(t_m) , \forall i$  where  $PO_m^i > 0$ 
9:   for  $j = 1, \dots, \min(M - t, R)$  do
10:     $Y_m^{i,j} = DCF_m^{i,j}(t_m) = \sum_{k>m} e^{-r(k-t)\Delta t} CF_k^{i,j} , \forall i$  where  $PO_m^i > 0$ 
11:     $p^j = \text{polyfit}(X, Y^j, 3)$ 
12:     $CV_m^{i,j} = \text{polyval}(p, X_m^i) , \forall i$  where  $PO_m^i > 0$ 
13:   end for
14:   for  $\min(M - m, R) > 1$  do
15:     for  $j = \min(M - m, R), \dots, 2$  do
16:       for  $i = 1, \dots, N$  do
17:         if  $PO_m^i + CV_m^{i,j-1} > CV_m^{i,j}$  then
18:            $CF_m^{i,j} = PO_m^i$ 
19:            $CF_k^{i,j} = CF_k^{i,j-1} , \forall k > m$ 
20:         end if
21:       end for
22:     end for
23:   end for
24:   for  $i = 1, \dots, N$  do
25:     if  $CV_m^{i,0} < PO_m^i$  then
26:        $CF_m^{i,0} = PO_m^i$ 
27:        $CF_k^{i,0} = 0 , \forall k > m$ 
28:     end if
29:   end for
30: end for
31: for  $j = 1, \dots, R$  do
32:    $v^j(t_0, S(t_0)) = \frac{1}{N} \sum_{i=1}^N DCF_0^{i,j} = \frac{1}{N} \sum_{i=1}^N \sum_{m=1}^M e^{-r \cdot m \Delta t} CF_m^{i,j}$ 
33: end for

```

Algorithm 3 The LSMC algorithm for the electricity contract.

```

1: for  $e = 0, \dots, N_{cap}$  do
2:    $CF_{M+1}^{i,e} = q_s(t_{M+1}, S^i(t_{M+1}), e)$  ,  $\forall i = 1, \dots, N$ 
3:    $ACF_{M+1}^{i,e} = CF_{M+1}^{i,e}$  ,  $\forall i = 1, \dots, N$ 
4: end for
5: for  $m = M, \dots, 1$  do
6:    $X^i = S^i(t_m)$  ,  $\forall i = 1, \dots, N$ 
7:   for  $e = 0, \dots, N_{cap}$  do
8:      $DACF^{i,e} = e^{-r\Delta t} ACF_{m+1}^{i,e}$  ,  $\forall i = 1, \dots, N$ 
9:      $p^e = \text{polyfit}(X, DACF^e, 3)$ 
10:     $CV_m^{i,e} = \text{polyval}(p^e, X_m^i)$  ,  $\forall i = 1, \dots, N$ 
11:   end for
12:   for  $e = 0, \dots, N_{cap}$  do
13:     for  $i = 1, \dots, N$  do
14:        $\Delta e^{i,*} =_{\Delta e \in \mathcal{A}(t_m, e)} \{PO_m^{i,\Delta e} + CV_m^{i,e+\Delta e} + Q^{\Delta e}\}$ 
15:        $CF_m^{i,e} = PO_m^{i,\Delta e^{i,*}} + Q^{\Delta e^{i,*}}$ 
16:        $ACF_m^{i,e} = CF_m^{i,e} + e^{-r\Delta t} ACF_{m+1}^{i,e+\Delta e^{i,*}}$ 
17:     end for
18:   end for
19: end for
20: for  $e = 0, \dots, N_{cap}$  do
21:    $v(t_0, S(t_0), e) = \frac{1}{N} \sum_{i=1}^N DACF_0^{i,e} = \frac{1}{N} \sum_{i=1}^N e^{-r\Delta t} ACF_1^{i,e}$ 
22: end for

```

References

- [1] EU Commission et al. Communication from the commission to the european parliament, the council, the european economic and social committee and the committee of the regions, a roadmap for moving to a competitive low carbon economy in 2050. *Brussels, 8.3. 2011. Available at: <http://ec.europa.eu>*, 2011.
- [2] M. Åhman, L.J. Nilsson, and B. Johansson. Global climate policy and deep decarbonization of energy-intensive industries. *Climate Policy*, 17(5):634–649, 2017.
- [3] S. Lechtenböhmer, L.J. Nilsson, M. Åhman, and C. Schneider. Decarbonising the energy intensive basic materials industry through electrification—implications for future eu electricity demand. *Dubrovnik*, 2015.
- [4] X. Luo, J. Wang, M. Dooner, and J. Clarke. Overview of current development in electrical energy storage technologies and the application potential in power system operation. *Applied energy*, 137:511–536, 2015.
- [5] V. Jülch. Comparison of electricity storage options using levelized cost of storage (lcos) method. *Applied Energy*, 183:1594–1606, 2016.
- [6] H. Chen, T.N. Cong, W. Yang, C. Tan, Y. Li, and Y. Ding. Progress in electrical energy storage system: A critical review. *Progress in natural science*, 19(3):291–312, 2009.
- [7] G.L. Kyriakopoulos and G. Arabatzis. Electrical energy storage systems in electricity generation: Energy policies, innovative technologies, and regulatory regimes. *Renewable and Sustainable Energy Reviews*, 56:1044–1067, 2016.
- [8] A. Poullikkas. A comparative overview of large-scale battery systems for electricity storage. *Renewable and Sustainable Energy Reviews*, 27:778–788, 2013.
- [9] H. Lund and W. Kempton. Integration of renewable energy into the transport and electricity sectors through v2g. *Energy policy*, 36(9):3578–3587, 2008.
- [10] E.H. Park Lee. *A socio-technical exploration of the Car as Power Plant*. PhD thesis, Delft University of Technology, 2019.
- [11] I. Staffell and M. Rustomji. Maximising the value of electricity storage. *Journal of Energy Storage*, 8:212–225, 2016.
- [12] H. Lund and G. Salgi. The role of compressed air energy storage (caes) in future sustainable energy systems. *Energy conversion and management*, 50(5):1172–1179, 2009.
- [13] F. Graves, T. Jenkin, and D. Murphy. Opportunities for electricity storage in deregulating markets. *The Electricity Journal*, 12(8):46–56, 1999.
- [14] D. Connolly, H. Lund, P. Finn, B.V. Mathiesen, and M. Leahy. Practical operation strategies for pumped hydroelectric energy storage (phes) utilising electricity price arbitrage. *Energy Policy*, 39(7):4189–4196, 2011.

-
- [15] G.P. Girish and S. Vijayalakshmi. Determinants of electricity price in competitive power market. *International Journal of Business and Management*, 8(21):70, 2013.
- [16] E. Schwartz and J.E. Smith. Short-term variations and long-term dynamics in commodity prices. *Management Science*, 46(7):893–911, 2000.
- [17] J.J. Lucia and E.S. Schwartz. Electricity prices and power derivatives: Evidence from the nordic power exchange. *Review of derivatives research*, 5(1):5–50, 2002.
- [18] M.T. Barlow. A diffusion model for electricity prices. *Mathematical finance*, 12(4):287–298, 2002.
- [19] F.E. Benth, J.S. Benth, and S. Koekebakker. *Stochastic modelling of electricity and related markets*, volume 11. World Scientific, 2008.
- [20] A. Eydeland and K. Wolyniec. *Energy and power risk management: New developments in modeling, pricing, and hedging*, volume 206. John Wiley & Sons, 2003.
- [21] R. Weron. Electricity price forecasting: A review of the state-of-the-art with a look into the future. *International journal of forecasting*, 30(4):1030–1081, 2014.
- [22] R. Carmona and M. Coulon. A survey of commodity markets and structural models for electricity prices. In *Quantitative Energy Finance*, pages 41–83. Springer, 2014.
- [23] D. Filipović, M. Larsson, and T. Ware. Polynomial processes for power prices. *Swiss Finance Institute Research Paper*, (18-34), 2018.
- [24] E. Wong. The construction of a class of stationary markoff processes. *Stochastic processes in mathematical physics and engineering*, (17):264–276, 1964.
- [25] F. Delbaen and H. Shirakawa. An interest rate model with upper and lower bounds. *Asia-Pacific Financial Markets*, 9(3-4):191–209, 2002.
- [26] H. Zhou. Itô conditional moment generator and the estimation of short-rate processes. *Journal of Financial Econometrics*, 1(2):250–271, 2003.
- [27] C. Cuchiero, M. Keller-Ressel, and J. Teichmann. Polynomial processes and their applications to mathematical finance. *Finance and Stochastics*, 16(4):711–740, 2012.
- [28] D. Filipović and M. Larsson. Polynomial diffusions and applications in finance. *Finance and Stochastics*, 20(4):931–972, 2016.
- [29] L. D’hiet and M. Vanmaele. *Polynomial Diffusions*. PhD thesis, Ghent University, 2018.
- [30] X. Kleisinger-Yu, V. Komaric, M. Larsson, and M. Regez. A multi-factor polynomial framework for long-term electricity forwards with delivery period. *arXiv preprint arXiv:1908.08954*, 2019.
- [31] S. Karlin and L.S. Shapley. Geometry of reduced moment spaces. *Proceedings of the National Academy of Sciences of the United States of America*, 35(12):673, 1949.
- [32] Z. Sun. Polynomial processes for energy markets. 2019. PowerPoint presentation.

-
- [33] Anonymous. Polynomial processes and energy prices. Master's thesis, University of Oxford, 2018. https://www.maths.ox.ac.uk/system/files/attachments/MT18_dissertation_Polynomial%20processes%20and%20energy%20prices.pdf.
- [34] A. Boogert and C. De Jong. Gas storage valuation using a monte carlo method. *The journal of derivatives*, 15(3):81–98, 2008.
- [35] M. Koller, T. Borsche, A. Ulbig, and G. Andersson. Defining a degradation cost function for optimal control of a battery energy storage system. In *2013 IEEE Grenoble Conference*, pages 1–6. IEEE, 2013.
- [36] L. von Sydow, L. Josef Höök, E. Larsson, E. Lindström, S. Milovanović, J. Persson, V. Shcherbakov, Y. Shpolyanskiy, S. Sirén, J. Toivanen, et al. Benchop—the benchmarking project in option pricing. *International Journal of Computer Mathematics*, 92(12):2361–2379, 2015.
- [37] C.W. Oosterlee and L.A. Grzelak. *Mathematical Modeling and Computation in Finance*. World Scientific, 2019.
- [38] A. Cartea and M.G. Figueroa. Pricing in electricity markets: a mean reverting jump diffusion model with seasonality. *Applied Mathematical Finance*, 12(4):313–335, 2005.
- [39] F. Fang and C.W. Oosterlee. A novel pricing method for european options based on fourier-cosine series expansions. *SIAM Journal on Scientific Computing*, 31(2):826–848, 2009.
- [40] D. Duffie, J. Pan, and K. Singleton. Transform analysis and asset pricing for affine jump-diffusions. *Econometrica*, 68(6):1343–1376, 2000.
- [41] D. Filipović and M. Larsson. Polynomial jump-diffusion models. *Swiss Finance Institute Research Paper*, (17-60), 2019.
- [42] F. Fang and C.W. Oosterlee. Pricing early-exercise and discrete barrier options by fourier-cosine series expansions. *Numerische Mathematik*, 114(1):27, 2009.
- [43] B. Zhang, L.A. Grzelak, and C.W. Oosterlee. Efficient pricing of commodity options with early-exercise under the ornstein–uhlenbeck process. *Applied Numerical Mathematics*, 62(2):91–111, 2012.
- [44] B. Zhang and C.W. Oosterlee. An efficient pricing algorithm for swing options based on fourier cosine expansions. *Journal of Computational Finance*, 16(4):1–32, 2013.
- [45] D.L. Wallace. Asymptotic approximations to distributions. *The Annals of Mathematical Statistics*, 29(3):635–654, 1958.
- [46] M. Ruijter, M. Versteegh, and C.W. Oosterlee. On the application of spectral filters in a fourier option pricing technique. *Journal of Computational Finance*, 19(1):75–106, 2015.
- [47] S. Pagliarani, A. Pascucci, and C. Riga. Adjoint expansions in local lévy models. *SIAM Journal on Financial Mathematics*, 4(1):265–296, 2013.

-
- [48] A. Borovykh, A. Pascucci, and C.W. Oosterlee. Pricing bermudan options under local lévy models with default. *Journal of Mathematical Analysis and Applications*, 450(2):929–953, 2017.
- [49] A. Borovykh. *Applications of stochastic processes to financial risk computation*. PhD thesis, alma, 2018.
- [50] F.A. Longstaff and E.S. Schwartz. Valuing american options by simulation: a simple least-squares approach. *The review of financial studies*, 14(1):113–147, 2001.
- [51] U. Dörr. Valuation of swing options and examination of exercise strategies by monte carlo techniques. *Mathematical Finance*, 10:27, 2003.
- [52] A. Ibáñez. Valuation by simulation of contingent claims with multiple early exercise opportunities. *Mathematical Finance: An International Journal of Mathematics, Statistics and Financial Economics*, 14(2):223–248, 2004.
- [53] O. Palizban and K. Kauhaniemi. Energy storage systems in modern grids—matrix of technologies and applications. *Journal of Energy Storage*, 6:248–259, 2016.
- [54] W. Kempton and S.E. Letendre. Electric vehicles as a new power source for electric utilities. *Transportation Research Part D: Transport and Environment*, 2(3):157–175, 1997.
- [55] W. Kempton, J. Tomic, S. Letendre, A. Brooks, and T. Lipman. Vehicle-to-grid power: battery, hybrid, and fuel cell vehicles as resources for distributed electric power in california. 2001.
- [56] J.L. Doob. The brownian movement and stochastic equations. *Annals of Mathematics*, pages 351–369, 1942.
- [57] C. Olofsson. Pricing swing options in the electricity market. 2015.